AMERICAN CHEMICAL SOCIETY (ACS)

Nigeria International Chemical Sciences Chapter

11th Annual Symposium

Theme: Emerging Technologies in Chemistry for Sustainable Development
Date: 8th -11th February, 2026
Venue: International Conference Center, University of Ibadan, Ibadan, Nigeria

Featuring:

2026 ACS Nigeria International Student Symposium Event
Theme: From Laboratory to Society: Student Innovations in Sustainable Chemical Technologies
Industry/Green Chemistry Programme
Women Chemist Committee/Global Women Chemistry Breakfast Event

BOOK OF PROCEEDINGS

ISBN: 978-978-67-0285-8

Published by ACS Nigeria

Members of Symposium Organizing Committee

International Advisory Committee

S/N	Name	Affiliation	Research Area	Country
1.	Prof. Joshua A. Obaleye	University of Ilorin, Ilorin, Kwara State	Inorganic Chemistry	Nigeria
2.	Prof. Edu Inam	University of Uyo, Uyo, Akwa Ibom State	Analytical/Environmental Chemistry	Nigeria
3.	Prof. Tolulope Fasina	University of Lagos, Nigeria	Inorganic Chemistry	Nigeria
4.	Prof. Jennifer Nielson	Brigham Young University	Liaison Officer	USA
5.	Prof. Ryan Richards	Colorado School of Mines	Liaison Officer	USA
6.	Dr. Sederra Ross	ACS Green Chemistry Institute	-	USA

Local Organizing Committee

S/N	Name	Affiliation	Position
1.	Prof. Ganiyat K. Oloyede	University of Ibadan	Chairman
2.	Dr. Esther Faboro	Bowen University, Oyo	Member
3.	Prof. Oluwayemi O. E. Onawumi	Ladoke Akintola University of Technology, Ogbomosho	Member
4.	Dr. Raymond Akong	University of Ibadan	Member
5.	Chemist Sodeeq Aderibigbe	National Open University of Nigeria	Member/Secretary
6.	Dr. Clement Odunayo Ajiboye	Lead City University	Member
7.	Mr. Hammed Babawale Quadri	University of Ibadan	Member
8.	Mr. O. A. Akinbi	University of Ibadan	Member
9.	Mr. Suleiman Temitayo Badmos	University of Ibadan	Member

Chair, Technical/Editorial Committee

Dr. Michael O. Afolayan
Sheda Science and Technology complex, Abuja, Nigeria

Reviewers

S/No.	NAME	AFFILIATION(S)	AREA OF SPECIALIZATION
1.	Dr. Eno-Obong Sunday Nicholas	University of Nigeria, Nsukka, Nigeria	Material and Inorganic Chemistry
2.	Dr. Fausat Afolami	Lagos State University of Science and Technology, Lagos, Nigeria	Analytical / Environmental Chemistry
3.	Dr. Victoria Ndukhaire	Sheda Science and Technology complex, Abuja, Nigeria	Organic Chemistry
4.	Dr. Blessing Sunday	Nassarawa State University, Keffi, Nigeria	Analytical Chemistry
5.	Dr. Stella Emmanuel	National Open University of Nigeria	Inorganic / Materials Chemistry
6.	Dr. Adewale Fadeyi	Sheda Science and Technology complex, Abuja, Nigeria	Organic Chemistry
7.	Dr. Olutayo Olajide	University of Abuja, Nigeria	Organic Chemistry
8.	Dr. Emmanuel Etim	Federal University of Technology, Ikot Abasi	Analytical / Environmental / Physical Chemistry
9	Dr. Gideon Okibe	Auburn University, USA	Natural Products and Medicinal Chemistry
10.	Dr. Felicia Umanah	Akwa Ibom State University	Chemistry Education

TABLE OF CONENTS

ISBN: 978-978-67-0285-8 DOI: https://doi.org/10.55455/acsnigeria.1.3.1-5

Comparative Physico-Chemical Analysis of Animal Fats from Abattoirs in Sokoto Metropolis for Sustainable Waste-to-Value and Environmental Management Applications

Owolabi Abdulmuiz Aduamigba[1]*, Oribukola Joshua Temitope[1], Ogundele Abiodun[1]
[1]Department of Chemistry, University of Ibadan, Ibadan, Nigeria
Corresponding Author's email: owolabiabdulmuiz@gmail.com
DOI https://doi.org/10.55455/acsnigeria.1.3.1-5

ABSTRACT

The increasing volume of lipid-rich waste generated from abattoirs and meat processing activities presents both environmental and economic concerns, particularly in regions with limited waste management infrastructure. In many Nigerian cities, rendered animal fats are often discarded without treatment, contributing to environmental pollution and sanitation issues. At the same time, these fats possess significant industrial value as raw materials for soap production, cosmetics, lubricants, and biofuel generation. In this study, fats rendered from cow, goat, camel, and sheep tissues collected within Sokoto Metropolis, Nigeria, were examined to determine their physicochemical characteristics and possible end-use applications. Physical properties (colour, melting point, specific gravity, and density) and chemical parameters (ash content, moisture content, acid value, free fatty acid, saponification value, iodine value, and peroxide value) were determined in triplicate (n = 3). All physical and chemical analyses strictly adhered to standard protocols recommended by the Association of Official Analytical Chemists. The results showed significant differences among the samples. Cow fat recorded the highest ash content (26.0 ± 0.264 %), moisture content (31.5 ± 0.265 %), and saponification value (98.035 ± 0.004 mg KOH/g), suggesting stronger potential in soap and detergent production. Camel fat exhibited the highest acid value (3.506 ± 0.004 mg KOH/g), free fatty acid (1.753 ± 0.003 %), and peroxide value (0.030 ± 0.003 meq/kg), indicating a higher tendency toward hydrolytic and oxidative degradation. Goat fat showed the highest iodine value (0.761 ± 0.003 g I_2/100 g), which may favor its use in biodiesel production due to a relatively higher level of unsaturation. Overall, the findings highlight the viability of converting animal fat waste into useful industrial feedstocks while reducing environmental burden.

KEYWORDS: animal fat, physicochemical analysis, biodiesel, waste valorization, industrial application.

1. INTRODUCTION

Large quantities of animal-derived waste are generated daily from slaughterhouses, meat processing facilities, and livestock markets across Nigeria.[1] Among these wastes, adipose tissues are often rendered into fats or simply discarded.[2] In many urban and semi-urban areas, indiscriminate disposal of these fatty wastes contributes to drainage blockage, offensive odour, and contamination of nearby soil and water systems.[3] Sustainable approaches that convert such wastes into useful materials are therefore increasingly important.[4]

Animal fats are composed primarily of triglycerides and have been utilized for centuries in food preparation and in the manufacture of soaps, candles, and skin-care products.[5] In recent years, renewed interest has emerged in their use as low-cost feedstocks for renewable energy production, particularly biodiesel.[6] Compared with edible vegetable oils, animal fats are less expensive and do not directly compete with food supply chains.[7] Their suitability for industrial use, however, depends strongly on their physicochemical composition.[8]

Parameters such as acid value, free fatty acid content, and peroxide value provide insight into the extent of hydrolysis and oxidation within fat samples.[9,8] Saponification value reflects the average molecular weight of the constituent fatty acids and can indicate suitability for soap production.[5] Iodine value reveals the degree of unsaturation, which affects oxidative stability and biodiesel performance.[6] In addition, physical characteristics such as density, specific gravity, and melting point influence handling, storage, and processing conditions.[10]

Sokoto Metropolis is one of the largest centers of livestock slaughter and trade in northern Nigeria.[3] Despite the abundance of animal fat generated in this region, there is limited published information comparing the properties of fats obtained from different species under the same environmental conditions. This work therefore evaluates the physicochemical properties of rendered fats from cow,

goat, camel, and sheep collected within Sokoto Metropolis and considers their suitability for selected industrial and bioenergy applications.

2. MATERIALS AND METHODS

2.1 Sample Collection

Fresh adipose tissues were obtained from slaughtered cow, goat, camel, and sheep at selected abattoirs within Sokoto Metropolis, Sokoto State, Nigeria. The samples were collected immediately after slaughter into clean polyethylene bags and transported to the laboratory for processing.

2.2 Rendering and Preparation of Fat Samples

Each adipose tissue sample was rinsed thoroughly with clean water to remove adhering blood and dirt. The tissues were then cut into smaller portions and heated gently in clean metallic containers to release the fat. The rendered fat was separated from the residual tissues and filtered through a fine-grade Muslin cloth (100 % cotton, pore size ≈ 100 μm) to remove suspended particles. The filtrate was stored in airtight sample bottles under dry, cool conditions prior to analysis.

2.3 Determination of Physical Properties

All physical measurements were conducted in triplicate (n = 3). Visual appearance and color were evaluated under natural sunlight. Melting point was evaluated by the open capillary tube method. Specific gravity (dimensionless ratio) and density (kg/m³) were determined at 25 °C.

2.4 Determination of Chemical Properties

All chemical determinations were performed in triplicate (n = 3). Moisture and volatile matter content were determined by oven-drying a known mass at 105 °C to constant weight. Total ash content was measured by dry ashing in a muffle furnace at 550 °C. Acid value and percentage free fatty acid (FFA, calculated as oleic acid equivalent) were determined by titration with standardized ethanolic 0.1 M KOH in a neutralized solvent mixture. Saponification value was determined by alcoholic potassium hydroxide reflux and back-titration with 0.5 M HCl in accordance with AOAC Official Method 920.160. The degree of unsaturation (iodine value) was determined using the Wijs halogen absorption technique. Primary oxidative stability (peroxide value) was evaluated by iodometric titration against standardized sodium thiosulfate solution.

All analytical protocols for physical and chemical parameter determinations implemented in this study strictly followed the standard methods approved and recommended by the Association of Official Analytical Chemists.[10]

3. RESULTS AND DISCUSSION

3.1 Physical Properties and Assessment

Table 1. Physical Properties of Selected Animal Fats (n = 3, Mean ± Standard Deviation)

Parameter	Sample A (Cow)	Sample B (Goat)	Sample C (Camel)	Sample D (Sheep)
Colour	Pale yellow	White	Cream colour	White
Melting Point (°C)	43.7 ± 0.1	45.2 ± 0.265	43.5 ± 0.173	44.4 ± 0.361
Specific Gravity (dimensionless)	0.985 ± 0.001	0.914 ± 0.004	0.968 ± 0.003	0.939 ± 0.002
Density (kg/m³)	985.000 ± 4.000	914.000 ± 2.000	968.000 ± 2.000	938.000 ± 1.154

Physical properties serve as vital indicators of sample purity, thermal behavior, and mass-transport dynamics required in industrial chemical processing. The visual colour assessment reflects pigment retention, thermal exposure during rendering, or potential contamination. Cow fat displayed a distinct pale-yellow hue due to carotenoid pigments retained from pasture grazing, whereas goat and sheep fats were pure white. From a waste-valorization perspective, white fats are highly preferred for cosmetic formulations, personal care products, and skin creams, as they eliminate the need for costly industrial

bleaching steps. Conversely, yellowish or cream-coloured fats, such as cow and camel fat, are better suited for biofuel generation or industrial grease production.

The observed melting points (43.5 °C – 45.2 °C) fall squarely within established literature ranges for refined animal tallows (42.-0 °C – 48.0 °C).[9,7] High melting points indicate an elevated proportion of long-chain saturated fatty acids, primarily palmitic and stearic acids. Goat fat recorded the highest melting point (45.2 ± 0.265 °C), pointing directly to its suitability for hard bar soap production, candle making, and heavy-duty industrial greases. In biodiesel applications, high melting points signify higher cetane numbers but necessitate fuel pre-heating systems to prevent cold-weather gelation.[8]

The observed density values (914.0 – 985.0 kg/m³) align closely with standard animal fat ranges (910.0 – 950.0 kg/m³).[10] Cow fat showed slightly elevated density (985.0 kg/m³), which can be attributed to residual bound water and suspended non-lipid particles from traditional open-pan rendering. Analytically, density and specific gravity govern fluid dynamics, mass-to-volume metering, and phase separation efficiency within industrial transesterification or saponification reactors.

3.2 Chemical Properties and Applications

Table 2. Chemical Properties of Selected Animal Fats (n = 3, Mean ± Standard Deviation)

Parameter	Sample A (Cow)	Sample B (Goat)	Sample C (Camel)	Sample D (Sheep)
% Moisture Content	31.5 ± 0.265	28.5 ± 0.100	10.5 ± 0.361	26.5 ± 0.360
% Ash Content	26.0 ± 0.264	21.5 ± 0.200	14.5 ± 0.360	22.0 ± 0.264
Acid Value (mg KOH/g)	3.086 ± 0.001	3.029 ± 0.004	3.506 ± 0.004	2.244 ± 0.003
Free Fatty Acid (%)	1.543 ± 0.003	1.515 ± 0.004	1.753 ± 0.003	1.112 ± 0.002
Saponification Value (mg KOH/g)	98.035 ± 0.004	55.259 ± 0.002	57.362 ± 0.003	43.478 ± 0.002
Peroxide Value (meq/kg)	0.025 ± 0.003	0.020 ± 0.002	0.030 ± 0.002	0.010 ± 0.001
Iodine Value (g I_2/100 g)	0.508 ± 0.003	0.761 ± 0.001	0.508 ± 0.004	0.254 ± 0.002

While commercial refined fats strictly require moisture below 1.0% and ash below 0.5%, the unrefined abattoir waste fats exhibited higher moisture (10.5 % – 31.5 %) and ash (14.5 % – 26.0 %) contents due to direct thermal rendering. Analytically, high moisture promotes triglyceride hydrolysis during storage, while high ash indicates inorganic mineral residues. In terms of end-use, high moisture interferes with base-catalyzed transesterification by causing unwanted emulsion and soap formation.[9] Therefore, pre-treatment steps involving centrifugal dewatering and fine filtration are essential before these waste streams can be efficiently valorized into biodiesel or chemical lubricants.

The determined acid values (2.24 – 3.51 mg KOH/g) and free fatty acid (FFA) levels (1.11 % – 1.75 %) are moderately lower than those typically reported for highly degraded waste cooking oils (>5.0 mg KOH/g), indicating that rendered tissues were processed shortly post-slaughter. Analytically, FFA content dictates the choice of catalytic pathway. Sheep, goat, and cow fats (1.11 % – 1.54 % FFA) can undergo direct homogeneous base-catalyzed transesterification, whereas camel fat (1.75 % FFA) approaches the threshold requiring a two-step acid-esterification process to prevent catalyst neutralization.[9,6]

Saponification value measures the alkali needed to saponify a given mass of fat, providing an inverse index of average molecular weight.[5] Lower overall saponification values compared to pure refined tallow (190 – 202 mg KOH/g) stem from non-lipid matrix inclusions in crude rendering. Nevertheless, cow fat recorded a significantly higher saponification value (98.035 mg KOH/g) relative to other species, directly demonstrating its superior reactivity for soap and commercial detergent manufacturing.

The iodine values (0.254 – 0.761 g I_2/100 g) are substantially lower than vegetable oil feedstocks (80 – 140 g I_2/100 g), confirming high structural saturation.[6] Analytically, iodine value measures double bond concentration, where lower unsaturation grants exceptional oxidative stability during extended storage. Goat fat exhibited the highest iodine value (0.761 g I_2/100 g), pointing to better cold-flow properties (lower cloud point) in biodiesel applications, whereas sheep fat (0.254 g I_2/100 g) offers maximum resistance to oxidative rancidity. Furthermore, peroxide values (0.010 – 0.030 meq/kg) remained well below the standard rancidity threshold (10.0 meq/kg), confirming minimal primary lipid oxidation and

validating that these waste fats maintain sufficient quality for high-value applications, including pharmaceutical ointments, cosmetics, and bio-based lubricants.

3.3 Integrated Valorization Matrix for Abattoir Waste Management

To establish a sustainable waste-to-value framework within urban abattoir management, the analytical results directly inform species-specific valorization pathways. Cow fat, characterized by its high saponification value (98.04 mg KOH/g) and density, is primarily targeted for soap and detergent manufacturing, which directly diverts organic pollutant loading from municipal aquatic discharges. Goat fat, exhibiting the highest iodine value (0.761 g I_2/100 g) and a clear white colour, serves as an optimal feedstock for biodiesel production and cosmetics, offsetting fossil fuel dependency while reducing solid waste accumulation.

Camel fat displays relatively lower moisture (10.5 %) but elevated free fatty acid content, making it best suited for bio-lubricant synthesis and energy recovery following two-step acid-esterification pre-treatment, thereby preventing soil contamination and offensive odour emissions from land dumping. Finally, sheep fat offers superior oxidative stability and a low iodine value (0.254 g I_2/100 g), rendering it ideally suited for industrial greases and extended-storage fuel blends, which further advances circular economy principles within local livestock waste networks.

4. CONCLUSION

Based on the obtained results, it was concluded that rendered animal fats obtained from common livestock species in Sokoto Metropolis differ significantly in both physical and chemical properties. Cow fat exhibited characteristics that favor soap and detergent production due to its high saponification value (98.035 ± 0.004 mg KOH/g). Goat fat may serve as a better biodiesel feedstock because of its comparatively higher iodine value (0.761 ± 0.001 g I_2/100 g) and lower peroxide content. Camel fat showed signs of greater hydrolytic and oxidative degradation (3.506 ± 0.004 mg KOH/g acid value), which indicates the need for pre-treatment before industrial utilization. Sheep fat displayed comparatively superior oxidative stability. Converting these slaughterhouse-derived waste fats into high-value industrial feedstocks offers a viable pathway for effective waste management and sustainable environmental management in urban centers.

ACKNOWLEDGEMENTS

The authors acknowledge the Department of Chemistry, Usmanu Danfodiyo University, Sokoto, Nigeria, and University of Ibadan for providing laboratory facilities and technical support.

REFERENCES

(1) Musa, J. J.; Adejumo, B. A. Environmental impacts of slaughterhouse waste disposal. Environ. Monit. Assess. 2023, 195 (4), Article 456.

(2) Bello, E. I.; Agge, M. A. Production and characterization of biodiesel from waste animal fat. Int. J. Energy Environ. Eng. 2016, 7 (4), 423–430.

(3) Sani, M.; Garba, A.; Bello, A. Assessment of slaughterhouse waste management practices in Sokoto Metropolis, Nigeria. IOSR J. Environ. Sci. Toxicol. Food Technol. 2020, 14 (8), 12–19.

(4) Alnaqbi, M. A.; Al-Zuhair, S.; Al-Marzouqi, A. H. Synthesis and optimization of biodiesel production from animal fat waste. Waste Biomass Valorization 2019, 10 (11), 3245–3255.

(5) Adejumo, B. A.; Adebiyi, O. A.; Omotoso, O. T. Characterization of animal fat for industrial and biodiesel production. Fuel 2023, 344, Article 128123.

(6) Singh, D.; Sharma, D.; Soni, S. L.; Sharma, S.; Kumari, D. Feedstock characterization for biodiesel production: A review. Energy Convers. Manage. 2024, 297, Article 117645.

(7) Banković-Ilić, I. B.; Stojković, I. J.; Stamenković, O. S.; Veljković, V. B. Waste animal fats as feedstocks for biodiesel production. Renewable Sustainable Energy Rev. 2014, 32, 238–254.

(8) Knothe, G.; Van Gerpen, J.; Krahl, J. The Biodiesel Handbook, 3rd ed.; AOCS Press, 2023.

(9) Encinar, J. M.; González, J. F.; Rodríguez-Reinares, A. Biodiesel from used frying oil by transesterification with methanol using homogeneous and heterogeneous catalysts. Fuel Process. Technol. 2007, 88 (5), 513–522.

(10) AOAC. Official Methods of Analysis, 22nd ed.; Association of Official Analytical Chemists: Washington, DC, 2023.

ISBN: 978-978-67-0285-8 DOI: https://doi.org/10.55455/acsnigeria.1.3.6-11

Nutrient Tracking for Water Quality Evaluation: A Case Study of Domestic and Industrial Discharges in Lagos State

Akeem Abayomi[1], Rotimi Oyebisi[1,2*], and Abolanle Abolaji[1]
[1] Department of Chemistry, University of Lagos, Lagos State, Nigeria
[2] Industrial Chemistry Programme, Bowen University, Iwo, Osun State, Nigeria
Corresponding Author's email: rotimi.oyebisi@bowen.edu.ng
DOI: https://doi.org/10.55455/acsnigeria.1.3.6-11

ABSTRACT

The release of nutrient-rich effluents from domestic and industrial sources pollutes surface waters, triggering eutrophication and hypoxia. This study assesses wastewater quality, nutrient levels, and regulatory compliance, highlighting implications for aquatic ecosystems and public health. Water samples were collected from seven points across domestic and industrial discharges weekly for three weeks, following standard sampling protocols. Physicochemical parameters such as pH, turbidity, conductivity, total dissolved solids (TDS), chloride, alkalinity, hardness, dissolved oxygen (DO), chemical oxygen demand (COD), and biochemical oxygen demand (BOD) were analyzed using standard methods, while UV-Visible spectrophotometry was used to determine nutrient indicators (phosphate and nitrate). The result showed wide variations across sites with pH ranging from 6.19 to 8.82, while high turbidity reflected elevated solids. COD (31.8 - 292 mg/L) and BOD (5.55 - 71.3 mg/L) indicated significant organic pollution and microbial activity, corresponding to low DO values. Phosphate and nitrate levels were moderate, ranging from 0.01 - 0.44 mg/L and 0.29 - 2.95 mg/L, respectively, and were within acceptable limits. Wastewater from domestic and industrial sources showed notable differences in characteristics compared to control samples. The study reveals that domestic and industrial wastewater significantly contribute to nutrient pollution, posing environmental risks to aquatic ecosystems. These findings emphasize the urgent need for enhanced, sustainable wastewater management practices to protect water resources.

KEYWORDS: Effluents, Hypoxia, Nutrients, Sustainability.

1. INTRODUCTION

Water is a vital natural resource under threat from untreated wastewater containing pollutants like organic matter, heavy metals, and nutrients[1]. These compromise water quality, harm aquatic ecosystems, and pose health risks, particularly in developing countries with inadequate treatment infrastructure. Lagos, with over 20 million inhabitants, generates massive volumes of untreated domestic and industrial wastewater daily, often discharged into waterways leading to nutrient accumulation, eutrophication, leading to hypoxia and habitat degradation[2 – 4]. The consequences include biodiversity loss, livelihood impacts, and waterborne diseases[5]. Several studies have documented high nutrient levels in Lagos surface waters, particularly nitrates and phosphates[1,6], however, there remains paucity of comparative analysis of nutrient concentrations and other physicochemical properties of domestic and industrial wastewater sources within the same geographical zone. These gaps pose a threat to achieving Sustainable Development Goals, including good health and well-being, clean water and sanitation, and life below water SDGs 3, 6 and 14, respectively. This study seeks to assess nutrient levels in domestic and industrial wastewater discharges across Lagos State, aiming to identify key gaps and inform effective wastewater management strategies.

2. MATERIALS AND METHODS

2.1 Study Area

The study was conducted in three major urban districts of Lagos State; Shomolu, Surulere, and Ikeja representing distinct socio-economic, residential and industrial characteristics with well geo-referenced sampling points (Table 1, Figure 1).

Table 1: Description of Sampling Locations

Sampling Points	Discharge Points	GPS Coordinate	Description of Study Area
Point A	Domestic Kitchen	6.53728 N 3.37732 E	Houses, shops and borehole
Point B	Domestic Laundry	6.53728 N 3.37732 E	Houses, shops and borehole
Point C	Canteen	6.53785 N 3.37490 E	Houses, small shops, eatery and borehole
Point D	Laundry Service	6.53789 N 3.37504 E	Houses, shops and borehole
Point E	Industry 1	6.47894 N 3.36202 E	Movement of heavy-duty vehicles, industrial operations and warehouses
Point F	Industry 2	6.58849 N 3.37591 E	Heavy vehicular movements, industrial operations and high traffic zone
Point G	Treated Effluent	6.58848 N 3.37592 E	Heavy vehicular movements, industrial operations and high traffic zone

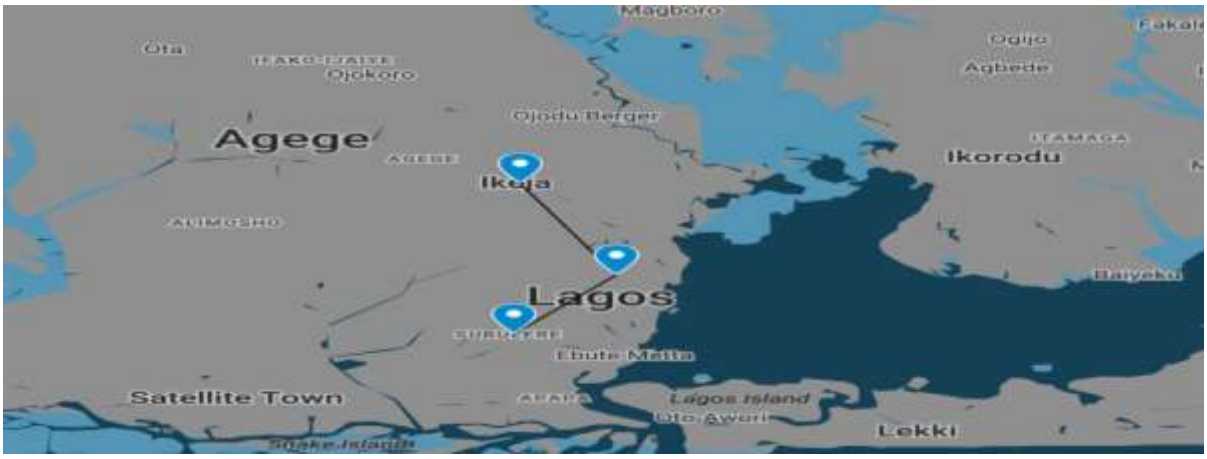

Figure 1. Map showing the study area

2.2 Sampling and Laboratory Analysis

Sampling occurred weekly over three events between June and July 2025, with 21 samples collected from domestic, commercial, and industrial discharge points, which were geo-referenced. Samples were collected in pre-cleaned 2.5 L polyethylene containers, stored in an ice chest, and transported to the laboratory. In-situ data were collected using a Horiba-U50 multi-parameter meter. Laboratory analysis followed APHA protocols, with phosphate and nitrate concentrations determined using a UV-Visible spectrophotometer at 880 nm and 420 nm, respectively[7,8].

3. RESULTS AND DISCUSSION

The physicochemical parameters and nutrient loads of the wastewaters demonstrated variability across the samples, as presented in Table 2 and Figures 2-5. Notably, samples F (from an industrial area with significant vehicular activity) and G (control sample) were clear, whereas the remaining samples were cloudy. Samples B, C, and D, obtained from domestic canteens and commercial laundry facilities, displayed a slightly soapy appearance. Furthermore, samples A, B, C, and D emitted an objectionable odour, in contrast to samples E, F, and G, which were unobjectionable. The pH of the samples was within the permissible threshold of 6.0 – 9.0 as set by NESREA and LASEPA, ranged from 6.19 – 8.82 for all the samples with a temperature range of 27.2 – 27.8 ^{O}C (Figure 2a). In Figure 2b, turbidity, TSS and TS were observed to be relatively high (Table 2) while TDS was observed to be lower than permissible threshold of 2,000 mg/L. Locations A, B, C and D were particularly observed to have higher threshold possibly because the wastewater being discharged were untreated resulting in low ORP values in the range of 50.7 – 163 mV and DO values ranging from 2.35 to 4.35 mg/L (Figure 2a). Similarly, BOD, COD, Chloride, Alkalinity and Hardness showed higher concentrations being discharged to the immediate drainage within the environment. While phosphate and nitrate were notably below the

permissible threshold, the risk of accumulated discharge to the environment following other physicochemical effect of wastewaters could be detrimental to the immediate water body.

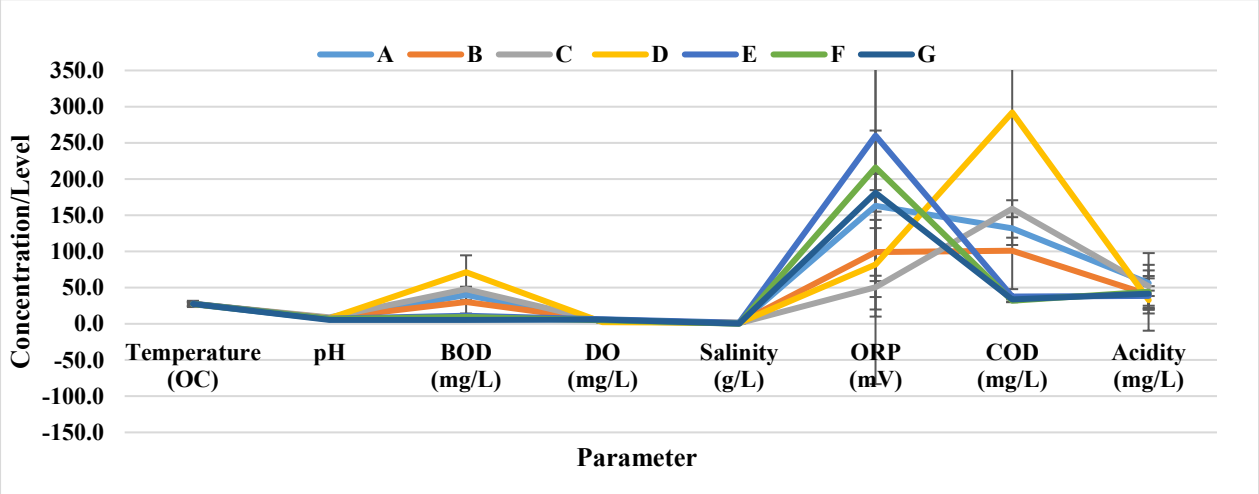

Figure 2a: Variation of Physicochemical Parameters at the Sampling Locations

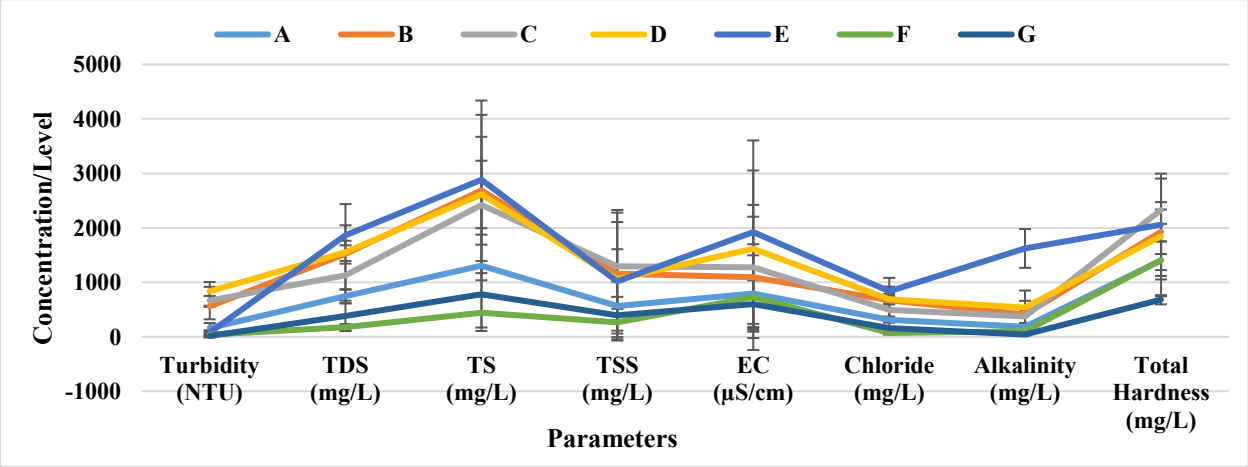

Figure 2b: Variation of Physicochemical Parameters at the Sampling Locations

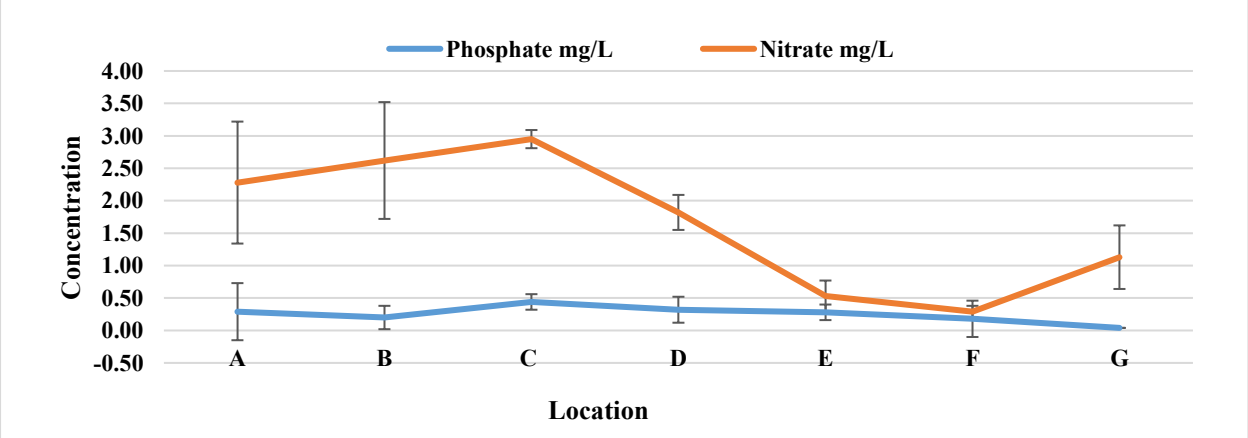

Figure 3: Results of Phosphate and Nitrate Concentrations across the Sampling Locations

Table 2: Range of Data and Permissible Limit of Effluent Discharges

Parameters	Range	NESREA/LASEPA LIMIT
Temperature, ^{O}C	27.2 - 27.8	NS
pH	5.51 - 8.82	6.0 - 9.0
BOD, mg/L	5.55 - 71.3	< 20
DO, mg/L	2.35 - 6.48	NS
Salinity, g/L	0.13 - 1.51	NS
Turbidity, NTU	15.9 – 833	<10
TDS, mg/L	179 – 1863	< 2000
TS, mg/L	443 – 2883	NS
TSS, mg/L	264 – 1292	< 750
EC, µS/cm	599 – 1921	<1000
ORP, mV	50.7 – 260	NS
COD, mg/L	31.8 – 292	< 40
Chloride, mg/L	73.7 – 836	< 350
Acidity, mg/L	32.6 - 56.1	NS
Alkalinity, mg/L	44 – 1622	NS
Total Hardness, mg/L	680 – 2328	NS
PO_4^{3-} mg/L	0.04 - 0.44	< 3.5
NO_3^- mg/L	0.29 - 2.95	< 10

National Environmental Standards and Regulations Enforcement Agency, 2011[9]
Lagos State Environmental Protection Agency, 2019 [10]
*NS - Not Specified

3.1 Relationship between physicochemical characteristics

The statistical correlation at $P < 0.05$ and $P < 0.01$(95% and 99% confidence limit, respectively) between physicochemical characteristics of the wastewater samples are presented in Table 3.

ISBN: 978-978-67-0285-8 DOI: https://doi.org/10.55455/acsnigeria.1.3.6-11

Table 3: Pearson Correlation of Different Parameters

	Temp., °C	pH	ORP mV	EC µS/cm	Turbidity NTU	DO mg/L	TDS mg/L	Salinity g/L	Acidity mg/L	Alkalinity mg/L	Total Hardness mg/L	Chloride mg/L	TS mg/L	TSS mg/L	COD mg/L	BOD mg/L	PO_4^{3-} mg/L	NO_3^- mg/L
Temp. °C	1																	
pH	0.739	1																
ORP mV	-0.520	-0.693	1															
EC µS/cm	0.375	0.536	-0.027	1														
Turbidity NTU	0.619	0.808(*)	-0.891(**)	0.425	1													
DO mg/L	-0.533	-0.416	0.774(*)	-0.068	-0.776(*)	1												
TDS mg/L	0.513	0.592	-0.202	0.900(**)	0.536	-0.095	1											
Salinity g/L	0.499	0.589	-0.191	0.907(**)	0.530	-0.086	1.000(**)	1										
Acidity mg/L	0.281	-0.044	-0.083	-0.491	-0.247	-0.074	-0.448	-0.464	1									
Alkalinity mg/L	0.167	0.240	0.380	0.886(**)	-0.012	0.364	0.789(*)	0.798(*)	-0.393	1								
Total Hardness mg/L	0.799(*)	0.912(**)	-0.398	0.745	0.630	-0.268	0.738	0.736	-0.046	0.549	1							
Chloride mg/L	0.500	0.588	-0.190	0.906(**)	0.529	-0.084	1.000(**)	1.000(**)	-0.462	0.798(*)	0.736	1						
TS mg/L	0.590	0.733	-0.371	0.862(*)	0.653	-0.184	0.978(**)	0.975(**)	-0.361	0.696	0.816(*)	0.975(**)	1					
TSS mg/L	0.656	0.886(**)	-0.603	0.723	0.778(*)	-0.308	0.853(*)	0.848(*)	-0.191	0.486	0.863(*)	0.848(*)	0.944(**)	1				
COD mg/L	0.519	0.501	-0.746	0.372	0.870(*)	-0.933(**)	0.401	0.395	-0.184	-0.066	0.403	0.392	0.463	0.520	1			
BOD mg/L	0.642	0.582	-0.786(*)	0.364	0.885(**)	-0.942(**)	0.415	0.406	-0.053	-0.068	0.491	0.404	0.495	0.577	0.985(**)	1		
PO_4^{3-} mg/L	0.798(*)	0.774(*)	-0.495	0.577	0.620	-0.559	0.497	0.491	0.270	0.314	0.850(*)	0.490	0.595	0.694	0.601	0.695	1	
NO_3^- mg/L	0.660	0.613	-0.870(*)	-0.014	0.699	-0.599	0.271	0.252	0.387	-0.274	0.413	0.252	0.424	0.624	0.559	0.655	0.520	1

***. Correlation is significant at the 0.05 level (2-tailed).**

****. Correlation is significant at the 0.01 level (2-tailed).**

ISBN: 978-978-67-0285-8 DOI: https://doi.org/10.55455/acsnigeria.1.3.6-11

Dissolved oxygen showed a positive relationship with ORP (r = 0.774) and negative with turbidity at (r = -0.776). Turbidity, which is a measure of light attenuation due to suspended particles positively correlated with suspended solids (r = 0.778), COD (r = 0.870) and BOD (r = 0.885), and negatively correlated with DO (r = - 0.776). this possibly explains the pollution status of the wastewater being discharged occasionally. Similarly, a negative relationship was observed in DO, COD and BOD at (r = -0.933 and r = -0.942), respectively. Furthermore, the high suspended solids observed in the wastewater samples also showed positive relationship with TDS, salinity, hardness and chloride at r = 0.853, r = 0.848, r = 0.863 and r = 0.848, respectively. These relationships reflect in the moderate relationship with phosphate and nitrate which has the tendencies of enriching connecting surface water and instigating oxygen stress in surface waters.

4. CONCLUSION

The study assessed nutrient levels and key water quality parameters in domestic and industrial wastewater discharges across Shomolu, Surulere, and Ikeja in Lagos State, Nigeria. Results showed domestic and industrial wastewater contribute to nutrient pollution, with high solids, turbidity, COD, and BOD levels. Phosphate and nitrate levels, though within limits, suggest ongoing nutrient enrichment that may cause eutrophication and oxygen stress in surface waters if not managed. The findings emphasize the need for community-level wastewater pretreatment, enforcing discharge regulations, and raising public awareness on sustainable waste practices to reduce nutrient loading and improve urban water quality.

ACKNOWLEDGEMENTS

The author acknowledges the Royal Society of Chemistry Researcher Development and Travel Grant (RSC-RDTG, Grant No: D25-7859075188) for supporting the study's poster presentation at the 11th Annual Symposium of the American Chemical Society, Nigeria Chapter. The Environmental Laboratory, Department of Chemistry, University of Lagos, is also acknowledged for providing laboratory access and resources in the actualization of the work, contributing to the success of the study.

REFERENCES

1. Abayomi, A.; Nimmo, M.; Williams, C.; Olayinka, K.O.; Osuntogun, B.; Alo, B. The Contribution of Roadside Soil to Phosphorus Loading in the Eutrophic Lagos Lagoon, Nigeria. *J. Env. Mon.***2011**, 20, 1-7
2. Nubi, O.A.; Adelopo, A.O. Pollution Load Assessment of Industrial Wastewater in Southwest Nigeria. *Env. Mon. Ass*, **2019**, 191(4), 240–252.
3. Adeyemi, A.; Ibitoye, A. Water Pollution and Public Health Implications in Lagos State, Nigeria. *J. Env. Stu. Pub. H*, **2020**, 14(1), 33–47.
4. Oyebisi, R.O.; Abayomi, A.A.; Oladosu, N.O.; Olayinka, K.O.; Alo, B.I. Assessing the cause of Increasing Iron Concentration in the Eutrophication of Lagos Coastal Water submitted to *J/ Sci. Res. Dev.* **2024**, 23 (1) 63-76
5. Adewumi, J.R.; Olanrewaju, M.A.; Ogedengbe, M.O. Wastewater Generation and Management in Lagos Metropolis. *Nigerian J. Env. Sci*, **2022**. 16(3), 55-65.
6. Oladosu, N.; Abayomi, A.; Olayinka, K.; Alo, B. Reverse flow injection techniques for the determination of nitrogen and phosphorus species in estuarine water of the Lagos Lagoon, Nigeria. *Int. J. Env. Ana. Che*, **2022**, 102 (16), 4862-4881.
7. APHA (American Public Health Association). Standard Methods for the Examination of Water and Wastewater (20th ed.). Washington, D.C.: American Public Health Association, **2017**.
8. Ademoroti, C.M.A. Environmental Chemistry and Toxicology. Ibadan: Foludex Press Ltd, **1996**
9. NESREA (National Environmental Standards and Regulations Enforcement Agency). National Environmental (Sanitation and Wastes Control) Regulations, S.I. No. 28 of 2009.Abuja: NESREA, **2011**.
10. LASEPA (Lagos State Environmental Protection Agency). Effluent Discharge Standards and Compliance Guidelines. Lagos: Ministry of the Environment, **2019**.

ISBN: 978-978-67-0285-8 DOI: https://doi.org/10.55455/acsnigeria.1.3.12-17

Phytochemical Evaluation and Antidiabetic Potential of Two Medicinal Plants *Launaea taraxacifolia* and *Alternanthera brasiliana*

Dasola A. Apata*[1], and Hawawu A. Olorunoje[2]
[1]Department of Applied Chemistry, Federal Polytechnic Ado Ekiti, Ekiti State, Nigeria.
[2]Department of Science Laboratory Technology, Federal Polytechnic Ado Ekiti, Ekiti State, Nigeria.
Corresponding Author's email: apata_da@fedpolyado.edu.mg
DOI: https://doi.org/10.55455/acsnigeria.1.3.12-17

ABSTRACT

The high rate of mortality has been attributed to the presence of disease such as diabetic and this has called for all possible interventions especially from botanical sources. The use of plant to treat and manage diabetic has continue to yield positive outcome among global population and this has given room for more exploration among researchers of medicinal plants. In this present work, phytochemical analysis and antidiabetic activity of methanol extract of *Launaea taraxacifolia*and *Alternanthera brasilia*were investigated. Methanol was used for the extraction of leaves of *Launaea taraxacifolia* and *Alternanthera brasilia* and phytochemicals were quantitatively determined. Antidiabetic activities of the plants extract were determined via *in vitro* alpha- amylase and alpha – glucosidase assay. The phytochemical analysis showed the present of alkaloids, terpenoids, flavonoids, phenols and tannis in the two plants. Quantitatively, *Launaea taraxacifolia* and *Alternanthera brasiliana* have total phenol of 203.50 ± 0.10 mgGAE/g and 127. 65 ± 0.12 mgGAE/g respectively. The two plant extracts were used at varying concentration and they displayed antidiabetic potential by inhibiting the two enzymes *in vitro.* The two plant extracts examined were observed to be concentration dependent., at 7.5 mg/mL, *Alternanthera brasiliana* and *Launaea taraxacifolia* gave 79.45% and 70.76 % inhibitory activities respectively while a lower concentration (1 mg/mL), a low inhibitory activity were observed in the two plant extracts. The presence of the phenols, alkaloids and flavonoids suggest the therapeutic potential of *Alternanthera brasiliana* and *Launaea taraxacifolia.* Also, the inhibitory actions of the plant extracts against the enzymes responsible for diabetic clearly suggest their antidiabetic potential.

KEYWORDS: Diabetic, phytochemical, *Launaea taraxacifolia,* alpha-amylase.

1. INTRODUCTION

Modern medicine has dwells more into botanicals thereby unfolding the therapeutic potential of plants. The ethnomedicinal study of plants as a potential source of therapeutic agent has become popular among researchers. The use of plants for the cure management of diseases has come to stay among the global populace, for it is found to be cheap, accessible and effective [1]. Diabetes mellitus (DM) is simply the inefficient use of insulin to effectively metabolize blood sugar thereby resulting into hyperglycemia. It is a chronic disease that impaired the normal functionality of the body system and also leads to formation of other ailments such as high blood pressure, stroke and so on. (DM) is the most widespread form of diseases across all continents which is majorly diagnosed in the elderly and it is becoming increasingly common in children and adolescents [3,4,5]. There are two main types of DM: Type 1 due to insulin insufficiency and Type 2 non-insulin dependent which account for 90-95% of diabetic patients [6,7,8, 9]. Nigeria is one of the African countries that its populace have been faced with. Among such plants are *Alternantherabrasiliana*, and *Launaeataraxacifolia*. *Alternanthera brasiliana*(*A. brasiliana*) is commonly referred to as JoyWeed or Brazilian joyweed, a species of the Amaranthaceae family. The presence of phenolic compounds in *A. brasiliana* contribute to its antimicrobial action by damaging microbial cell walls and inhibiting enzyme activity [10, 11]. The acute and sub-acute toxicity of*A. brasiliana* have been conducted by Bilal *et al*., 2025[12]and revealed no adverse effects on heart, kidney or liver tissues at doses up to 3000 mg/kg; LD_{50}.The Extracts of *A.brasiliana* have been found to exhibit significant antimicrobial effects against various strains of bacteria and fungi, including *Staphylococcus aureus*, *Escherichia coli*, and *Candida albicans*[13] and also against; *Mycobacterium smegmatis* and herpes simplex virus (HSV) [14], *Launaeataraxacifolia* (*L. taraxacifolia*) commonly known as wild lettuce that is underutilized leafy vegetable and is indigenous to West Africa, but it is scarcely consumed for both nutritional and medicinal purposes. In Nigeria, it is locally known as *efoyanrin* (Yoruba), *namijindayi* (Hausa), and *agblòke* (Ghana). Wild lettuce belongs to the *Asteraceae* family and is recognized for its rich phytochemical profile, which includes flavonoids, saponins, tannins, alkaloids, terpenoids, and phenolic compounds [15,16].The plant also enhance the regulation of insulin and thus inhibit the carbohydrate digesting enzymes which suggest *L. taraxacifolia* as a potential antidiabetic [17]. *Launaeataraxacifolia* has long been valued in African traditional medicine for its wide range of therapeutic applications. In Nigeria and Ghana, decoctions and leaf extracts are commonly employed in the treatment of diabetes, malaria, hypertension, measles, and eye

infections such as conjunctivitis [18,19]. The leaves are also applied topically for wound healing, skin infections, and yaws, reflecting the plant's antimicrobial and anti-inflammatory potential [20]. The leaves of *L. taraxacifolia* were also reported to contain phenols [21], glycosides[22]and flavonoids [23] which make it a good potential antioxidant, immune enhancer, cardiac treatment and anti-inflammatory agent. *L. taraxacifolia* is the only Asteraceae species which has no trichomes [24]. It is also consumed as a salad ingredient or cooked in stew [25]. *L. taraxacifolia* contains useful amounts of bioactive chemicals and minerals. It has been shown to possess antioxidant [26], anti-inflammatory [27], antimicrobial[28], anticancer [29], neuro-nephroprotective [30], and cardio protective properties [31].

2. MATERIALS AND METHODS

2.1 Plant collection

The leaves of *A. brasiliana*and*L.taraxacifolia* were collected on Federal Polytechnic Ado Ekiti Campus, Ekiti State Nigeria. The plant material was identified and authenticated by Mr Oyebode of Botany unit of Applied biology department,Federal Polytechnic Ado Ekiti, Ekiti State, Nigeria, and voucher specimens (FPA 730 and FPA 731 respectively) were deposited at the school Herbarium.

2.2 Plant Preparation and Extraction

The collected plant sample was cleaned of the dust and soil. It was air dried at room temperature (25^{o}C) for six-weeks until constant weight was obtained. The dried sample was pulverized and stored in an air tight container prior to extraction. A 250 g of pulverized sample was soaked with 2.5 liter methanol for 72 hours. The extract was concentrated under a reduced pressure to a small volume by means of rotary evaporator.

2.3 Quantitative Phytochemical Screening of *A. brasiliana* and *L.taraxacifolia* leaves

The determination of phytochemicals in the extracts of the plants were conducted with methods used by Shaik and Patil, 2020 [32]. Four different phytochemicals; alkaloids, flavonoids, terpenoids and phenols.

2.4 In vitro Antidiabetic Assay

The antidiabetes potentials of the two plants at varying concentration (1, 2.5, 5, 7.5 and 10 mg/ mL)were carried out *in vitro* against alpha-amylase and alpha glucosidase inhibitory assay. The analysis was carried out in duplicate.

2.5 Alpha Amylase Activity

The assay was evaluated using a modified procedure of McCue *et al*[33]. A 100 µL of the plant extracts and 100 µL of 0.02 M phosphate bufferpH6.9 with 0.006 M sodium chloride) containing α-amylase from Aspergillus oryzae (0.5 mg/mL) were added to each tube and incubated at 40 °C for 10 min. After pre-incubation, 100 µL of 1% starch solution in 0.02 M sodium phosphate buffer (pH 6.9 with 0.006 M sodium chloride) was added to each tube. The reaction was halt with 200 µL of dinitrosalicylic acid. The test tubes were incubated in a water bath for 5 min, and cooled at room temperature. The alpha amylase inhibitory activity was determined.

2.6 Alpha glucosidase Inhibition Assay

The inhibitory activity of the plant extracts on alpha-glucosidase was evaluated according to the method described by McCue *et al* [33]. Alpha-glucosidase was derived from *Saccharomyces cerevisiae*. A 100 µL of α-glucosidase was dissolved in 100 µL of phosphate buffer pH6.8 which was pre-incubated with 50 µL of the sample for 10 min. Then 50 µL of 20 µL phosphate buffer (pH 6.9) was then added to start the reaction. The reaction mixture was incubated at 37°C for 20 min and stopped by adding 2 µL of 0.1 M Na2CO3. The glucosidase activity was determined by measuring the yellow-colored paranitrophenol released from pNPG at 405 nm.

2.7 Statistical Analysis

The data obtained from the study were analyzed using Analysis of variance (ANOVA) using R(3.5.1) with Turkey HSD post – hoc. A p-value of less than 0.05 was considered a statistically significant value were expressed as mean ± SEM of experimental replication.

3. RESULTS AND DISCUSSION

3.1 Phytochemical Analysis

The presence of secondary metabolites in plant contributes immensely to their bioactivities properties.. Phytochemicals such as flavonoids, alkaloids and phenols to mention but few have been known to be responsible for the therapeutic nature of botanicals [34,35]. The selected plants were evaluated quantitatively of Phytochemicals; flavonoids, terpenoids, phenols and alkaloids. *L. taraxacifolia* happened to have a higher concentration of all the phytochemicals analyzed than *A. brasiliana*. which was a bit high in except alkaloid The results as presented in table 1 show that *L. taraxacifolia* possess a higher concentration of phenol (203.50 ± 0.10) and lower concentration of alkaloid (8.45 ± 0.19) as compared to *A. brasiliana*(10.50± 0.15). The presence of phenol, alkaloid, terpenoid and flavonoid in the extracts signify antioxidant and anti- inflammatory potential as was also reported by Barua *et al* [36]. Various investigations have also shown that aqueous fraction of these plants exhibit pharmacological properties like antidiabetic, anticancer and anticonvulsant properties [37,38].

Table 1: Phytochemical analysis of *A. brasiliana* and *L. taraxacifolia* leaves extract

Phytochemicals	*L. taraxacifolia*	*A. brasiliana*
Phenol	203.50 ± 0.10	127. 65 ± 0.12
Flavonoid	19.65 ± 0.17	11.54 ± 0.15
Terpenoid	29.29 ± 0.11	5.40 ± 0.10
Alkaloid	8.45 ± 0.19	10.50± 0.15

3.2 Antidiabetic activity

Diabetes is one of diseases that have been known to contribute to the high rate of mortality in the human populace especially in Africa continent including Nigeria. So the search for therapeutic agent from botanical origin which are believed to be less toxic, readily available and affordable is inevitable [39]. Although some of the synthetic drugs have made huge successes in regulating blood sugar level, but their side effects are unaffordable and this table is a major concern in the middle and low income countries [40]. And Nigeria is one of the Africa countries that are richly endowed with medicinal plant. In this investigation, we explore the antidiabetic activities of *A. brasiliana* and *L. taraxacifolia* leaves extract *in vitro* through alpha amylase and alpha glucosidase inhibitory assay.Alpha amylase enzyme controls the breakdown of carbohydrate and disaccharides into simple sugar (glucose) there by making monosaccharides available in the body including blood stream.Therefore, alpha amylase inhibitory activity is one of the major routes to evaluate the hyperglycemia lowering efficacy of plant extracts. More so, alpha amylase enzyme inhibitor helps to manage type 2 diabetes and reduce blood glucose level of diabetic patients [41,42]. The methanol extract of *A. brasiliana* and *L. taraxacifolia demonstrated* increasing percentage inhibition as the tested concentration increased. As presented in table 2, the inhibitory effect of *A. brasiliana* at initial concentration (1 mg/mL) gave 47.06± 0.17% , higher than 29.09 ± 0.00% that was observed with *L. taraxacifolia,* but at subsequent concentrations, a remarkable inhibitory effect were observed for *L. taraxacifolia* higher than that observed for*A. brasiliana.*This results obtained are in line with the study performed by Ayele *et al* [43].

Table 2: Alpha amylase inhibitory activity of *A. brasiliana* and *L. taraxacifolia* leaves extract

Concentration	*L. taraxacifolia*	*A. brasiliana*

of Extract (mg/mL)		
1	29.09 ± 0.00	47.06± 0.17
2.5	41.23 ± 0.11	42.24 ± 0.15
5	49.43 ± 0.14	44.56 ± 0.16
7.5	54.42 ± 0.19	46.40± 0.12
10	60.90± 0.13	54.78± 0.13

Alpha glucosidase is the enzyme responsible for transferring broken starch and carbohydrate to the blood stream thereby increasing the blood sugar level and consequently causing diabetes. Table 3 showed the outcome of alpha glucosidase inhibitory effect of *A. brasiliana* and *L. taraxacifolia* leaves extract. At a higher dose of 10 mg/mL, both *A. brasiliana* and *L. taraxacifolia* gave 91.17± 0.19 and 96.81± 0.19 respectively. But at 5 and 7.5 mg/mL, a remarkable percentage inhibition of 67.43 ± 0.10% and 79.45± 0.15% respectively were observed higher than that obtained for *L. taraxacifolia* (59.18 ± 0.11% and 70.76 ± 0.19%).A similar results were also obtained by Ayele *et al* [44], Vallinayaki and Rajeshkumar [45] where *Mimosa Peduca*and *Scutellariatourneforti*i methanol extract gave comparable percentage inhibition and also comparable the work of Sapkota *et al* [46].The overall assessment depict *L. taraxacifolia having* a higher antidiabetic potential than *A. brasiliana which* may be attributed to the presence of phytochemicals analyzed.

Table 3: Alpha glucosidase inhibitory activity of *A. brasiliana* and *L. taraxacifolia* leaves extract

Concentration of Extract (mg/mL)	*L. taraxacifolia* % inhibition	*A. Brasiliana* % inhibition
1	24.75 ± 0.10	16. 06 ± 0.12
2.5	43.56 ± 0.17	29.54 ± 0.15
5	59.18 ± 0.11	67.43 ± 0.10
7.5	70.76 ± 0.19	79.45± 0.15
10	96.81± 0.19	91.17± 0.19

4. CONCLUSION

Based on our investigations, the methanol extract of *A. brasiliana* and *L. taraxacifolia* demonstrated in vitro alpha amylase and alpha glucosidase inhibitory activities, suggesting potential antidiabetic relevance. However, further phytochemical characterization, IC_{50} determination, *in vivo* validation and toxicity studies are needed before therapeutic claims can be made.

REFERENCES

1. Atanasov, A. G., Zotchev, S. B., Dirsch, V. M., &Supuran, C. T. (2021). *Natural products in drug discovery: Advances and opportunities in the modern era*. Nature Reviews Drug Discovery, 20(3), 200–216. https://doi.org/10.1038/s41573-020-00114-z
2. Weir GC, Gaglia J, Bonner-Weir S. Inadequate β-cell mass is essential for the pathogenesis of type 2 diabetes. Lancet Diabetes Endocrinol. 2020;8(3):249-256.
3. Shuey MM, Lee KM, Keaton J, et al. A genetically supported drug repurposing pipeline for diabetes treatment using electronic health records. EBioMedicine. 2023;94(8):122-131.
4. Wang X, Long D, Hu X, Guo N. Gentiopicroside modulates glucose homeostasis in high-fat-diet and streptozotocin-induced type 2 diabetic mice. Front Pharmacol. 2023;14(8):1172360.

5. Mehta, S.; Sharma, A.K.; Singh, R.K(2021): Therapeutic journey of *Andrographispaniculata (Burm.f.) Nees* from natural to synthetic and nanoformulations. *Mini-Rev. Med. Chem*. 21, 1556–1577
6. Vaughan P, Gilson L, Mills A. Diabetes in developing countries: its importance for public health. Health Pol Plan. 1989;4 (2):97–109.
7. Welz AN, Emberger-Klein A, Menrad K. Why people use herbal medicine: insights from a focus-group study in Germany. BMC Complement Altern Med. 2018;18(1):1–9.
8. Joseph B, Jini D. Antidiabetic effects of Momordicacharantia (bitter melon) and its medicinal potency. Asian Pacific J Trop Dis. 2013;3(2):93– 102. https:// doi. org/ 10. 1016/ S2222-1808(13) 60052-3.
9. World Health Organization. (2022). *Medicinal plants and traditional medicine in health systems*. Geneva: WHO Press.
10. Ahmed, F., Adebayo, A. H., &Abdullahi, M. (2021). *Pharmacological and therapeutic properties of Alternantherabrasiliana: An overview*. African Journal of Traditional, Complementary and Alternative Medicines, 18(1), 43–52.
11. Ogunmefun, O. T., Ajayi, O. I., & Adebayo, O. R. (2021). *Antioxidant and antimicrobial activities of tannin-rich extracts from medicinal plants*. African Journal of Pharmaceutical Research & Development, 13(2), 72–80.
12. Bilal, M., Hassan, M., & Khan, M. A. (2025). *Nephroprotective and diuretic effects of Alternantherabrasiliana leaf extract in experimental models*. BMC Complementary Medicine and Therapies, 25(2), 45–59.
13. Nwinyi, O. C., Ajiboye, T. O., & Ibrahim, M. (2020). *Antimicrobial activity of Alternantherabrasiliana extracts against selected pathogens*. African Journal of Microbiology Research, 14(6), 252–260.
14. Silva, R. L., Acuña, U. M., & Lima, A. C. (2024). *Pharmacological review of Alternantherabrasiliana (Joy weed): Ethnomedicinal uses and bioactivities*. Frontiers in Pharmacology, 15, 147293.
15. Olugbami, J. O., Ajani, E. O., &Adeoye, A. O. (2022). *In vitro antidiabetic activities of Alternantherabrasiliana extracts through alpha-amylase and alpha-glucosidase inhibition*. International Journal of Pharmacognosy and Phytochemical Research, 14(1), 23–29.
16. Iyabo AM, Hauwa A. Uterotonic effect of aqueous extract of LaunaetaraxacifoliaWilld on rat isolated uterine horns. Afr J Biotechnol. 2019;18(19):399–407.
17. Adinortey MB, Sarfo JK, Kwarteng J, Adinortey CA, Ekloh W, Kuatsienu LE, et al. The Ethnopharmacological and nutraceutical relevance of Launaeataraxacifolia (Willd.) Amin ex C. Jeffrey Evid Based Complement Alter Med. 2018;2018(01):1–13.
18. Adedayo BC, Oyeleye SI, Oboh G. Inhibition of some enzymes implicated in diabetes mellitus by raw and blanched extracts of African lettuce (Launaeataraxacifolia). Biokemistry. 2020;32(1):69–76.
19. Adebisi AA. LaunaeaTaraxacifolia (Willd) Amin ex C Jeffrey. Record from Protabase. Diera: PROTA (Plant Resources of Tropical Africa); 2004.
20. B.C. Anyanwu, I.E. Otuokere, J.O. Echeme, *et al.* Isolation and characterization of a secondary metabolite from the aerial parts of launaea (Lactuca) taraxacifolia J ChemSoc Niger, 46 (4) (2021), pp. 661-672.
21. Kuyoro S, Akinloye O, Ololade Z, Kayode O, Badejo O. Anti-diabetic properties of crude Methanolic leaf extract of Launaeataraxacifolia (wild lettuce). Niger J BiochemMol Biol. 2017;32(1):67–77.
22. Andrade-cetto A, Vasquez CR. Gluconeogenesis inhibition and phytochemical composition of two Cecropia species. J Ethnopharmacol 2010;130(1):93–7.
23. . Adedeji O, Jewoola O. Importance of leaf epidermal characters in the Asteraceae Family. Not Bot HortiAgrobot Cluj-Napoca. 2008;36(2):7–16.
24. Burkill HM. The Usefulness of Plants of West Africa. Edition 2, vol. 2(1). Kew, ISBN 10094764301X: R Bot GardIthakaHarb Incorporation; 1985. p. 1–2.
25. Koukoui O, Senou M, Agbangnan P, Seton S, Koumayo F, Azonbakin S, et al. Effective in-vivo cholesterol and triglycerides lowering activities of Hydroethanolic extract of LaunaeaTaraxacifolia leaves. Int J Pharm Sci Res. 2017;8(5):2040–7.
26. Ololade ZS, Kuyoro S, Ogunmola O, Abiona O. Phytochemical, antioxidant, anti-arthritic, anti-inflammatory and bactericidal potentials of the leaf extract of Lactucataraxacifolia. Glob J Med Res B Pharma Drug DiscovToxicol Med. 2017;17(2):19–28.

27. Thomford NE, Mkhize B, Dzobo K, Mpye K, Rowe A, Parker MI, et al. African lettuce (Launaeataraxacifolia) displays possible anticancer effects and herb-drug interaction potential by CYP1A2, CYP2C9, and CYP2C19 inhibition. Omi A J Integr Biol. 2016;20(9):528–37.
28. Akintunde JK, Woleola MT. Impairment of neuro-renal cells on exposure to cosmopolitan polluted river water followed by differential protection of Launeataraxacifolia in male rats. CompClin Path. 2019;01(01):1–15.
29. Salisu T, Ottu B, Okpuzor J. Histopathologic studies of aqueous extracts of five selected local edible vegetables in isoproterenol-induced myocardial infarction in male Wistar albino rats. Planta Med. 2014;80(01):2–39.
30. Thomford NE, Awortwe C, Dzobo K, Adu F, Chopera D, Wonkam A, et al. Inhibition of CYP2B6 by medicinal plant extracts: implication for use of efavirenz and nevirapine based highly active antiretroviral therapy (HAART) in resource-limited settings. Molecules. 2016;21(221):1–15.
31. Shaikh JR and Patil M. Qualitative tests for preliminary phytochemical screening: An overview. Int J Chem Stud. 2020; 8(2):603–608.
32. McCue P, Kwon YI, Shetty K. Anti-amylase, anti-glucosidase and anti-angiotensin i-converting enzyme potential of selected foods. J Food Biochem. 2005;29(3):278-294.
33. Abebe W, Zhang W, Zhang S, Xie G. Chemical composition and antimicrobial activity of essential oil from Justiciaschimperiana. J Pharmacogn Natural Prod. 2018;04(02):2–4.
34. Lawal AM, Lawan MM, Apampa SA. Phytochemical analysis and thin layer chromatography profiling of crude extracts from GuieraSenegalensis (Leaves). J Biotechnol Biomed Sci. 2019;3(3):7–12.
35. Barua CC, Begum SA, Pathak DC, Bora RS. Wound healing activity of AlternantherabrasilianaKuntze and its antioxidant profiles in experimentally induced diabetic rats. J Appl Pharm Sci. 2013; 3(10):161-166.
36. Melesie Taye G, Bule M, Alemayehu Gadisa D, Teka F, Abula T.In vivo antidiabetic activity evaluation of aqueous and 80% methanolic extracts of. leaves of Thymus schimperi (Lamiaceae) in alloxan-induced diabetic mice. Diabetes Metab Syndr Obes: Targets Ther. 2020;13(11):3205-3212.
37. Cui G, Lai F, Wang X, Chen X, Xu B. Design, synthesis and biological evaluation of indole-2-carboxylic acid derivatives as IDO1/TDO dual inhibitors. Eur J Med Chem. 2020;188(2):111985
38. Crudele L, Gadaleta RM, Cariello M, Moschetta A. Gut micro- biota in the pathogenesis and therapeutic approaches of diabetes. EBioMedicine. 2023;97:1-13.
39. Fasanmade OA, Dagogo-Jack S. Diabetes care in Nigeria. Ann Glob Health. 2018;81(6):821-829.
40. Padhi S, Nayak AK, Behera A. Type II diabetes mellitus: a review on recent drug based therapeutics. Biomed Pharmacother. 2020; 131(11):110708.
41. Ezedum N. Protection of traditional knowledge and its relevance to national economic growth and development in Nigeria. Nigerian Juridical Rev. 2022;17(7):88-108
42. Safamansouri H, Nikan M, Amin G, et al. α-Amylase inhibitory activity of some traditionally used medicinal species of labiatae. J Diabetes Metab Disord. 2014;13(11):1-5
43. Faloye KO, Famuyiwa SO, Ayoola MD, Ndinteh DT. Isolation and characterization of two new polyphenols from the antidiabetic fraction of pod extract of Caesalpiniapulcherrima Swartz. Eur J Med Plants. 2020;31(20):48-56.
44. Ayele AG, Kumar P, Engidawork E. Antihyperglycemic and hypoglycemic activities of the aqueous leaf extract of RubusErlangeriengl (Rosacea) in mice. Metabolism Open. 2021;11(11):100118.
45. Vallinayaki KN, RajeshkumarShanmugam: Evaluation of Antidiabetic Activity and Cytotoxic Effect of Strontium Nanoparticles Synthesized Using Mimosa Pudica. College and Hospital, Saveetha Institute of Medical and Technical Sciences, Saveetha University, Chennai, Tamil Nadu, India.
46. Sapkota BK, Khadayat K, Sharma K, Raut BK, Aryal D, Thapa BB, et al. Phytochemical analysis and antioxidant and antidiabetic activities of extracts from Bergeniaciliata, Mimosa pudica, and Phyllanthusemblica. Advances in Pharmacological and Pharmaceutical Sciences 2022;2022.

ISBN: 978-978-67-0285-8 DOI: https://doi.org/10.55455/acsnigeria.1.3.18-21

Effect of Temperature on the Adsorption of *Lonchocarpus cyanescens* Dye Extract on TiO_2 Semiconductor

John Moriamo O.[a,b] , Ogunbayo Taofeek B.[b], Olopade Mutteu A.[c], Isanbor Chukwuemeka [b], Babatunde Alice. I.[b], Alayande Samson O.[d], Msagati Titus A. M.[e]

[a]Department of Chemistry, Sikiru Adetona College of Education, Science and Technology, Omu-Ajose, Ogun state

[b]Department of Chemistry, University of Lagos, Lagos

[c]Department of Physics, University of Lagos, Lagos

[d]Department of Industrial Chemistry, Abiola Ajimobi Technical University, Ibadan, Oyo

[e]Institute of Nanotechnology and Water Sustainability (NanoWS), College of Science, Engineering and Technology, University of South Africa, Florida Park, South Africa

Corresponding Author's email: tbentos22@gmail.com

DOI: https://doi.org/10.55455/acsnigeria.1.3.18-21

ABSTRACT

The dye-sensitized solar cell (DSSC) has huge benefits with respect to competing technologies, but challenges remain in attaining a high power conversion efficiency and stability in the long term. In this study, we made an effort to optimize the DSSC by investigating the effect of dye- sensitizer temperature on the amount of dye adsorbed on the TiO_2 semiconductor during the fabrication process using different concentrations of a natural dye extracted from the leaves of *Lonchocarpus cyanescens*. The studied temperatures are 30 °C, 35 °C, 40 °C and 45 °C with concentrations 1.67g/L, 3.33 g/L, 5.00g/L, 6.67 g/L, 8.33 g/L and 10.00g/L. The results revealed that the percentage adsorption of dye increased from 30 °C to 35 °C to 40 °C and then decreased at 45 °C for all dye concentrations. This suggests that the optimal temperature for the adsorption of *Lonchocarpus cyanescens* dye extract on TiO_2 semiconductor is 40 °C, and adsorption is both physisorption and chemisorption. The information obtained in this study will aid in gaining access to clean and affordable energy, a key factor in the development of any nation.

KEYWORDS: *Lonchocarpus cyanescens*, semiconductor, optimize, DSSC, adsorption.

1. INTRODUCTION

The generation of electricity using solar cells is becoming more popular and it is high time the dye-sensitized solar cell (DSSC), became more functional as a viable alternative to the silicon solar cells. A major factor in determining the quality of a dye-sensitized solar cell is the adsorption process.The semiconductor surface adsorbs dye and gets sensitized to absorb visible light so as to initiate the flow of electrons which eventually get injected into the conduction band to generate electricity.The dye molecules are deposited by soaking the mesoporous semiconductor layer in a solution containing the dye.

The adsorption technology has been widely utilized due to its high efficiency, simple procedural process and cost effectiveness.[1] It is the transfer of organic substances from a liquid phase onto the surface of a solid phase. It can be either physical, caused by Van der Waals force or chemical, caused by chemical bonds such as covalent bond or ionic interaction. The efficiency of adsorption of dyes on the TiO_2 semiconductor material is important and carried out because the performance of DSSCs is known to be closely related to the equilibrium amount of adsorbed dye on TiO_2.[2] It is at the root of the four major processes (light absorption, electron injection, dye regeneration and charge transport) of the DSSC operation.

The interaction between TiO_2 nanoparticle and functional groups of the dye would then drive the electron transfer from the dye molecules to the conduction band of the semiconductor TiO_2.[3] This is very important in enhancing the photoelectric conversion efficiency of the DSSC. Although the operating principle of the DSSC is well understood, it is a complicated system involving four major parts and several working processes and so enhancing their performance is not an easy task since it is mutually influenced by many factors. Several variables, such as the solvent polarity, pH of sensitizer solution, thickness of film, annealing or sintering temperature of films, temperature of the dye solution, dye sensitisation time, co-sensitisation etc. may act independently or dependently to affect the efficiency of the DSSC and so can be carefully determined and/or manipulated to enhance its performance, by

selecting the optimum values of parameters during the fabrication process to favor the performance of DSSCs.
Hence, there is a need to understand the effect of these factors/working parameters on the efficiency of DSSCs and various methods have been developed for exploring the knowledge of how to improve the performance of DSSCs.[4] For a breakthrough on the performance of DSSC and to preserve its durability, scientists and engineers need to optimize every material within the DSSC. The hope is very high that in the near future the DSSC is going to compete successfully with the silicon cells in terms of efficiency and its commercialisation will be realised within a few years with more efforts devoted to it.[5]

2. MATERIALS AND METHODS

Titanium (iv) oxide TiO_2, titanium (iv) chloride $TiCl_4$, ethanol (Sigma Aldrich), glass substrates, crude extract of *Lonchocarpus cyanescens* and analytical balance.
The synthesis of titanium (iv) oxide and the preparation of plant materials are as stated in our previous study.[6] TiO_2 colloidal paste was prepared by mixing TiO_2 nanoparticles with aqueous solution of $TiCl_4$ to achieve optimal crack-free mesoporous films and good adhesion to glass substrate. This involves dispersing the TiO_2 powder in the aqueous solution and then crushing and grinding with a mortar and pestle for about 1 hour until a uniform suspension is obtained. Different concentration of leaves extract of *Lonchocarpus cyanescens*, 1.67 g/L, 3.33 g/L, 5.00 g/L, 6.67 g/L, 8.33 g/L and 10.00g/L were prepared in ethanol solution. Films of TiO_2 on the glass plate spread by doctor blading method, [7] were soaked in the dye solutions for 16 hours 20 minutes in a small beaker. The experiment was carried out at four different temperatures, 45 °C, 40 °C, 35 °C and 30 °C and the mass of the adsorbed dye was determined gravimetrically using the analytical balance.

3. RESULTS AND DISCUSSION

The evaluation of the effect of temperature on the adsorption of dye in the DSSC is critical in its optimization. The Figure below shows the variation of the adsorption of Lonchocarpus cyanescens using different concentrations on the TiO_2 at different temperatures.

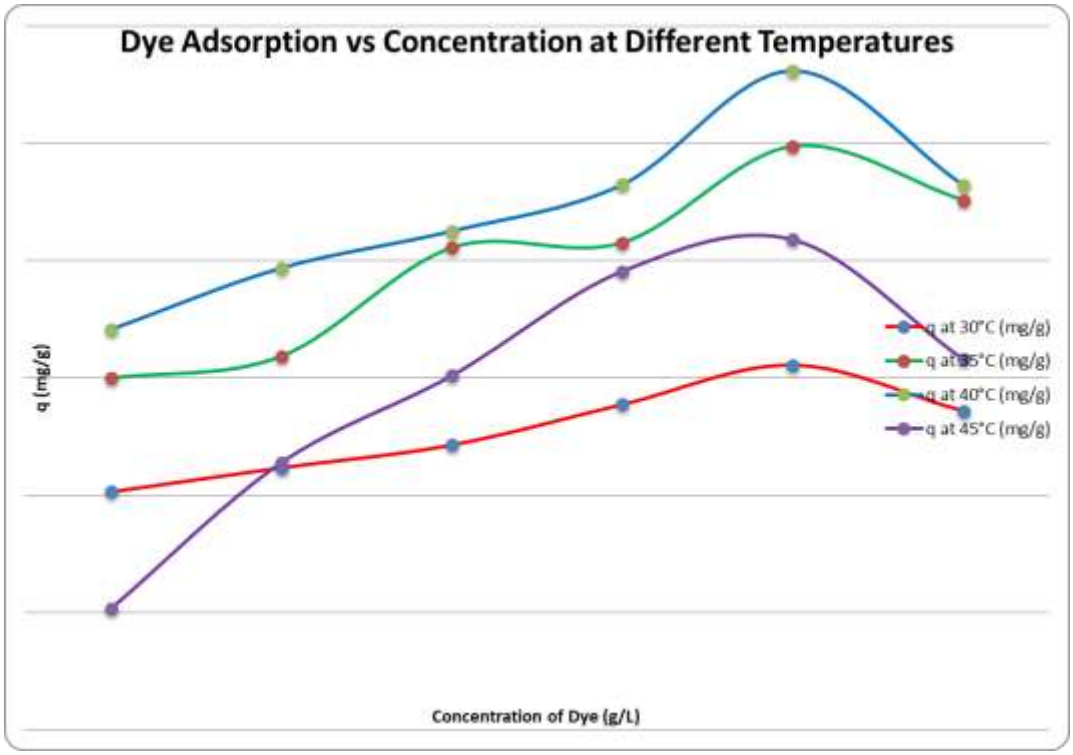

Figure 1: Graph of the amount of adsorbed dye (q) versus concentration at different temperatures

The effect of temperature was studied at 30 °C, 35 °C, 40° C and 45 °C. As displayed on the graph above, result shows that the adsorption of dye was found to increase from 30 °C to 35 °C to 40 °C and then decreased at 45 °C (Figure 1), This was observed at all concentrations, suggesting that adsorption is both physisorption and chemisorption. This has been reported by Hirose et al.[8] The result also shows that adsorption of LC is not favoured at high temperature as it was found to decrease at the highest studied temperature (45 °C). Similar study by Rahman et al. showed the effect of dye temperature on the efficiency of cells at temperature of 30 °C, 50 °C, 60 °C, 70 °C and 80 °C.[9] The result from their study, reveals that optimum dye loading and efficiency were obtained at 50 °C.

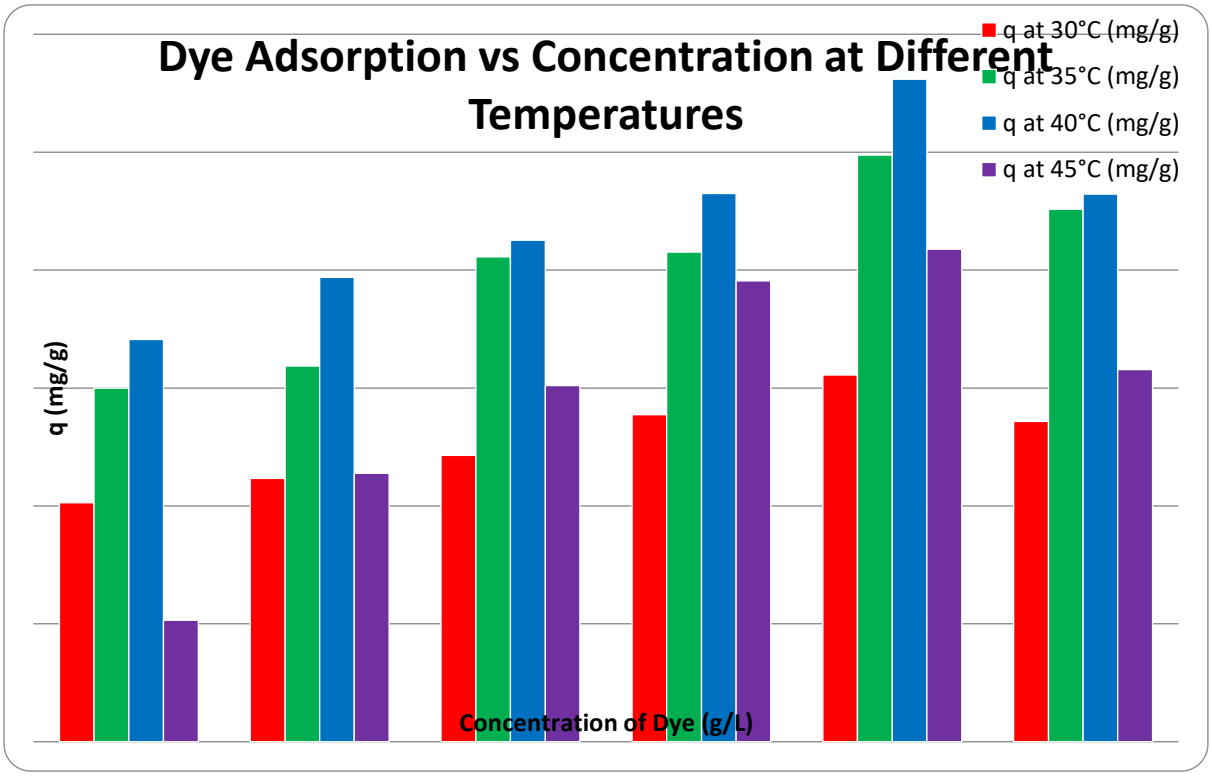

Figure 2: Bar chat displayof the amount of adsorbed dye (q) versus concentration at different temperatures

Adsorption of LC is generally observed to increase with increasing concentration as shown in Figure 2. However, there appear to be a critical adsorption at the fifth concentration (8.33 g/L), at this concentration, adsorption of crude extract of *Lonchocarpus cyanescens* was found to be the highest at all studied temperatures. A decrease in the amount of dye adsorbed was observed at the highest studied concentration in this work after the critical concentration for all temperatures. The reason for this is that the surface of TiO_2 may no longer adsorb after a particular concentration, and dye may have a maximum adsorption concentration. This result is in agreement with the study on effect of concentration of chlorophyll extract from binahong leaves, *Anredera cordifolia* on TiO_2 as adsorbents.[10]

Their result, showed an increase in efficiency as concentration increases until it got to a threshold concentration after which it decreased. Also, Chang et al. in their study demonstrated that dye layer increases with increasing dye adsorption time;[11] however, beyond an optimum concentration, the dye layer obstructs the charge transfer from the conduction band of the TiO_2 surface to the electrolyte.[12] In this study, the optimal adsorption temperature for crude *Lonchocarpus cyanescens* on the TiO_2 semiconductor is at 40 °C and a dye uptake of 112.360mg/g was possible and adsorption is both physisorption and chemisorption as a decrease was observed at a higher temperature. Both physical and chemical adsorption may occur on a surface at the same time. A layer of molecules may be physically adsorbed on top of an underlying chemisorbed layer and on the same surface can display physiosortion at one temperature and chemisorption at a higher temperature.[13] The basic knowledge of

adsorption equilibrium and kinetics is a fundamental to design an adsorption system, [14] of which the DSSC is one.

4. CONCLUSION

It is important to obtain the maximum amount of dye adsorbed by the TiO_2 semiconductor during the fabrication process of the dye sensitized solar cell as the efficiency of the cell most of the time is directly dependent on it. This study revealed that there is a particular temperature to attain the highest dye uptake for every dye that will be used as a sensitizer in the DSSC. There is therefore the need to carefully optimize all varying parameters of the DSSC especially the temperature of the sensitizer solution.

REFERENCES

1. Siyal, A.; Shamsuddin, M. R.; Khan, M.; Rabat, N. E.; Zulfiqar, M.; Man, Z.; Siame, J.; Azizli, K. A. A. Review on geopolymers as emerging materials for the adsorption of heavy metals and dyes. *J. Environ. Manag,* **2018,** 224, 327-339.
2. Perez, C.; Kador, L.; Peng, B.; Thelakat, M. Characterization of the Adsorption of Rubpy Dyes on Mesoporous TiO_2 Films with UV-Vis, Raman, and FTIR Spectroscopies. *J. Phys. Chem. B*, **2006**, 110, 8723-8730.
3. Narayan, M. N. Review: Dye sensitized Solar Cells based on Natural photosensitizers. *Renew. Sustain. Energy Rev.,* **2012,** 16:208-215.
4. Arifin, Z.; Soeparman, S.; Widhiyanuriyawan, D.; Agus, P. A.; Dharmanto, D. Synthesis, characterization, and fabrication of hollow fibers of Zn-doped TiO_2 for dye sensitized solar cells. *J.Eng. Sci. and Technol.*, **2017,** 12(5), 1227-1239.
5. Lee, C.; Li, C.; Ho, K. Use of organic materials in dye-sensitized solar cells. *Mater. Today*, **2017**, 20(5), 267-283.
6. John, M. O.; Ogunbayo, T. B.; Ikechukwu, P. E.; Chukwuemeka, I.; Olopade, M. A.; Babatunde, A. I.; Olaleru, S. A.; Olugbuyiro, J. A. O.; Alayande, S. O.; Msagati, T. A. M. Enhanced photoelectrochemical activity of green-capped TiO_2 photoelectrodes for DSSC application. *ChemistrySelect*, **2025,** 10, e02349, 1-8.
7. Onah, E. O.; Offiah, S. U.; Chime, U. K.; Whyte, G. M.; Raphael. M.; Obodo, R. M.; Ekechukwu, O. V.; Ahmad, I.; Ugwuoke, P. E.; Ezema, F. I. Comparative photo-response performances of dye sensitized solar cells using dyes from selected plants. *Surf. and Interfaces,* **2020**, 20(100619), 1-12.
8. Hirose, F.; Shikaku, M.; Kimura, Y.; Niwano, M. IR Study on N719 Dye Adsorption with High Temperature Dye Solution for Highly Efficient Dye-Sensitized Solar Cells. *J. Electrochem. Soc.*, **2010,** 157, B1578-B1581.
9. Rahman, M. Y.; Rozab, L.; Samsuric, S. A.; Umar, A. A. Effect of N719 Dye Dipping Temperature on the Performance of Dye-Sensitized Solar Cell. *Russ. J. Electrochem*, **2017,** 54(10), 863-868.
10. Muryani, B. Y.; Sarifah, N.; Kusumawardani, D. R.; Nurosyid, F. Effect Concentration of dye solution Binahong Leaves to the Efficiency of Dye-Sensitized Solar Cell (DSSC). *AIP Conf. Proc.*, **2019**, 1-5.
11. Chang, W.; Lee, C.; Yu, W.; Lin, C. Optimization of dye adsorption time and film thickness for efficient ZnO dye-sensitized solar cells with high at-rest stability. *Nanoscale Res. Lett.*, **2012,** *7,* 1-10.
12. Faqir, P.; Aini, N. A.; Mardhiyah, Z.; Nurosyid, F. Effect of concentration of red dragon fruit (*Hylocereus costaricensis*) peels extract as a dye of Dye-Sensitized Solar Cell (DSSC) on DSSC efficiency. *AIP Conf. Proc*., **2019,** 2202, 2-7.
13. Webb, P. A. Introduction to Chemical Adsorption Analytical Techniques and their Application to catalysis MIC Technical Publications Micromeritics Instrument Corp., Norcross, Georgia 30093, **2003,** 1-12.
14. Azizian, S.; Eris, S. Adsorption isotherms and kinetics. *Interface Sci. Technol.*, **2021**, 33, 445-509.

ISBN: 978-978-67-0285-8 DOI: https://doi.org/10.55455/acsnigeria.1.3.22-29

Fish-Bone-Derived Porous Carbon/Hydroxyapatite Composite for Sustainable Treatment of Local Sludge Wastewater

Thompson Izuagie
Department of Chemistry, National Open University of Nigeria, Abuja
Corresponding Author's email: tizuagie@noun.edu.ng
DOI: https://doi.org/10.55455/acsnigeria.1.3.22-29

ABSTRACT

Fish-bone waste was valorized into a porous carbon/hydroxyapatite composite and evaluated for sustainable treatment of local sludge wastewater. Catfish bones collected in Sokoto State were washed, oven-dried, pulverized, impregnated with H_3PO_4 (1:3) for 24 h, carbonized at 350 °C for 30 min, neutralized, dried, and applied in a filtration column. The resulting material was characterized by FTIR, XRD, SEM, and EDX. FTIR revealed O–H, C–H, and oxygen-containing surface functionalities alongside prominent phosphate-associated bands, while XRD showed crystalline reflections consistent with retention of the calcium-phosphate mineral phase. SEM revealed a rough, porous carbonaceous matrix containing dispersed mineral domains, and EDX confirmed C, O, P, and Ca as the predominant elements, collectively supporting formation of a carbon/hydroxyapatite composite. Filtration markedly improved sludge-water quality, achieving 92.77% COD, 89.02% BOD_5, and 96.40% turbidity removal. The pH increased from 3.40 to 7.20, while dissolved oxygen increased from 0.56 to 6.20 mg/L. High removal efficiencies were also obtained for Cd (99.51%), Cr (92.93%), Cu (91.43%), and Zn (92.00%). These findings demonstrate the potential of fish-bone waste as a low-cost, sustainable precursor for producing a multifunctional carbon/mineral adsorbent for wastewater treatment and resource valorization.

KEYWORDS: fish bone; porous carbon; hydroxyapatite; sludge wastewater; heavy metals.

1. INTRODUCTION

Increasing pressure on freshwater resources, population growth, urbanization, and inadequate wastewater management have intensified the need for sustainable technologies that can improve wastewater quality while facilitating safe water reuse.[1,2] Wastewater and sludge-associated aqueous streams are chemically complex and may contain suspended and dissolved solids, biodegradable and oxidizable organic matter, nutrients, inorganic ions, and potentially toxic metals. The persistence of metal contaminants is of particular concern because they are non-biodegradable and may accumulate in environmental compartments if inadequately treated.[3–7] Consequently, the development of affordable treatment materials capable of removing multiple classes of contaminants while minimizing secondary waste and resource consumption remains an important objective of sustainable water management.

Among available treatment approaches, adsorption has received considerable attention because of its operational simplicity, flexibility, relatively low energy requirements, and suitability for both centralized and decentralized applications.[2,8–10] Recent developments have increasingly focused on porous and waste-derived adsorbents as alternatives to comparatively expensive conventional materials. Porous materials can provide large accessible surfaces and diverse adsorption sites for wastewater contaminants, while carbonaceous adsorbents offer tunable pore structures and surface functionalities that support interactions with both inorganic and organic species.[11,12] Biomass- and biowaste-derived carbon materials are particularly attractive from a sustainability perspective because their production can simultaneously valorize residual resources and generate functional materials for environmental remediation.[13–16]

Fish-processing residues represent a potentially valuable feedstock within this waste-to-resource framework. Fish bones contain an organic matrix together with a substantial calcium-phosphate mineral fraction, predominantly associated with hydroxyapatite (HAp). Unlike conventional lignocellulosic precursors used primarily to produce carbonaceous adsorbents, thermal processing of fish bone can therefore generate a heterogeneous carbon–mineral material in which residual carbonaceous structures coexist with HAp-rich inorganic phases.[17] Recent work has demonstrated that pyrolysis and activation of fish-bone biowaste can produce porous HAp-rich adsorbents containing residual carbon structures and surface functional groups suitable for aqueous contaminant removal.[18] This distinctive composition provides an opportunity to exploit fish-bone waste directly as a precursor for multifunctional adsorbents rather than removing its mineral fraction before carbonization.

Hydroxyapatite is particularly relevant to metal-contaminated wastewater because its calcium-phosphate framework exhibits strong affinity toward several metal ions through mechanisms that may include surface complexation, ion exchange, dissolution–precipitation, and incorporation into the mineral lattice. Accordingly, HAp-based materials have emerged as promising low-cost adsorbents for heavy metals and other aqueous pollutants.[19,20] Fish-bone-derived HAp has demonstrated effective Cd(II) removal from aqueous systems and real industrial wastewater[20], while recent investigations have further demonstrated substantial adsorption of Cr^{3+}, Ni^{2+}, and Zn^{2+} by HAp derived from different fish species, with removal performance strongly influenced by fish species, thermal treatment, and solution pH.[21] Waste-derived HAp can therefore contribute simultaneously to contaminant immobilization and the productive utilization of calcium-phosphate-rich biological residues.

Combining a porous carbonaceous phase with naturally occurring HAp may offer additional advantages over either component considered independently. The carbonaceous fraction can contribute porosity, accessible surface area, and oxygen-containing functional groups, whereas the calcium-phosphate phase can provide chemically active sites with strong affinity for metal ions. Such complementary characteristics may broaden the range of interactions available for contaminant sequestration. The feasibility of this composite approach is supported by studies demonstrating that waste-derived HAp-containing composites can exhibit high porosity and substantial adsorption capacities for metal ions and other wastewater contaminants.[22] More broadly, the integration of waste-derived carbon materials with functional inorganic phases is consistent with current efforts to develop multifunctional adsorbents that couple high treatment performance with resource recovery and circular-economy principles.

Against this background, the present study investigates a fish-bone-derived porous carbon/hydroxyapatite composite for sustainable treatment of local sludge wastewater. By converting locally available fish-bone waste into a functional carbon–mineral adsorbent, the study explores an approach that integrates waste valorization, contaminant removal, and sustainable wastewater management.

2. MATERIALS AND METHODS

2.1 Preparation of fish-bone adsorbent

Catfish bones were separated from residual tissue, washed with distilled water and oven-dried at 150 °C for 24 h. The dried material was crushed and sieved to approximately 110 mesh. Fish-bone powder was impregnated with 75% H_3PO_4 at a solid-to-acid ratio of 1:3 for 24 h, filtered, dried and carbonized in a furnace at 350 °C for 30 min. After cooling, the product was washed with NaOH solution and deionized water until the washings reached approximately neutral pH. The material was then dried and pulverized before use. This preparation procedure is consistent with established approaches involving acid modification and thermal conversion of fish-bone waste into carbonaceous/HAp-containing adsorbent materials[18,23].

2.2 Wastewater collection and filtration

Sludge wastewater was collected from Madorawa, Bodinga Local Government Area, Sokoto State. Large particulate matter was removed before treatment. The prepared fish-bone material was used in a burette-column filtration arrangement in which cotton supported the adsorbent bed. Wastewater was contacted with the adsorbent and passed through the column, and the filtrate was collected for analysis as described elsewhere.[16]

2.3 Characterization and water-quality analyses

FTIR spectra were recorded over 4000–400 cm^{-1} to examine surface functional groups. XRD was used to assess crystalline phases and structural order; the study adopted a typical 2θ range of approximately 10–80° using Cu Kα radiation (λ = 1.5406 Å). SEM was used to examine morphology, while EDX associated with the SEM analysis was used to assess elemental composition. Physicochemical parameters were determined before and after treatment using standard methods.[24] Heavy-metal concentrations of Cd, Cr, Cu and Zn were determined by atomic absorption spectroscopy (AAS). Removal efficiency was calculated as $R\ (\%) = [(C_i - C_f)/C_i] \times 100$, where C_i and C_f are the

concentrations before and after filtration, respectively. For dissolved oxygen, the direction of improvement was reported as an increase rather than removal.

3. RESULTS AND DISCUSSION

3.1 Structural and surface characterization of the Fish-Bone-Derived Porous Carbon/Hydroxyapatite Composite

The FTIR spectrum of the fish-bone-derived material (Figure 1a) exhibits a weak, broad absorption in the hydroxyl stretching region at approximately 3370–3540 cm^{-1}, together with a C–H stretching feature around 2875 cm^{-1}. The most prominent absorptions occur below approximately 1400 cm^{-1}, particularly within the 1200–900 cm^{-1} fingerprint region. Rather than being attributed exclusively to carbonaceous functionalities, these bands are more appropriately interpreted as contributions from overlapping P–O vibrations of the retained calcium-phosphate phase and C–O-containing surface groups of the carbonaceous matrix. This interpretation is consistent with recent studies of fish-bone-derived hydroxyapatite (HAp), in which characteristic phosphate stretching vibrations have been reported at approximately 1000–1080 cm^{-1}, together with hydroxyl and residual organic functionalities.[21] Similarly, HAp extracted from fish bone has shown characteristic phosphate bands at approximately 1044 and 963 cm^{-1}.[25] The FTIR spectrum therefore indicates the coexistence of surface-functionalized carbonaceous matter and a retained phosphate-rich mineral phase, supporting assignment of the material as a carbon/HAp composite rather than phase-pure porous carbon.

The XRD pattern (Figure 1b) contains several relatively sharp diffraction reflections superimposed on a broader background, indicating the coexistence of crystalline and comparatively disordered components. Such a pattern is inconsistent with assignment of the material as exclusively amorphous carbon and instead demonstrates retention of a crystalline inorganic phase following carbonization at 350 °C. This interpretation agrees with recent characterization of fish-bone-derived HAp, for which well-defined XRD reflections characteristic of crystalline HAp have been observed.[25] More importantly, Zhang et al. (2026) recently demonstrated that pyrolysis and activation of fish bone can yield an HAp-rich adsorbent containing a residual carbon structure, providing direct precedent for the coexistence of carbonaceous and calcium-phosphate phases in thermally processed fish-bone materials.[18] When considered alongside the phosphate-associated FTIR bands and the Ca- and P-rich EDX response, the present XRD pattern therefore strongly supports identification of the material as a porous carbon/hydroxyapatite composite.

The SEM micrograph (Figure 1c) reveals an irregular, rough and highly textured morphology characterized by interconnected cavities and agglomerated domains. The porous matrix is interspersed with angular, comparatively compact particles that are morphologically distinct from the surrounding carbonaceous structure. In conjunction with the FTIR and XRD results, these features are consistent with HAp-rich mineral domains retained within and on the surface of a porous carbonaceous matrix. Comparable heterogeneous and porous morphologies have been observed in fish-bone-derived HAp materials, while porosity has been associated with improved accessibility of aqueous contaminants to adsorption sites. Recent work on thermally treated fish bone likewise demonstrates that pyrolysis and activation can improve the porosity and surface functionality of HAp-rich fish-bone adsorbents.[18] The interconnected cavities observed here may consequently facilitate access of dissolved species to external and internal adsorption sites and reduce diffusion distances within the adsorbent. Nevertheless, the SEM image provides morphological rather than quantitative porosity information; parameters such as specific surface area, pore volume and pore-size distribution would require complementary gas-adsorption measurements.

The EDX spectrum and elemental maps (Figure 1d) provide further evidence for the composite nature of the material. The analysis is dominated by C, O, P and Ca, with smaller contributions from Na and Si. The strong carbon signal confirms retention of a substantial carbonaceous component, whereas the simultaneous occurrence of Ca, P and O is consistent with the calcium-phosphate/HAp phase identified from FTIR and XRD. Fish-bone-derived HAp is similarly characterized by Ca- and P-rich compositions,

and recent studies routinely combine SEM–EDX with FTIR and XRD to establish the chemical and structural characteristics of such materials.[21] The elemental maps additionally show that C, O, P and Ca are distributed throughout the examined region, although local variations are evident, consistent with a heterogeneous carbon–mineral architecture. The EDX-derived Ca/P atomic ratio of approximately 1.34 is lower than the theoretical value of 1.67 for stoichiometric hydroxyapatite and should therefore not be interpreted as evidence of phase-pure stoichiometric HAp. Rather, it may reflect a calcium-deficient or compositionally heterogeneous phosphate-containing phase, contributions from other Ca- or P-containing species, and the local and semi-quantitative nature of EDX analysis. Accordingly, EDX is used primarily here to establish elemental identity and spatial association rather than precise bulk stoichiometry.

Together, the FTIR, XRD, SEM and EDX results provide mutually reinforcing evidence that carbonization of fish bone at 350 °C preserved a substantial fraction of the native calcium-phosphate mineral while converting part of the organic component into a porous carbonaceous matrix. The resulting material is therefore more appropriately described as a fish-bone-derived porous carbon/hydroxyapatite composite than as phase-pure activated or nanoporous carbon. This dual-phase architecture is potentially advantageous for wastewater treatment because the carbonaceous component can contribute accessible pores and surface functional groups, while HAp provides chemically active phosphate- and calcium-associated sites capable of interacting with metal ions. HAp-based materials have been reported to remove metals through combinations of surface complexation, ion exchange and dissolution–precipitation processes, depending on the adsorbate and solution conditions. Fish-bone-derived HAp has, for example, demonstrated effective Cd^{2+} removal from real wastewater, supporting its potential as a waste-derived adsorbent for metal-contaminated aqueous systems. More recent studies further demonstrate the capacity of fish-bone-derived HAp and HAp-containing composites to remove multiple metal ions from water and wastewater.

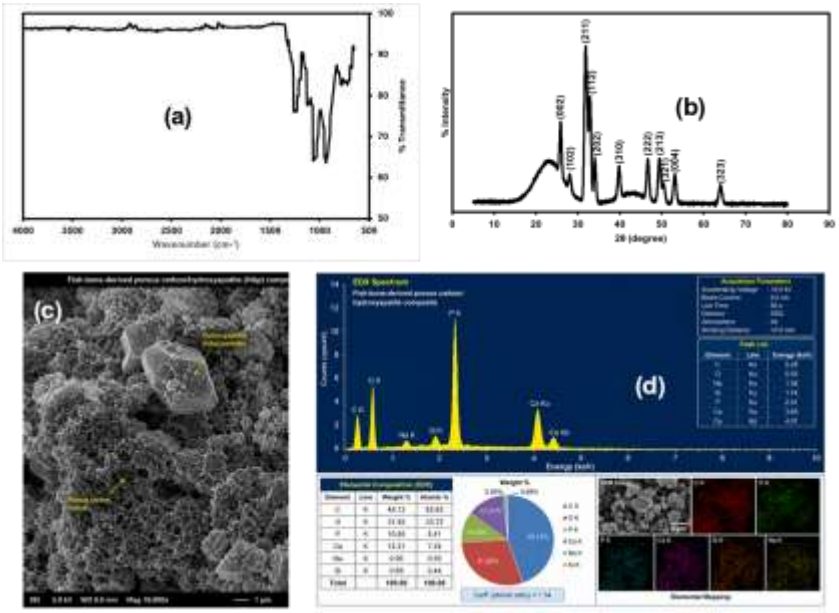

Figure 1. Characterization of the fish-bone-derived porous carbon/hydroxyapatite (HAp) composite: **(a)** FTIR spectrum showing characteristic surface functional groups; **(b)** XRD pattern confirming the crystalline phases of the composite; **(c)** SEM micrograph showing the porous carbon matrix and embedded HAp-rich particles; and **(d)** EDX spectrum, elemental composition, and elemental mapping confirming the presence and distribution of C, O, P, Ca, Na, and Si.

3.2 Physicochemical performance of composite

Filtration with the fish-bone-derived porous carbon/hydroxyapatite composite substantially improved the physicochemical characteristics of the sludge water (Table 1). The initially acidic pH increased from 3.40 to 7.20, bringing the treated water within the stated acceptable range of 6.5–8.5. This shift is

important because pH influences contaminant speciation, adsorption behaviour and overall treatment performance. WHO similarly recognizes pH as an important operational water-quality parameter.[26]

Electrical conductivity (EC) decreased from 940 to 245 µS/cm (73.94%), while total dissolved solids (TDS) declined from 604 to 198 mg/L (67.22%), indicating substantial reduction of dissolved ionic constituents. The final values were below the NSDWQ limits reported in Table 1. WHO also recognizes TDS as an important indicator of drinking-water acceptability, although no health-based guideline value is established for TDS.[27]

Marked reductions were observed in oxygen-demanding and particulate pollutants. COD decreased from 249 to 18.0 mg/L, corresponding to 92.77% removal, while BOD_5 declined from 41.0 to 4.50 mg/L (89.02%). Turbidity exhibited the highest removal efficiency, decreasing from 75.0 to 2.70 NTU (96.40%). Effective turbidity reduction is particularly important because suspended and colloidal particles can impair water quality and interfere with subsequent treatment and disinfection processes[26,27]

Concurrently, dissolved oxygen increased from 0.56 to 6.20 mg/L, consistent with the substantial reduction in oxygen-demanding constituents. Overall, the simultaneous improvements in pH, EC, TDS, COD, BOD_5, turbidity and DO demonstrate effective attenuation of dissolved, particulate and organic pollutant loads. These results indicate strong treatment performance of the fish-bone-derived composite, although compliance with these physicochemical parameters alone should not be interpreted as confirmation of drinking-water safety without complementary microbiological and contaminant-specific assessments.[26]

Table 1. Physicochemical characteristics of sludge water before and after filtration.

Parameter	Before filtration	After filtration	Change/Removal (%)	WHO/NSDWQ guideline/limit[28,29]	Assessment after filtration
pH	3.40	7.20	—	6.5–8.5	Within acceptable range
EC (µS/cm)	940	245	73.94	1,000 µS/cm†	Within NSDWQ limit
TDS (mg/L)	604	198	67.22	500 mg/L†	Within NSDWQ limit
DO (mg/L)	0.56	6.20	+1007.14‡	-	-
COD (mg/L)	249	18.0	92.77	-	-
BOD_5 (mg/L)	41.0	4.50	89.02	-	-
Turbidity (NTU)	75.0	2.70	96.40	≤5 NTU	Within commonly applied drinking-water limit

† Nigerian Standard for Drinking Water Quality (NSDWQ), NIS 554:2015, Standards Organisation of Nigeria (SON).[28]

3.3 Heavy-Metal Removal

The fish-bone-derived porous carbon/hydroxyapatite composite demonstrated high removal efficiencies for all four target metals (Table 2). Cd decreased from 0.570 to 0.0028 mg/L, corresponding to 99.51% removal, and the residual concentration was within the WHO guideline value of 0.003 mg/L.

Cr decreased from 0.580 to 0.0410 mg/L (92.93% removal), also below the WHO guideline of 0.05 mg/L, while Cu declined from 0.910 to 0.0780 mg/L (91.43% removal), substantially below its 2.0 mg/L guideline value. Zn decreased from 3.500 to 0.2800 mg/L (92.00% removal); WHO does not establish a health-based guideline value for Zn at concentrations normally encountered in drinking water.[26,27]

The consistently high removal (>91%) is compatible with the complementary surface chemistry of the carbon/HAp composite. Oxygen-containing carbon functionalities may contribute through surface complexation and electrostatic interactions, while hydroxyapatite can immobilize metal ions through ion exchange, surface complexation and dissolution–precipitation processes, as reported for waste-derived HAp adsorbents.[20] However, adsorption kinetics, isotherms and post-adsorption characterization would be required to establish the dominant removal mechanisms quantitatively.

Table 2. Concentrations and removal efficiencies of selected heavy metals in sludge water before and after filtration.

Heavy metal	Before filtration (mg/L)	After filtration (mg/L)	Removal (%)	WHO guideline (mg/L)[26,27]	Assessment after filtration
Cd	0.570	0.0028	99.51	0.003	Within WHO guideline
Cr	0.580	0.0410	92.93	0.05	Within WHO guideline
Cu	0.910	0.0780	91.43	2.0	Within WHO guideline
Zn	3.500	0.2800	92.00	No WHO health-based given value	Substantially reduced

4. CONCLUSION

A porous carbon/hydroxyapatite composite was prepared from waste catfish bones through H_3PO_4 impregnation followed by carbonization at 350 °C. FTIR, XRD, SEM and EDX analyses collectively confirmed a porous carbonaceous matrix containing retained calcium-phosphate/hydroxyapatite phases. The composite markedly improved sludge-water quality, achieving 92.77% COD, 89.02% BOD_5 and 96.40% turbidity removal, accompanied by a substantial increase in dissolved oxygen. High removal efficiencies were also obtained for the target heavy metals, reaching 99.51% for Cd, 92.93% for Cr, 91.43% for Cu and 92.00% for Zn. These findings demonstrate the potential of fish-bone waste as a low-cost and sustainable precursor for producing a multifunctional carbon/mineral adsorbent for wastewater treatment. Further studies should incorporate BET surface-area and pore-size analyses, calibrated XRD phase identification, adsorption kinetics and isotherms, regeneration and reuse studies, and post-adsorption characterization to establish adsorption mechanisms, long-term performance and practical applicability before large-scale deployment or claims regarding drinking-water safety are considered.

REFERENCES

(1) UNESCO. *The United Nations World Water Development Report 2024: Water for Prosperity and Peace*; 2024. https://www.unesco.org/en/articles/united-nations-world-water-development-report-2024-water-prosperity-and-peace (accessed 2025-12-06).

(2) Izuagie, T.; Oyem, I. M.; Umar, B.; Isah, A.; Abdulsalami, I. O.; Oyem, H. H. Sustainable Water Treatment in Sub-Saharan Africa: Recent Advances in Multifunctional Materials and Digital Tools for Complex Contaminant Removal. *Sustainability Science and Technology* **2026**, *3* (2), 022001. https://doi.org/10.1088/2977-3504/ae565e.

(3) Kominko, H.; Gorazda, K.; Wzorek, Z. Sewage Sludge: A Review of Its Risks and Circular Raw Material Potential. *Journal of Water Process Engineering* **2024**, *63*, 105522. https://doi.org/10.1016/j.jwpe.2024.105522.

(4) Mulopo, J. A Systematic Overview of Current Advancements for Chemical, Material, and Energy Production Using Sewage Sludge for Industrial Ecology and Sustainability Transition. *Environmental Sustainability* **2024**, *7* (1), 5–29. https://doi.org/10.1007/s42398-023-00301-9.

(5) Feng, J.; Burke, I. T.; Chen, X.; Stewart, D. I. Assessing Metal Contamination and Speciation in Sewage Sludge: Implications for Soil Application and Environmental Risk. *Rev. Environ. Sci. Biotechnol.* **2023**, *22* (4), 1037–1058. https://doi.org/10.1007/s11157-023-09675-y.

(6) E. J. Itumoh; O. P. Aghamelu; T. Izuagie. Influence of Mining and Agricultural Activities on the Quality of Groundwater from Some Rural Areas of South-Eastern Nigeria. *Global Nest Journal* **2015**, *17* (2), 406–417.

(7) EJ Itumoh; T Izuagie; NO Omaka; A Uba; M Shuaibu; IA Dogonyaro; A Isah; AU Dange; SI Isah. Trace Metals Analysis of Soil and Water Samples from a Limestone Mining Site in Sokoto State Nigeria. *Journal of Physical Sciences and Innovation* **2011**, *3*, 62–71.

(8) Patel, H. Fixed-Bed Column Adsorption Study: A Comprehensive Review. *Appl. Water Sci.* **2019**, *9* (3), 45. https://doi.org/10.1007/s13201-019-0927-7.

(9) Malloum, A.; Akpotu, S. O.; Adegoke, K. A.; Okeke, E. S.; Omotola, E. O.; Ohoro, C. R.; Amaku, J. F.; Conradie, J.; Olisah, C.; Akpomie, K. G. Advances in Molecular Simulations of Dye Adsorption from Wastewater. *J. Mol. Liq.* **2025**, *439*, 128732. https://doi.org/10.1016/j.molliq.2025.128732.

(10) Hira, N. E; Lock, S. S. M.; Shoparwe, N. F.; Lock, I. S. M.; Lim, L. G.; Yiin, C. L.; Chan, Y. H.; Hassam, M. Review of Adsorption Studies for Contaminant Removal from Wastewater Using Molecular Simulation. *Sustainability* **2023**, *15* (2), 1510. https://doi.org/10.3390/su15021510.

(11) Liu, X.; Hao, Q.; Fan, M.; Teng, B. Carbonaceous Adsorbents in Wastewater Treatment: From Mechanism to Emerging Application. *Science of The Total Environment* **2024**, *955*, 177106. https://doi.org/10.1016/j.scitotenv.2024.177106.

(12) Al-Jubouri, S. M.; Al-Batty, S.; Al-Hamd, R. Kh. S.; Sims, R.; Hakami, M. W.; SK, M. H. Sustainable Environment through Using Porous Materials: A Review on Wastewater Treatment. *Asia-Pacific Journal of Chemical Engineering* **2023**, *18* (4). https://doi.org/10.1002/apj.2941.

(13) Kumar, K.; Kumar, R.; Kaushal, S.; Thakur, N.; Umar, A.; Akbar, S.; Ibrahim, A. A.; Baskoutas, S. Biomass Waste-Derived Carbon Materials for Sustainable Remediation of Polluted Environment: A Comprehensive Review. *Chemosphere* **2023**, *345*, 140419. https://doi.org/10.1016/j.chemosphere.2023.140419.

(14) Nazir, G.; Rehman, A.; Hussain, S.; Mahmood, Q.; Fteiti, M.; Heo, K.; Ikram, M.; Aizaz Ud Din, M. Towards a Sustainable Conversion of Biomass/Biowaste to Porous Carbons for CO_2 Adsorption: Recent Advances, Current Challenges, and Future Directions. *Green Chemistry* **2023**, *25* (13), 4941–4980. https://doi.org/10.1039/D3GC00636K.

(15) Izuagie, T.; A. Muazu, S.; A. Anka, H. Nanoporous Carbon from Waste Egg Shells Modified with Copper-Nanoparticles – An Efficient Material for Removal of Microbial Contaminants from Polluted Water. *International Journal of Science for Global Sustainability* **2023**, *8* (4), 9. https://doi.org/10.57233/ijsgs.v8i4.360.

(16) Izuagie, T.; Sirajo, M.; Abubakar, M. Immobilization of Polyoxometalate-Ionic Liquid on Coconut Shell Nanoporous Carbon Support: An Improved Material for Water Purification. *Caliphate Journal of Science and Technology* **2022**, *4* (2), 213–220. https://doi.org/10.4314/cajost.v4i2.11.

(17) Rigueto, C. V. T.; de Oliveira, R.; Gomes, K. S.; Alessandretti, I.; Nazari, M. T.; Rosseto, M.; Krein, D. D. C.; Loss, R. A.; Dettmer, A. From Waste to Value-added Products: A Review of Opportunities for Fish Waste Valorization. *Environmental Quality Management* **2023**, *33* (1), 203–221. https://doi.org/10.1002/tqem.22040.

(18) Zhang, X.; Liu, Z.; He, T.; Ma, Y.; Tan, C.; Huang, Y.; Zheng, J.; Chen, H. Hydroxyapatite-Rich Adsorbent Derived from Thermal Treatment of Fishbone Biowaste for Wastewater Cleaning. *Journal of Water Process Engineering* **2026**, *89*, 110283. https://doi.org/10.1016/j.jwpe.2026.110283.

(19) Amenaghawon, A. N.; Anyalewechi, C. L.; Darmokoesoemo, H.; Kusuma, H. S. Hydroxyapatite-Based Adsorbents: Applications in Sequestering Heavy Metals and Dyes. *J. Environ. Manage.* **2022**, *302*, 113989. https://doi.org/10.1016/j.jenvman.2021.113989.

(20) Foroutan, R.; Peighambardoust, S. J.; Hosseini, S. S.; Akbari, A.; Ramavandi, B. Hydroxyapatite Biomaterial Production from Chicken (Femur and Beak) and Fishbone Waste through a Chemical Less Method for Cd2+ Removal from Shipbuilding Wastewater. *J. Hazard. Mater.* **2021**, *413*, 125428. https://doi.org/10.1016/j.jhazmat.2021.125428.

(21) Moreno Carpinteyro, M.; Peñas Esteban, F. J.; Benito, A. D. Fishbone-Derived Hydroxyapatite from Distinct Species: Effect of Calcination and PH on Heavy Metal Adsorption from Water. *Environments* **2026**, *13* (2), 102. https://doi.org/10.3390/environments13020102.

(22) Trung, T. S.; Minh, N. C.; Cuong, H. N.; Phuong, P. T. D.; Dat, P. A.; Nam, P. V.; Hoa, N. Van. Valorization of Fish and Shrimp Wastes to Nano-Hydroxyapatite/Chitosan Biocomposite for Wastewater Treatment. *Journal of Science: Advanced Materials and Devices* **2022**, *7* (4), 100485. https://doi.org/10.1016/j.jsamd.2022.100485.

(23) Juliana, M.; Dewi, D. A. S. Characterization of Acid-Treated Carbon from Snapper (*Lutjanidae*) and Red Grouper (*Epinephelus spp.*) Bones Using HCl and H_3PO_4; *Jurnal Teknologi dan Industri Pangan* **2026**, *37* (1), 44–54. https://doi.org/10.6066/jtip.2026.37.1.44.

(24) William C. Lipps; Ellen Burton Braun-Howland; Terry E. Baxter. *Standard Methods for the Examination of Water and Wastewater*, 24th ed.; American Public Health Association; American Water Works Association; Water Environment Federation: Washington, DC, 2023.

(25) Gnanasekaran, R.; Yuvaraj, D.; Muthu, C. M. M.; Ashwin, R.; Kaarthikeyan, K.; Kumar, V. V.; Ramalingam, R. J.; Al-Lohedan, H.; Reddy, K. Extraction and Characterization of Biocompatible Hydroxyapatite (Hap) from Red Big Eye Fish Bone: Potential for Biomedical Applications and Reducing Biowastes. *Sustainable Chemistry for the Environment* **2024**, *7*, 100142. https://doi.org/10.1016/j.scenv.2024.100142.

(26) World Health Organization. *Guidelines for Drinking-Water Quality: Fourth Edition Incorporating the First, Second and Third Addenda*; Geneva, Switzerland, 2026. https://www.who.int/publications/i/item/9789240121225 (accessed 2026-08-23).

(27) World Health Organization. *Guidelines for drinking-water quality: Fourth edition incorporating the first addendum – Chapter 12: Chemical fact sheets. WHO*. https://cdn.who.int/media/docs/default-source/wash-documents/water-safety-and-quality/dwq-guidelines-4/gdwq4-with-add1-chap12.pdf (accessed 2026-02-25).

(28) Standards Organisation of Nigeria. *Nigerian Standard for Drinking Water Quality*; Abuja, 2015. https://africacheck.org/sites/default/files/Nigerian-Standard-for-Drinking-Water-Quality-NIS-554-2015.pdf (accessed 2026-08-23).

(29) Frisbie, S. H.; Mitchell, E. J. Arsenic in Drinking Water: An Analysis of Global Drinking Water Regulations and Recommendations for Updates to Protect Public Health. *PLoS One* **2022**, *17* (4), e0263505. https://doi.org/10.1371/journal.pone.0263505.

ISBN: 978-978-67-0285-8 DOI: https://doi.org/10.55455/acsnigeria.1.2.30-41

Investigating Bioactive Compounds from *Parkia biglobosa* Stem Bark for theTreatment of Elephantiasis: A Virtual Screening and Drug Design Approach

Zainab Veracious Balogun* and Abdulkabir Oladele Oladimeji
Industrial Chemistry Unit, Department of Chemical Sciences, Olusegun Agagu University of Science and Technology, Okitipupa, Ondo State, Nigeria.
Corresponding Author's email: veraciousz20@gmail.com
DOI: https://doi.org/10.55455/acsnigeria.1.2.30-41

ABSTRACT

Elephantiasis (L*ymphatic filariasis*) is a neglected tropical disease that causes severe swelling and disability. Current treatments such as albendazole are useful but limited by side effects and drug resistance, so there is a need for new, safer therapies. In this study, the stem of *Parkia biglobosa* (African locust bean tree), a plant widely used in African traditional medicine, was examined for bioactive compounds. The present study investigated the phytochemical composition and bioactivity of *Parkia biglobosa* stem essential oil and extract. GC-MS analysis revealed major constituents including 2-amino-6-methylbenzoic acid (29.82%), 2,4-di-tert-butylphenol (20.40%), 9,10-methanoanthracen-11-ol (5.31%), α-phellandrene (4.48%), and pentacosane (4.79%). Drug-likeness evaluation using SwissADME indicated one Lipinski's rule violation, attributed to the high molecular weight of certain constituents. Antioxidant activity was assessed using FRAP, DPPH, and ABTS assays. The essential oil exhibited strong ABTS scavenging activity (average 86.78%), while the stem extract showed concentration-dependent potency in the DPPH assay (95.28% at 100 mg/ml). Both samples demonstrated weak ferric reducing activity in the FRAP assay. Molecular docking further revealed favorable binding interactions of selected phytochemicals with protein 8E4F, suggesting potential therapeutic relevance. These findings highlight *Parkia biglobosa* stem essential oil and extract as promising sources of natural antioxidants with drug-like properties, warranting further pharmacological exploration.

KEYWORDS: Bioactive compounds, *Parkia biglobosa,* Elephantiasis, Drug design, Virtual screening.

1. INTRODUCTION

Elephantiasis also known as lymphatic filariasis, is a neglected tropical disease caused by parasitic filarial worms such as *Wuchereriabancrofti*, *Brugia malayi*, and *Brugia timori*. The disease is transmitted through the bites of infected mosquitoes, primarily *Culex*, *Anopheles*, and *Aedes* species. First recorded in ancient Egyptian texts and later documented in ancient India, elephantiasis is characterized by severe swelling of limbs and genitals due to lymphatic obstruction caused by the parasites.

Parkia biglobosa, commonly referred to as the African locust bean tree, is a multipurpose tree native to sub-Saharan Africa, particularly in savannah regions of West Africa. It belongs to the family Fabaceae (Leguminosae) and is widely known for its food, medicinal, and economic value. Traditionally, the seeds are fermented to produce a local condiment called "dawadawa" or "iru," widely used in Nigerian and Ghanaian cuisine. However, beyond the seeds, other parts of the tree, including the bark, stem, leaves, and pods, have shown great potential in traditional medicine.

Numerous studies have been conducted to evaluate the pharmacological and phytochemical properties of *Parkia biglobosa*: Odeyemi et al. (2015) reported antimicrobial activity in stem bark extracts against *Staphylococcus aureus* and *Escherichia coli*. Akinmoladun et al. (2014) found flavonoids, saponins, tannins, alkaloids, and glycosides in ethanolic and aqueous extracts of the plant's stem and roots. Ogunmoyole et al. (2018) assessed antioxidant potential of methanolic extracts of the root and stem, demonstrating significant radical scavenging activities. Adedapo et al. (2011) showed anti-inflammatory and analgesic activity in aqueous extracts from the bark and leaves. Adebayo et al. (2019) analyzed essential oil compositions using GC-MS and identified compounds such as alpha-pinene, linalool, eugenol, and caryophyllene in the volatile fractions of the leaves and bark. Ajaiyeoba et al. (2003**)** confirmed antifungal properties of the root and bark against *Candida albicans* and dermatophytes. Balogun et al. (2020) explored the immunomodulatory effects of the stem extracts on lymphocyte proliferation and cytokine expression. Ezekwesili-Ofili et al. (2021**)** investigated the hepatoprotective effects of methanolic extracts in Wistar rats with paracetamol-induced liver damage.

Despite these findings, there is a paucity of comprehensive studies combining cold maceration, rotary evaporation, hydro distillation, andGC-MS to examine the volatile profile of the **s**tem of *Parkia biglobosa*. This project aims to fill that research gap by using an integrated approach. Additionally, this project is driven by the hypothesis that the phytochemicals derived from the stem bark of *Parkia biglobosa* may offer therapeutic relevance in the management or potential cure of elephantiasis, a neglected tropical disease caused by lymphatic filarial parasites. The investigation into its phytochemical constituents may pave the way for future pharmaceutical applications against lymphatic filariasis.

2. MATERIALS AND METHODS

2.1 Reagent and Materials

Methanol, ethyl acetate, n-hexane, distilled water, ice block, beaker, round-bottom flask, measuring cylinder, funnel, retort stand, Clevenger apparatus, rotary evaporator, bucket, keg, cotton wool, muslin cloth, GC-MS, MOE, CHEMDRAW, UCSF Chimera, Plip, SWISSADME.

2.2 Plant Collection and Preparation

Fresh stem samples of Parkia biglobosa were collected in February 2025 from a forest in Ibarapa Local Government Area, Oyo State, Nigeria. The plant was authenticated by Dr. Odewo at the Forestry Research Institute of Nigeria (FRIN). Samples were air-dried under shade for four weeks, then ground into coarse powder. A total of 2515 g of the powder was extracted with methanol and ethyl acetate (4 L each) at room temperature for five days with intermittent agitation. Extracts were filtered and concentrated under reduced pressure at 40°C using a rotary evaporator.

2.3 Hydro distillation

Essential oil was obtained from 40 g of powdered sample using a Clevenger-type apparatus for 45 minutes (in two portions) and stored under refrigeration.

2.4 GC–MS Analysis

Samples were analyzed using an Agilent 8890 GC coupled with a 5795 MS. Helium (99.999%) served as the carrier gas on an HP-5MS column (30 m × 0.320 mm, 0.25 µm). The oven temperature was programmed from 80°C (2 min) to 240°C at 12°C/min (held 6 min). A 1 µL sample was injected, and compound identification was performed using the NIST library and retention times.

2.5 Ligand and Protein Preparation

Ligands were drawn and optimized in ChemDraw and exported for docking. The target protein (PDB ID: 8E4F) was retrieved from the Protein Data Bank and prepared in Chimera by removing water molecules, adding hydrogens, and defining active sites.

2.6 Molecular Docking and Interaction Analysis

Docking was performed using MOE software. Binding affinities were evaluated using London dG and GBVI/WSA dG scoring functions. Top poses were analyzed, and interactions were profiled using PLIP to identify hydrogen bonds, hydrophobic interactions, and other key contacts.

2.7 ADMET Prediction and Candidate Selection

Pharmacokinetic properties were predicted using SwissADME. Compounds were prioritized based on docking scores, interaction profiles, and drug-likeness for further validation.

2.8 Antioxidant Assays

(a). FRAP Assay: Ferric reducing antioxidant power was determined using the method of Sharmaet al. (2024). Extract (200 µL) was mixed with 3.0 mL FRAP reagent, incubated for 10 min, and absorbance measured at 593 nm. Results were expressed as µmol Fe^{2+} equivalents/g extract.

(b). DPPH Assay: DPPH scavenging activity was evaluated using the method of Khalid et al. (2023). Sample (1 mL, 1 mg/mL) was mixed with 4 mL DPPH solution (30 mg/L), incubated for 30 min in the dark, and absorbance read at 520 nm.

(c). ABTS Assay: ABTS scavenging activity was determined using the method of Gulcin et al. (2024). Sample (1 mL) was added to 4 mL ABTS solution, incubated for 6 min in the dark, and absorbance measured. Inhibition (%) for DPPH and ABTS was calculated as:

$$\frac{Absorbance\ of\ control - Absorbance\ of\ sample}{Absorbance\ of\ control}\ x\ 100$$

3. RESULTS AND DISCUSSION

3.1 Results

The GC–MS analysis revealed a diverse range of metabolites, including aromatic acids, terpenoids, hydrocarbons, esters, fatty acids, and sulfur-containing compounds. These constituents varied in their retention times and relative percentage compositions, suggesting a complex mixture of volatile and semi-volatile metabolites. The essential oil contained twenty-one (21) identifiable compounds. Among these, 2-amino-6-methylbenzoic acid (29.82%) and 2,4-di-tert-butylphenol (20.40%) were the predominant constituents, accounting for nearly half of the total composition. Other notable compounds include alpha-phellandrene (4.48%), pentacosane (4.79%), and eucalyptol (4.31%), which have been reported in literature for their antioxidant, antimicrobial, and anti-inflammatory properties. The presence of long-chain alkanes such as octacosane, hexacosane, and docosane, as well as fatty acids and esters, further highlights the chemical diversity of the extract.

This compositional profile is significant as it reflects the potential pharmacological properties of Parkia biglobosa stem essential oil, with phenolic and terpenoid compounds likely contributing to its antioxidant and therapeutic activities.

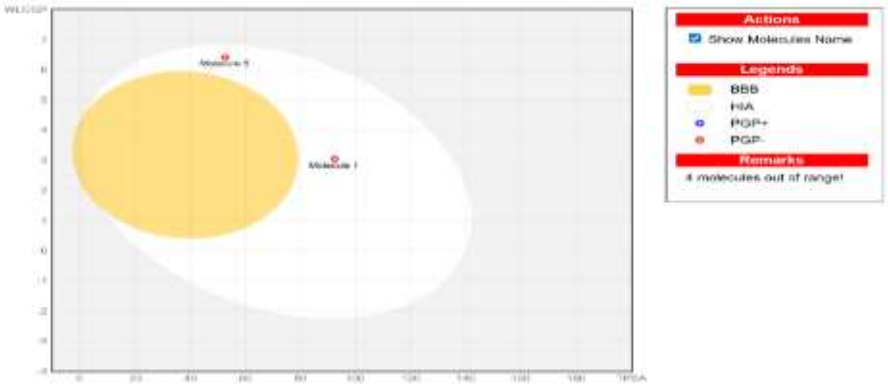

Figure 1: Boiled-Egg Model Illustrating Gastrointestinal Absorption (HIA) and Blood–Brain Barrier (BBB) Permeation of the Test Molecules.

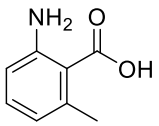

2-amino-6-methylbenzoic acid

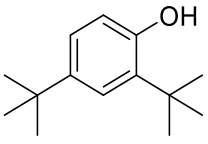

2,4-di-tert-butylphenol

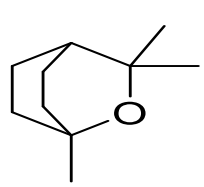

Eucalyptol

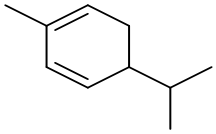

alpha-phellandrene

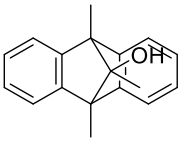

9,10,-Methanoanthracen-11-ol,9,10-dihydro-9,10,11-trimethyl

pentacosane

Figure 2: Structures of the Constituents of the Essential Oil
The structures above are the chemical structures of major constituents identified in the essential oil.

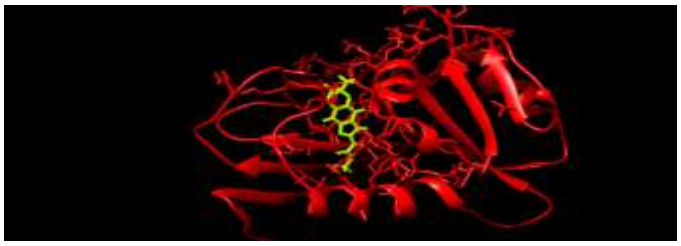

Figure 3: Binding interaction of Albendazole with Protein (8E4F) active site.

Figure 4: Binding interaction of Octacosane with Protein (8E4F) active site.

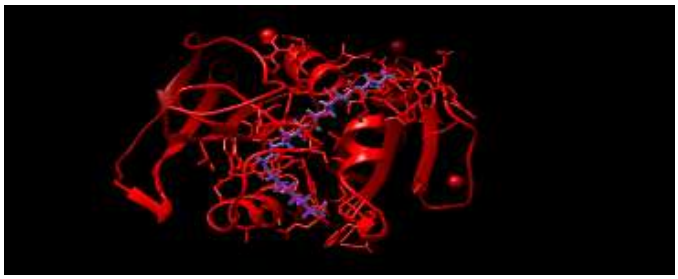

Figure 5: Binding interaction of Hexacosane with Protein (8E4F) active site.

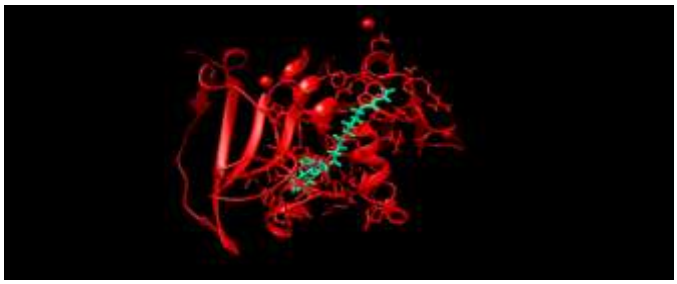

Figure 6: Binding interaction of Carbonic acid, eicosyl vinyl ester with Protein (8E4F) active

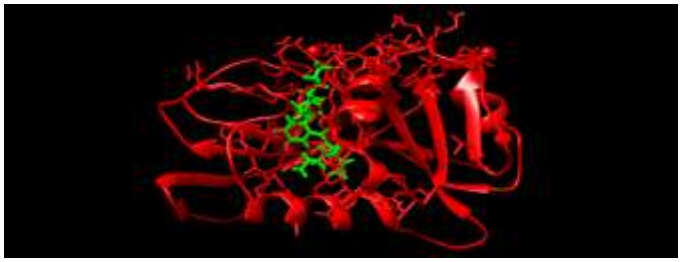

Figure 7: Binding interaction of 1,2-Benzenedicarboxylic acid, bis(2-propylpentyl) ester with Protein (8E4F) active site.

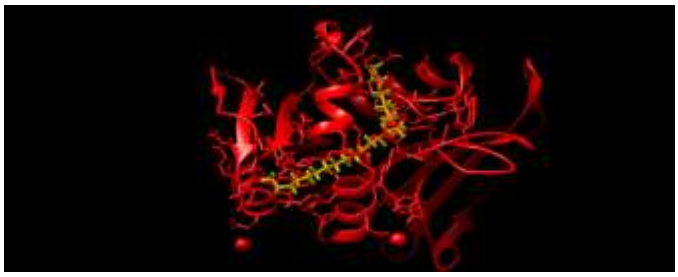

Figure 8: Binding interaction of Pentacosane with Protein (8E4F) active site.

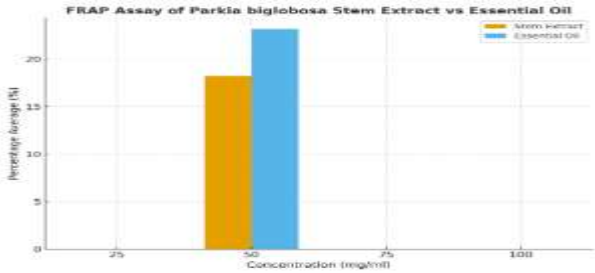

Figure 9: FRAP Assay of *Parkia biglobosa* stem Extract vs Essential Oil

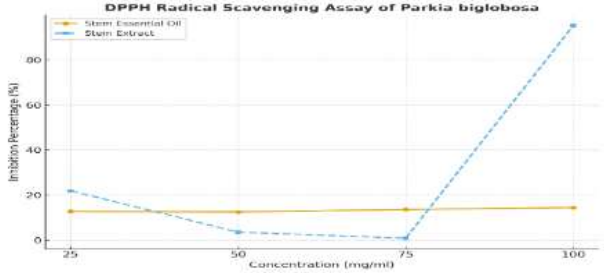

Figure 10: DPPH Radical Scavenging Assay of *Parkia biglobosa* Stem Extract vs Essential Oil

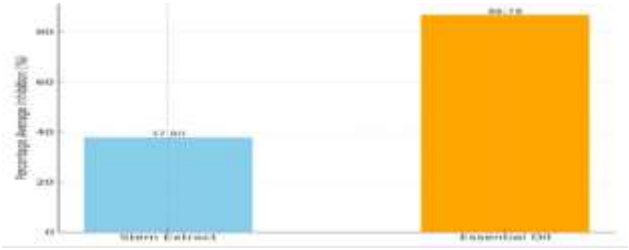

Figure 11: ABTS Scavenging Assay of *Parkia biglobosa* Stem Extract vs Essential

Table 1: Percentage composition of Essential oil of stem of Parkia biglobosa

S/N	Constituents	Chemical formular	KOVAT Index	Retention time (Min)	Percentage composition (%)
1.	Trans-2-methyl-3-propyloxirane	$C_6H_{12}O$	-	3.38	2.47
2.	2-Amino-6-methylbenzoic acid	$C_8H_9NO_2$	-	3.46	29.82
3.	Alpha-phellandrene	$C_{10}H_{16}$	-	4.15	4.48
4.	1-Methyl-3-(1-methylethyl)-benzene	$C_{10}H_{14}$	1010	4.43	2.20
5.	Limonene	$C_{10}H_{16}$	-	4.48	2.46
6.	Eucalyptol	$C_{10}H_{18}O$	1030	4.55	4.31
7.	9,10-Methanoanthracen-11-ol,9,10-dihydro-9,10,11-trimethyl	$C_{18}H_{18}O$	-	5.46	5.31
8.	Dodecanal	$C_{12}H_{24}O$	-	9.40	2.06
9.	Eicosane	$C_{20}H_{42}$	-	10.34	1.62
10.	2,4-Di-tert-butylphenol	$C_{14}H_{22}O$	-	10.64	20.40
11.	Dodecanoic acid	$C_{12}H_{24}O_2$	1580	11.17	1.75
12.	Octacosane	$C_{28}H_{58}$	-	12.56	2.31
13.	Hexacosane	$C_{26}H_{54}$	-	12.98	1.81
14.	Docosane	$C_{22}H_{46}$	-	14.55	2.45
15.	Pentacosane	$C_{25}H_{52}$	-	14.92	4.79
16.	1-Hexadecanethiol	$C_{16}H_{34}S$	-	15.42	1.75
17.	1,2-Benzenedicarboxylic acid, bis(2-propylpentyl) ester	$C_{24}H_{38}O_4$	-	15.61	3.15
18.	Eicosane	$C_{20}H_{42}$	-	16.52	1.61
19.	Carbonic acid, eicosyl vinyl ester	$C_{23}H_{44}O_3$		16.88	1.86
20.	Octacosane	$C_{28}H_{58}$	-	17.00	1.81
21.	Sulfurous acid, 2-ethylhexyl hexyl ester	$C_{14}H_{30}O_3S$	-	17.27	1.60
	Total				**100**

Table 2: Constituents with top-ranked binding energies compared to standard drug

S/N	Molecules	Binding energy(kcal/mol)
1.	Albendazole	-6.7578
2.	Octacosane	-9.3733
3.	Hexacosane	-9.1402
4.	Carbonic acid, eicosyl vinyl ester	-8.9437
5.	1,2-Benzenedicarboxylic acid, bis(2propylpentyl) ester	-8.8271

6.	Pentacosane	-8.7618

Table 3: Protein-Ligand interaction between target protein and tested ligands

Ligand	Hydrogen Bond Interactions	Hydrophobic Interactions	Key Residues Involved	Binding Characteristics
Albendazole (Standard)	2 (ILE-10A: 2.78 Å, ILE-114A: 2.15 Å)	4 (ILE-19A, LYS-57A, VAL-58A, TYR-120A)	Polar+ hydrophobic residues	Strong and specific binding due to combined hydrogen bonds and hydrophobic stabilization.
Octacosane	None	8 (ALA-12A, ILE-19A, PHE-36A, LYS-57A, VAL-58A, LYS-79A, LEU-122A, VAL-145A)	Predominantly hydrophobic residues	Extensive hydrophobic interactions, stable fit but lacks polar specificity.
Hexacosane	None	6 (ALA-12A, PHE-36A ×3, LEU-69A, VAL-145A)	PHE-36A (repeated), VAL-145A	Hydrophobic-driven stabilization, less versatile than octacosane.
Carbonic acid, eicosyl vinyl ester	None	4 (PHE-36A, LYS-57A, LEU-77A, LYS-79A)	Non-polar and basic residues	Stable hydrophobic binding but less extensive than hydrocarbons.
1,2-Benzenedicarboxylic acid, bis(2-propylpentyl) ester	None	10 (ALA-12A, ILE-19A, PHE-36A ×2, LYS-57A ×2, ILE-62A, LEU-69A, VAL-145A ×2)	Multiple hydrophobic residues	Highest number of hydrophobic contacts, suggesting strongest binding among phytochemicals.
Pentacosane	None	6 (PHE-36A, LYS-57A, LEU-77A, LYS-79A, GLU-118A, VAL-145A)	Hydrophobic + GLU-118A	Moderate hydrophobic stabilization, similar to hexacosane.

Table 4: Drug-likeness Predictions of Selected Compounds Computed by SwissADME

S/N	Chemical formular	Molecular weight (g/mol)	TPSA (Å²)	LogP (Consensus)	GI Absorption	BBB Permeant	P-gp substrate	Lipinski violation
1	$C_{12}H_{15}N_3O_2S$	265.33	92.31	2.29	High	No	No	0
2	$C_{28}H_{58}$	394.76	0.00	10.81	Low	No	Yes	1
3	$C_{26}H_{54}$	366.71	0.00	10.09	Low	No	Yes	1
4	$C_{23}H_{44}O_3$	368.59	35.53	7.73	Low	No	No	1
5	$C_{24}H_{38}O_4$	390.56	52.60	6.16	High	No	No	1
6	$C_{25}H_{52}$	352.68	0.00	9.72	Low	No	Yes	1

Table 5: Ferric Reducing Antioxidant Power (FRAP) Assay of Parkia biglobosastem bark essential oil

Concentration mg/ml	Blank	Absorbance sample	Percentage average
25	0.268	0.260	
50	0.268	0.535	23.21

75	0.268	15.1816
100	0.268	31.2391

Table 6: DPPH Radical Scavenging Assay of Parkia biglobosastem essential oil

Concentration mg/ml	Blank	Absorbance sample	Inhibition percentage
25	1.180	1.029	12.80
50	1.180	1.032	12.54
75	1.180	1.019	13.64
100	1.180	1.009	14.49

Table 7: ABTS [2,2'-azino - bis (3-ethylbenzothiazoline-6-sulfonic acid)] Scavenging activityof Parkia biglobosa stem Essential Oil

Concentration mg/ml	Blank	Absorbance sample	Inhibition percentage
25	1.337	0.214	83.99
50	1.337	0.216	83.84
75	1.337	0.162	87.88
100	1.337	0.115	91.40
Percentage Average			**86.78**

Table 8: Ferric Reducing Antioxidant Power (FRAP) Assay of Parkia biglobosaroot Extract

Concentration mg/ml	Blank	Absorbance sample	Percentage Average
25	0.268	0.268	
50	0.268	0.356	18.22
75	0.268	15.6487	
100	0.268	20.7871	

Table 9: DPPH Radical Scavenging Assay of Parkia biglobosastem Extract

Concentration mg/ml	Blank	Absorbance sample	Percentage Average
25	0.268	0.268	
50	0.268	0.356	18.22
75	0.268	15.6487	
100	0.268	20.7871	

Table 10: ABTS [2,2'-azino-bis (3-ethylbenzothiazoline-6-sulfonic acid)] Scavenging activityof Parkia biglobosa stem Extract

Concentration mg/ml	Blank	Absorbance sample	Inhibition percentage
25	1.780	1.334	25.06
50	1.780	1.121	37.02

75	1.780	1.003	43.65
100	1.780	0.971	45.45
Percentage Average			**37.80**

3.2 Discussion

3.2.1 Essential Oil

From Table 1 above, the most abundant compound detected from the GC-MS analysis was 2-amino-6-methylbenzoic acid (29.82%), an aromatic carboxylic acid derivative. Aromatic acids and related nitrogen-containing derivatives are known to contribute to antimicrobial and pharmacological properties in plant extracts (Akpuaka et al.,2013). Another highly abundant constituent was 2,4-di-tert-butylphenol (20.40%), a phenolic antioxidant commonly reported in essential oils and plant-derived fractions. This compound has been documented to exhibit strong antioxidant, antimicrobial, and anti-inflammatory activities (Gao et al., 2011). The high proportions of these two compounds suggest that they may account for much of the extract's potential bioactivity.

3.2.2 Molecular docking result

The molecular docking study provided insights into the binding affinities of phyto-constituents identified from Parkia biglobosa stem extract in comparison with the standard drug albendazole. Binding energy values (ΔG) are critical indicators of the strength and stability of ligand–protein interactions, with more negative values reflecting stronger binding potential.

Among the analyzed molecules as shown in Table 2 above, long-chain alkanes such as Octacosane (–9.3733 kcal/mol), Hexacosane (–9.1402 kcal/mol), Docosane (–8.5759 kcal/mol), and Pentacosane (–8.7618 kcal/mol) exhibited the highest binding affinities, surpassing the reference albendazole (–6.7578 kcal/mol). Similarly, Carbonic acid, eicosyl vinyl ester (–8.9437 kcal/mol) and 1,2-Benzenedicarboxylic acid, bis(2-propylpentyl) ester (–8.8271 kcal/mol) also demonstrated strong binding interactions, suggesting that they may contribute significantly to the bioactivity of the extract.

3.2.3 Protein-Ligand interaction profile

The protein-ligand interaction results from Table 3 highlight the nature of interactions between the target protein and the tested ligands (Albendazole and selected phytochemicals). The interactions involve both hydrogen bondingandhydrophobic contacts, which are critical for stabilizing ligand binding within the protein active site as shown in figure 4.2 above.

3.2.4 UCSF Chimera

Molecular docking using UCSF Chimera revealed that Albendazole (Figure 3), the standard drug, formed stable hydrogen bond and hydrophobic interactions with the protein (8E4F) active site, serving as a reference. Among the phytochemicals, Octacosane, Hexacosane, and Pentacosane (Figure 4–8) mainly showed hydrophobic interactions due to their hydrocarbon chains, suggesting weaker binding affinity. In contrast, Carbonic acid, eicosyl vinyl ester and 1,2-benzenedicarboxylic acid ester exhibited stronger interactions through polar and aromatic groups, indicating better potential activity. Overall, the results suggest that the polar and aromatic constituents of Parkia biglobosa essential oil may contribute more significantly to bioactivity than the straight-chain hydrocarbons, which aligns with earlier reports on plant-derived bioactive compounds (Kumar et al., 2021; Zaki et al., 2022).

3.2.5 ADME Prediction and Pharmacological Evaluation

The predicted properties of the tested compounds are summarized in Table 4, and their distribution in the BOILED-Egg model is illustrated in Figure 1 above. The diagram represents the BOILED-Egg predictive model, which is widely applied in drug discovery to evaluate the likelihood of compounds being absorbed in the gastrointestinal tract and/or crossing the blood–brain barrier (BBB). The two

descriptors plotted are WLOGP (lipophilicity, y-axis) and Topological Polar Surface Area (TPSA, x-axis), both of which strongly influence molecular pharmacokinetics.
The yellow region corresponds to the BBB-permeable space, indicating compounds that are likely to cross into the central nervous system. The white region represents the optimal space for human intestinalabsorption (HIA), highlighting compounds expected to show favorable oral bioavailability. Each molecule is plotted as a circle, with the outline color denoting P-glycoprotein (P-gp) interaction:
Red outline (PGP-) indicates molecules that are not substrates of P-gp, meaning they are not actively effluxed from cells. Blue outline (PGP+), which does not appear here, would denote molecules that are subject to P-gp efflux, potentially lowering absorption or distribution.
significantly reduce its potential as a drug candidate.

The Boiled-Egg model demonstrates that Molecule 5 is a strong candidate for CNS-active drug design, while Molecule 1 has potential for systemic (non-CNS) applications with good intestinal absorption. The four out-of-range compounds highlight possible limitations in bioavailability, requiring optimization.

3.2.6 FRAP Assay of Parkia biglobosa Stem Extract vs. Essential Oil

The ferric reducing antioxidant power (FRAP) of Parkia biglobosa stem extract and essential oil is illustrated in Figure 9. Both samples exhibited relatively low and inconsistent percentage values compared to the ABTS and DPPH assays. The stem extract recorded 18.22% inhibition at 50 mg/ml, with no substantial activity at other concentrations, while the essential oil showed 23.21% inhibition at 50 mg/ml, also with weak or negligible values across the remaining concentrations.

These results suggest that neither the stem extract nor the essential oil demonstrated strong ferric reducing ability under the tested conditions.

3.2.7 DPPH Radical Scavenging Assay of Parkia biglobosa Stem Extract vs. Essential Oil

As shown in Figure 10, the stem essential oil showed consistently low inhibition values (12.80 –14.49%) across concentrations, indicating relatively weak radical scavenging potential in the DPPH system. In contrast, the stem extract displayed variable activity, with very low inhibition at 50–75 mg/ml (3.61% and 0.92%, respectively), but a sharp increase to 95.28% inhibition at 100 mg/ml. This suggests that the antioxidant effect of the extract may be concentration-dependent, becoming highly active at higher doses, whereas the oil remains weak in this assay.

These results highlight that the DPPH assay response differs from the ABTS assay, where the oil was dominant. Such differences are often attributed to the polarity of antioxidant compounds and the solubility of radicals in the assay medium (Molyneux et al. 2004; Prior et al., 2005). Hence, while the essential oil performed better in the ABTS assay, the extract demonstrated stronger radical scavenging activity in the DPPH assay at higher concentrations.

3.2.8 ABTS Scavenging Activity of Parkia biglobosa Stem Extract and Essential Oil

The bar chart (Figure 2) compares the average percentage inhibition of Parkia biglobosa stem extract and essential oil in the ABTS assay. The results show that the stem extract exhibited a moderate antioxidant activity with 37.80% average inhibition, while the essential oil displayed a significantly higher activity with 86.78% average inhibition. This suggests that the essential oil contains more potent or higher concentrations of radical-scavenging phytochemicals compared to the crude extract.

These findings are consistent with studies where essential oils, rich in monoterpenes and phenolic compounds, generally demonstrate stronger ABTS radical scavenging activities than polar extracts (Brand-Williams et al., 1995; Re et al., 1999). Thus, the essential oil of Parkia biglobosa shows greater potential as a natural antioxidant source compared to its stem extract.

4. CONCLUSION

This study demonstrated that *Parkia biglobosa* stem harbors diverse phytochemicals with significant pharmacological potential against lymphatic filariasis. Virtual screening revealed that long-chain hydrocarbons and ester derivatives exhibited stronger binding affinities to the filarial protein 8E4F than

albendazole, the current standard drug. Interaction profiling highlighted the predominance of hydrophobic contacts, while ADMET analysis identified a subset of compounds with acceptable oral bioavailability and drug-likeness. Additionally, antioxidant assays confirmed the therapeutic relevance of the plant by demonstrating free radical scavenging activity. Collectively, these findings validate the ethnomedicinal use of *Parkia biglobosa* stem bark and provide a computational basis for the development of novel anti-filarial agents. Future work should focus on in vitro validation, toxicity studies, and structural optimization of the lead compounds to enhance their efficacy and pharmacokinetic properties.

5. RECOMMENDATIONS

The promising phytochemicals identified in *Parkia biglobosa* stem bark through docking and ADMET predictions should be isolated and subjected to laboratory-based in vitro and in vivo studies to confirm their anti-filarial efficacy and safety.

Compounds such as octacosane, hexacosane, pentacosane, and ester derivatives with strong binding affinities should undergo structural modifications to reduce excessive lipophilicity and improve solubility for enhanced pharmacological performance.

Since albendazole remains a standard treatment, combined therapy with *Parkia biglobosa* phytochemicals should be investigated to evaluate potential synergistic effects, reduced drug resistance, and minimized side effects.

Comprehensive toxicological studies are needed to evaluate long-term safety, potential mutagenicity, and cytotoxicity of the bioactive compounds before clinical applications.

Variations in phytochemical composition due to geography, season, or extraction methods should be addressed by developing standardized extraction protocols to ensure reproducibility and therapeutic consistency.

The identified compounds should be incorporated into larger virtual screening and cheminformatics pipelines, exploring derivatives and analogues that may yield more potent anti-filarial candidates.

Government and research institutions should support phytomedicine research on *Parkia biglobosa* and other African medicinal plants, as they provide cost-effective and culturally acceptable alternatives for managing neglected tropical disease.

REFERENCES

(1) Benzie, I. F. F.; Strain, J. J. Ferric Reducing Antioxidant Power (FRAP) as a Measure of “Antioxidant Power”: The FRAP Assay. Anal. Biochem. 1996, 239 (1), 70–76.

(2) Daina, A.; Michielin, O.; Zoete, V. SwissADME: A Free Web Tool to Evaluate Pharmacokinetics, Drug-Likeness and Medicinal Chemistry Friendliness of Small Molecules. Sci. Rep. 2017, 7, 42717.

(3) Daina, A.; Zoete, V. A BOILED-Egg to Predict Gastrointestinal Absorption and Brain Penetration of Small Molecules. ChemMedChem 2016, 11 (11), 1117–1121.

(4) Jumper, J.; Evans, R.; Pritzel, A.; Highly Accurate Protein Structure Prediction with AlphaFold. Nature 2021, 596 (7873), 583–589.

(5) Lipinski, C. A.; Lombardo, F.; Dominy, B. W.; Feeney, P. J. Experimental and Computational Approaches To Estimate Solubility and Permeability in Drug Discovery and Development Settings. Adv. Drug Deliv. Rev. 2001, 46 (1–3), 3–26.

(6) Mysinger, M. M.; Carchia, M.; Irwin, J. J.; Shoichet, B. K. Directory of Useful Decoys, Enhanced (DUD-E): Better Ligands and Decoys for Better Benchmarking. J. Med. Chem. 2012, 55 (14), 6582–6594.

(7) Roestos, C.; Lytoudi, K.; Mavromelanidou, O.; Zoumpoulakis, P.; Sinanoglou, V. Antioxidant Capacity of Selected Plant Extracts and Their Essential Oils. Antioxidants 2013, 2 (1), 11–22.

(8) Sari, M.; Biondi, D. M.; Kaabeche, M.; Mandalari, G.; D'Arrigo, M.; Bisignano, G.; Saija, A.; Daquino, C.; Ruberto, G. Chemical Composition, Antimicrobial and Antioxidant Activities of the Essential Oil of Several Populations of Origanum glandulosumDesf. Flavour Fragr. J. 2006, 21 (6), 890–898.

(9) Schuster, D.; Laggner, C.; Langer, T. Pharmacophore Modeling and Virtual Screening: Concepts, Workflows, and Applications. Methods Mol. Biol. 2020, 2114, 311–334.

(10) Silva, S. L.; Chaar, J. S.; Figueiredo, P. S.; Yano, T. Cytotoxic Evaluation of Essential Oil from Casearia sylvestris Sw on Human Cancer Cells and Erythrocytes. Acta Amazonica 2008, 38 (1), 107–112.

(11) Sterling, T.; Irwin, J. J. ZINC 15 – Ligand Discovery for Everyone. J. Chem. Inf. Model. 2015, 55 (11), 2324–2337.

(12) Su, M.; Yang, Q.; Du, Y.; Feng, G.; Liu, Z.; Li, Y.; Wang, R. Comparative Assessment of Scoring Functions: CASF-2016 Update. J. Chem. Inf. Model. 2019, 59 (2), 895–913.

(13) Su, Y. C.; Ho, C. L. Composition and in Vitro Cytotoxic Activities of the Leaf Essential Oil of Beilschmiediaerythrophloia from Taiwan. Nat. Prod. Commun. 2013, 8 (2), 143–144.

(14) van de Waterbeemd, H.; Camenisch, G.; Folkers, G.; Chretien, J. R.; Raevsky, O. A. Estimation of Blood–Brain Barrier Crossing of Drugs Using Molecular Size and Shape, and H-Bonding Descriptors. J. Drug Target. 1998, 6 (2), 151–165.

(15) van de Waterbeemd, H.; Gifford, E. ADMET in Silico Modelling: Towards Prediction Paradise? Nat. Rev. Drug Discov. 2003, 2 (3), 192–204.

(16) Vilar, S.; Cozza, G.; Moro, S. Medicinal Chemistry and the Molecular Operating Environment (MOE): Application of QSAR and Molecular Docking to Drug Discovery. Curr. Top. Med. Chem. 2008, 8 (18), 1555–1572.

(17) Wójcikowski, M.; Ballester, P. J.; Siedlecki, P. Performance of Machine-Learning Scoring Functions in Structure-Based Virtual Screening. Sci. Rep. 2017, 7, 46710.

ISBN: 978-978-67-0285-8 DOI: https://doi.org/10.55455/acsnigeria.1.3.42-49

Utilisation of Mining Waste Clays for the Production of Geopolymer Binders: Process Optimisation

Adebayo M., Adeleye[1,3]*, Gbenga M., Ayininuola[2], Mary B., Ogundiran[1]
[1] Department of Chemistry, University of Ibadan, Ibadan, Oyo State, Nigeria.
[2]Department of Civil Engineering, University of Ibadan, Ibadan, Oyo State, Nigeria.
[3]Department of Chemical Sciences, Joseph Ayo Babalola University, Ikeji Arakeji, Osun State.
Corresponding Author's email: badeleye@gmail.com
DOI: https://doi.org/10.55455/acsnigeria.1.3.42-49

ABSTRACT

The replacement of Portland cement with geopolymer binder (GB) is gaining global attention due to reduced carbon footprint in compliance with the United Nations agenda on sustainable development goals. The major drawback to geopolymer technology is the cost and unavailability of its aluminosilicate precursors. Therefore, this study investigated the utilisation of mining waste clays (MWCs) as sustainable precursors for the production of GBs, with a particular focus on process optimisation. The MWCs samples collected from Nigerian mining sites, namely Ijero, Owode, Ibeshe and Awo, were pre-treated by screening, drying, and sieving. These were characterised using the DTA/TGA technique for their thermal properties. The MWCs were calcined at varying temperatures of 420 ^{0}C – 850 ^{0}C range, at a time range of 3 – 14 h, NaOH concentrations in the range 4 – 10 M, and with varying NaOH/Na_2SiO_3 activator ratios 1:1 - 1:2.5. The GBs produced at these varied parameters were tested for their respective compressive strength to establish optimal process conditions. The dehydroxylation of MWCs into the reactive amorphous phase occurred within the range of 420-740 ºC. Optimised process conditions for GBs production were 600-740ºC calcining temperature, 6hrs calcining time, 8M NaOH concentration and 1:1.5 NaOH/Na_2SiO_3 ratio. The compressive strength of the geopolymer binders ranged from 26.1 to 33.7 MPa, meeting the applicable ASTM strength requirements. Process conditions were optimised for the production of GBs from MWCs.

KEYWORDS: Mining waste clays, climate change, geopolymer binders, carbon-footprint reduction.

1. INTRODUCTION

High and excessive energy requirements have been found to be a flaw associated with the manufacture of Portland cement. According to report by [1], the energy requirement for the manufacturing of PLC is just next to that of steel and aluminium. In addition, in the course of production or manufacture of Portland cement, a huge amount of dust gets released into the environment, which constitutes a major health concern. Coupled with these problems, a major adverse impact from cement manufacture is the high quantity of carbon (iv) oxide (CO_2) being released into the atmosphere during production. Studies have been ongoing to find more sustainable environmentally friendly alternatives to Portland cement in compliance with the UN goals on a sustainable environment. Consequently, geopolymer binders have gained much attention in this regard, because they can utilise aluminosilicate materials as precursor and, in the presence of an alkaline activator, provide a mechanically and environmentally superior alternative to the conventional Portland cement binders [2, 3]. The production of geopolymer binders generally involves the alkaline activation of silica and alumina-rich solid precursors. During the geopolymerisation process, reactive Si and Al species are dissolved from the precursor by the activator under alkaline conditions and are subsequently polycondensed to form a three-dimensional aluminosilicate network. The resulting binder can exhibit high compressive strength and other favourable engineering properties. The use of waste materials as precursors is a form of waste valorisation [4, 5]. Geopolymer technology may not be considered more advantageous over Portland cement ultimately, until there is proper identification of suitable low-cost precursor, and well optimized process conditions; to achieve waste valorisation and green process advantage respectively [6]. So many precursors have been investigated, including fly ash, volcanic materials, blast furnace slag, agricultural waste, metakaolin, and some mineral wastes. However, the sustainability of most of these precursors can not be guaranteed, due to changing technological process pathways generating these materials as by-products. This has aroused interest in naturally occurring wastes, such as waste clays [3, 4].

Clay is no doubt an aluminosilicate material, but is less reactive without thermal treatment, due to the ordered structure of the crystalline raw form. Thermal activation is usually employed to modify the mineral structure, remove structural hydroxyl groups and increase the availability of reactive

aluminosilicate species. Studies have reported the use of thermally treated clays as effective precursors for low-carbon geopolymer binders, although the optimal calcining temperature varies based on clay mineralogy and chemical composition [4, 7]. This variability is important because excessive calcination may cause structural reorganisation or sintering, whereas inadequate calcination may leave substantial quantities of unreactive crystalline phases. Therefore, investigating the appropriate calcining temperature and duration for a particular clay resource is an essential aspect of determining the geopolymer process.

Activators are a major part of the process of geopolymerisation, which provide the alkaline environment and soluble silica needed for the dissolution of the aluminosilicate precursor's component species. Activators include calcium hydroxide, sodium hydroxide and sodium silicate, etc. However, variations in hydroxide concentration, silicate content and hydroxide-to-silicate ratio can substantially influence precursor dissolution, gel formation, setting behaviour and mechanical strength. Therefore, optimisation of the activator composition is essential for achieving adequate mechanical performance and also to avoid excessive activator consumption [6, 8].

Therefore, this study investigated the optimisation of processing conditions for the production of geopolymer binders from mining waste clays obtained from mining locations spread across four different states of Nigeria: Ekiti State (Ijero), Ogun State (Owode), Lagos State (Ibeshe) and Osun State (Awo). The chemical and thermal characteristics of the studied clays were determined. The effects of calcining temperature, and duration were studied. The NaOH/Na_2SiO_3 activator ratio on the compressive strength of the resulting geopolymer binders were determined; to establish suitable processing conditions for the different mining waste clays. The study therefore went beyond just the identification of mining waste clays as potential geopolymer precursors and sought to establish experimentally derived processing conditions for their effective conversion into mechanically effective geopolymer binders. The outcome is intended to provide a practical process basis for the valorisation of Nigerian mining waste clays as locally available precursors for sustainable, low-carbon construction materials.

2. MATERIALS AND METHODS

2.1 Materials

Samples of raw mining waste clays were randomly scooped from the mining grounds in each of the four selected mining locations: Ijero (Ekiti State), Ibeshe (Lagos State), Owode (Ogun State), and Awo (Osun State) mining sites. These were labelled EK, LA, OG and OS, respectively. Industrial-grade Na_2SiO_3 solution (26% wt SiO_2, 11 % wt Na_2O, and 63% wt SiO_2) and sodium hydroxide pellets were purchased from a credible chemical company.

Fig. 1: Map Showing Selected Mining Locations in the Southwest Region of Nigeria

The selected locations where sampling of the mining waste clays took place is represented on map in Fig. 1. Instruments used for this study included: Simultaneous thermal properties and mass loss analysers, which had Thermogravimetric analyser and Differential thermal analyser (TGA/DTA); NETZSCH STA 449 F3 Jupiter model, with temperature range set at 40 - 900 ^{0}C, heating rate of 10^{0}C per minute; Digital furnace (Vecstar furnaces 1100 series and Carbolite AAF, type 301 MC 16-GB-C 1.01), with a heating rate of 7.8 ^{0}C/minute was used; an oven and an analytical weighing balance, at the Department of Chemistry laboratories, University of Ibadan; Compression test machines: ELE

International, ADR Touch 2000 Standard Compression Machine, at Civil Engineering workshop, University of Ibadan.

2.2 Methods

2.2.1 Pre-treatment of mining waste clays

The collected MWC samples from Ijero (EK), Owode (OG), Ibeshe (LA) and Awo (OS) were initially screened manually to remove visible foreign materials, including stones, gravel, plant residues and other coarse impurities. The screened samples were oven-dried at 105 °C, pulverised and homogenised. The dried samples were subsequently passed through a 212-μm mesh sieve to obtain a relatively uniform particle-size fraction. The processed samples were stored in labelled airtight containers before thermal characterisation and calcination.

2.2.2 Preparation of activators

The activator mixture was composed of sodium hydroxide and sodium silicate. Pellets of sodium hydroxide were dissolved in cooled distilled water in plastic containers to achieve NaOH concentrations of 4, 6, 8, and 10 M. Sodium silicate solution was made available in a plastic container.

2.2.3 Thermal characterisation and calcining of the mining waste clay samples

The four mining waste clays were separately pulverised, sieved with a 212-micron mesh sieve, dried in the oven at 105 °C, and kept in appropriately labelled plastic buckets. These raw mining waste clays were characterised for their thermal properties using the thermogravimetry/differential thermal analysis method (TGA/DTA). The determination of the thermal properties of the samples was done to establish phase changes occurring during calcination and to determine the dehydroxylation temperatures of the clays. Hence, based on the values observed from the respective DTA curves of the clays, they were thereafter calcined in the furnace at varying temperatures in the 420 – 850 °C range.

2.2.4 Preparation of geopolymer binders and optimisation

The procedure used for the production of geopolymer binders included mixing of calcined mining waste clays and activator into paste or molten material, which was fed into moulds of 40 x 40 x 40 cm^3. These were kept for demoulding till after 3 days. Solid cubes of geopolymer binders resulted. Using this procedure, laboratory-scale experiments were performed, starting with the optimisation of calcination temperature by using clays calcined at the varied temperatures of the 420 – 850 °C range. At the same time, other parameters were kept at 6 hours calcining time, 8 M NaOH concentration and activator mixing ratio of 1:1($NaOH/Na_2SiO_3$), as observed in previous studies [9]. Replicate geopolymer samples were produced for all the temperatures selected for each of the four clays, respectively. The resulting geopolymers were subjected to compressive strength tests at 7, 14, 21, and 28 days of curing time. The temperature value that produced the geopolymer with the highest compressive strength was considered the optimum calcining temperature. This procedure was repeated to optimise other parameters; varying calcining time of 3, 6, 10, 14 and 20 hrs; varying NaOH concentration within the range 4, 6, 8 and 10 M; and varying activator ($NaOH/Na_2SiO_3$) mix ratios of 1:1, 1:1.5, 1:2, and 1:2.5 for all the clays respectively.

3. RESULTS AND DISCUSSION

3.1 Thermal Properties of the Clays by DTA/TGA technique

The thermograms resulting from thermal characterisation using DTA/TGA are represented in Fig. 2. The TGA/DTA results simultaneously monitored and presented the mass loss of clays with increasing temperature during dehydroxylation. According to [10], dehydroxylation, which has been understood to depend essentially on the clays' layered structures and the amount of hydroxyl groups, had been preceded by the removal of the interlayer water molecules and those absorbed from the atmosphere.

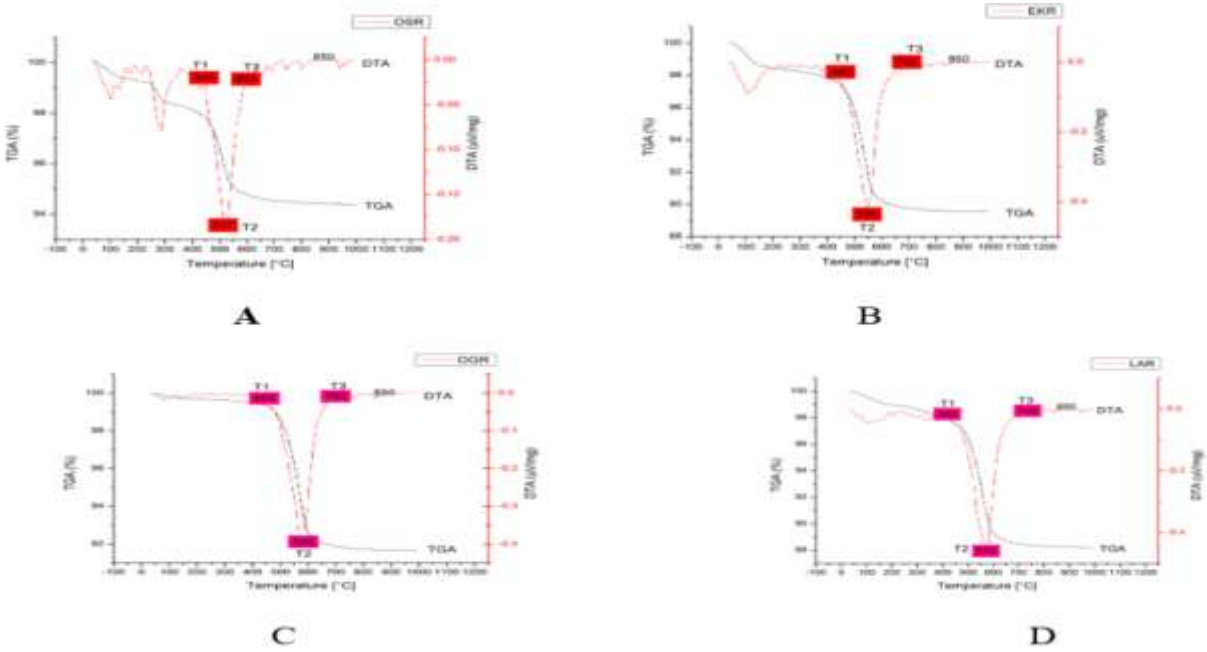

Fig.2 Thermograms of mining waste clays; A (OS); B (EK); C (OG); D (LA)

Dehydroxylation, however, requires more intense thermal treatment, leading to the loss of hydroxyl groups chemically bonded to the octahedral sheets. This causes a collapse of the crystalline structure, leading to the amorphisation of the clay. This phenomenon takes place at different temperatures for different clays, depending on the mineral composition. For the clays studied, the temperature range on DTA/TGA thermograms provided necessary information to predict the dehydroxylation temperature points for each clay source and also enhance identification of the constituent clay minerals.

There exist different groups of clay minerals, based on their silica-to-alumina ratio (SiO_2/Al_2O_3) and the way their structural sheets are layered. When the clay minerals consist of the tetrahedral-octahedral sheets, and the silica and alumina sheets form a layer by shared oxygen atoms, and these layers are held together by hydrogen bonding, this is referred to as a 1:1 clay mineral. An example of this type is the kaolinite clay mineral. However, when tetrahedral – octahedral- tetrahedral sheets are formed, and the silica, alumina, and silica sheets form a layer by shared oxygen atoms with an interlayer space, this is referred to as a 2:1 clay mineral type. The interlayer always contains adsorbed water molecules and other ions. Examples of this group of clay minerals include montmorillonite, illite, and chlorite [11]. The thermograms of the clay samples suggest the points of transformation of the kaolinite to metakaolinite, which is the reactive form of clay.

Generally, for all the clays, the temperature range for the dehydroxylation of kaolinite which occurred between 430^0C and 740^0C, had the most intense mass loss among the three peaks in the respective thermograms, suggesting a relatively large presence of kaolinite alongside the composition of the 2:1 clay types suggested by the XRF results. This assumption is further ascertained by the XRD results, revealing intense kaolinite peaks for the clays. At a temperature range above 800^0C, the occurrence here was the dehydroxylation of some 2:1 clay minerals; illite, montmorillonite, and mullite [12]. All the clays used in this study, as represented by the thermogrammes, exhibited all the dehydration and dehydroxylation phenomena

3.2 Optimisation of calcining temperature of the mining waste clays

The results of the compressive strength of the geopolymers produced from clays calcined at the varying temperatures are presented in Fig. 3. From the results, the optimal calcination temperatures for the clays are 700, 740, 600, and 700 (^{0}C) for OG, LA, OS, and EK, respectively. From these values, the clays can be calcined at temperatures within the range of 600 to 740 (^{0}C). Correlating the compressive strength test results with the thermograms (Fig. 2), it was observed that the calcination of clays at the T3 dehydroxylation (post-peak) temperatures gave the best geopolymer performance, across all the clays. This suggests that the thermal process of clay conversion to metakaolin continued after the peak and had only come to completion at the post-peak point. For all the investigated clays, strength generally

increased with curing age. The reduction in strength at 850 °C suggested that excessive calcination may be detrimental to geopolymer precursor reactivity.

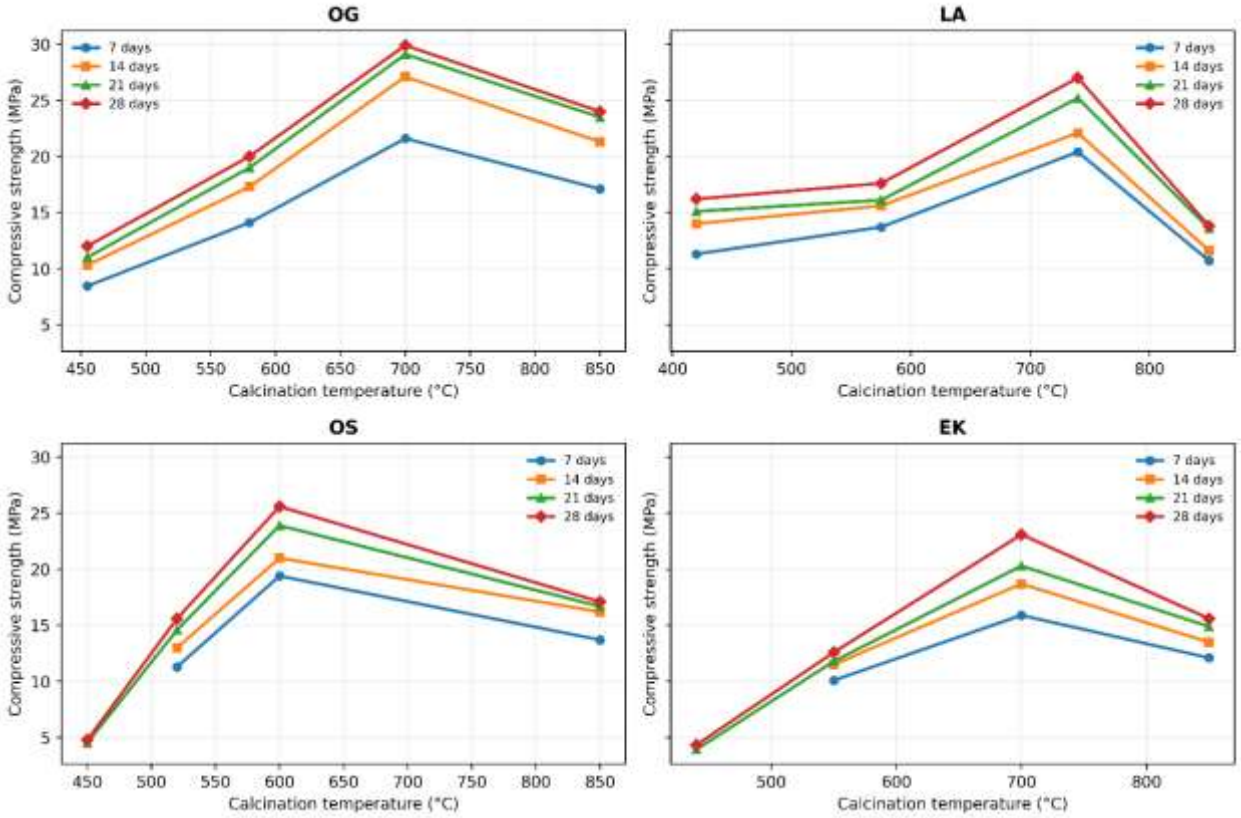

Fig. 3: Compressive Strength of Geopolymers at Varying Calcination Time

3.3 Optimisation of Calcination Time of the Mining Waste Clays

The results of the compressive strength of the geopolymers at varying calcining time duration are presented in Figure 4. The results suggest that the optimal calcination time for the clays is 6 hours at the optimised temperature. The decline in the compressive strength at higher temperatures suggests that at a calcination time longer than 6 hours, the clays experienced transformation to less reactive crystalline phase minerals.

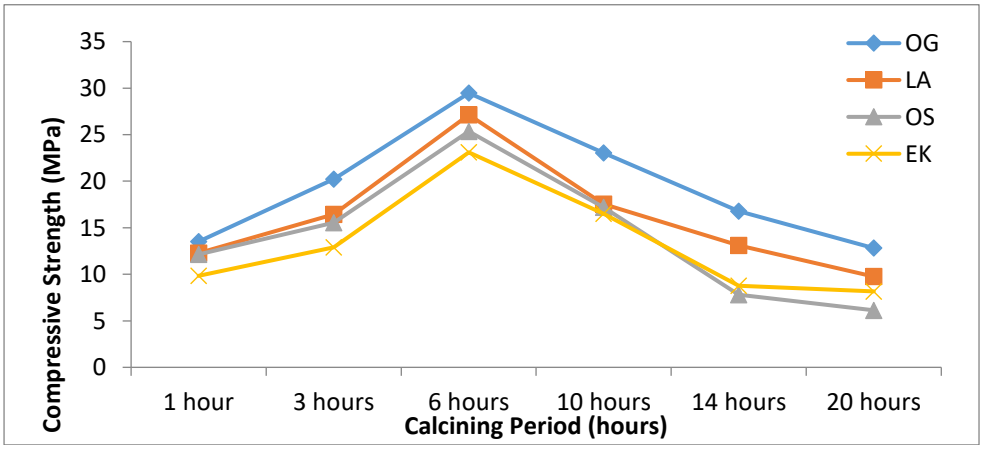

Fig. 4: Compressive Strength of Geopolymers of Different Clays at Varying Calcination Time

3.4 Optimisation of NaOH Concentration

The concentration of NaOH used in the making of the activator for geopolymer production was optimised to determine which concentration was most suitable. The results are presented in Figure 5.

It was observed from the results that the geopolymers produced with NaOH of 8 M concentration had the highest compressive strength across all the selected clays.

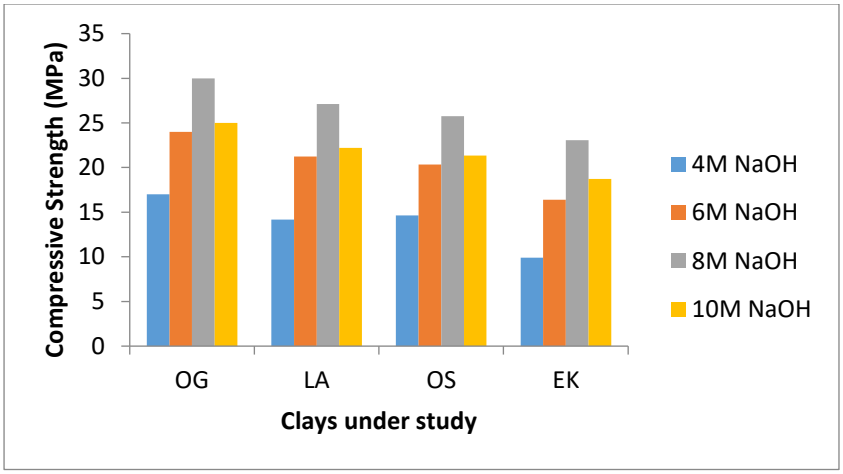

Fig. 5: Compressive Strength of Geopolymers of Different Clays with Varying Concentrations of NaOH

3.5 Optimisation of Activator Mixing Ratio ($NaOH/Na_2SiO_3$)

The results of the optimisation of the mixing ratio of activator consisting of Na_2SiO_3 and NaOH as presented in Fig. 6 suggested that a careful balance of the constituent species in these two activator components largely influenced the mechanical strength development of the geopolymers. This ratio may have provided the most favourable alkaline environment for the best strength development for geopolymer. The highest 28-day compressive strengths were obtained at a $NaOH/Na_2SiO_3$ ratio of 1:1.5, with values of 33.7, 29.8, 28.3 and 26.1 MPa for OG, LA, OS and EK based binders, respectively. However, further increase to 1:2.5 adversely affected the strength, suggesting that excess availability of soluble silica species in Na_2SiO_3 could be causing changes in dissolution kinetics, mixture viscosity and gel formation.

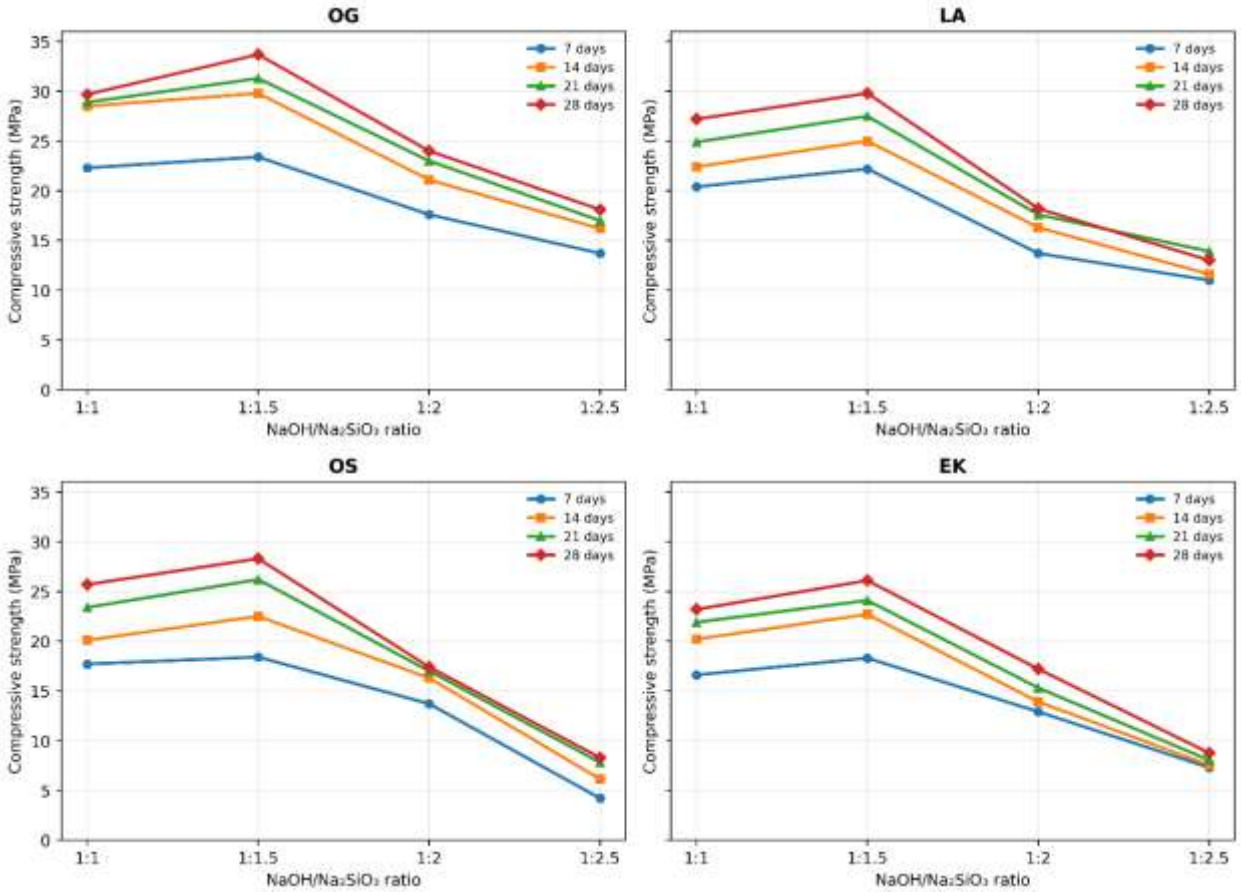

Fig. 6: Compressive Strength (MPa) of the Geopolymers with Varying NaOH/ Na_2SiO_3 ratio

4. CONCLUSION

This study demonstrated the suitability of Nigerian mining waste clays (MWCs) as sustainable aluminosilicate precursors for geopolymer binder production and established the optimal values for the major process conditions. Thermal analysis confirmed significant dehydroxylation and transformation of the clay minerals to reactive phases within approximately 430–740 °C, with the optimum calcination temperature varying among the clay sources. Based on compressive strength development, the optimum temperatures were 700 °C for OG, 740 °C for LA, 600 °C for OS and 700 °C for EK, while 6 h was identified as the optimum calcination time. An 8 M NaOH concentration and 1:1.5 NaOH/Na_2SiO_3 activator ratio produced the most favourable strength development across the investigated clays. At the optimum activator ratio, the 28-day compressive strengths reached 33.7, 29.8, 28.3 and 26.1 MPa for OG, LA, OS and EK, respectively. Excessive calcination and higher sodium silicate proportions resulted in reduced strength, indicating the importance of controlling thermal treatment and activator composition. Overall, the findings establish that locally sourced Nigerian mining waste clays can be effectively converted into reactive geopolymer precursors through appropriate process optimisation, providing a sustainable route for waste valorisation and the development of lower-carbon alternative binders to conventional Portland cement.

REFERENCES

[1] Temuujin, J., & van Riessen, A. (2009). Effect of fly ash preliminary calcination on the properties of geopolymer. Journal of Hazardous Materials, 164(2–3), 634–639. https://doi.org/10.1016/j.jhazmat.2008.08.065

[2] Nodehi, M., & Taghvaee, V. M. (2022). Alkali-activated materials and geopolymer: A review of common precursors and activators addressing circular economy. Circular Economy and Sustainability, 2(1), 165–196. https://doi.org/10.1007/s43615-021-00029-w

[3] Elzeadani, M., Bompa, D. V., & Elghazouli, A. Y. (2022). One part alkali activated materials: A state-of-the-art review. Journal of Building Engineering, 57, 104871. https://doi.org/10.1016/j.jobe.2022.104871

[4] Lekshmi, S., Sudhakumar, J., & Thomas, S. (2023). Application of clay in geopolymer system: A state-of-the-art review. Materials Today: Proceedings. https://doi.org/10.1016/j.matpr.2023.04.083

[5] Khan, R., Iqbal, S., Soliyeva, M., et al. (2025). Advanced clay-based geopolymer: Influence of structural and material parameters on its performance and applications. RSC Advances, 15, 12443–12471. https://doi.org/10.1039/D4RA07601J

[6] Rathod, N., Chippagiri, R., & Ralegaonkar, R. V. (2023). Cleaner production of geopolymer materials: A critical review of waste-derived activators. Materials Today: Proceedings. https://doi.org/10.1016/j.matpr.2023.03.502

[7] Ayati, B., Newport, D., Wong, H., & Cheeseman, C. (2022). Low-carbon cements: Potential for low-grade calcined clays to form supplementary cementitious materials. Cleaner Materials, 5, 100099. https://doi.org/10.1016/j.clema.2022.100099

[8] Firdous, R., Nikravan, M., Mancke, R., Vöge, M., & Stephan, D. (2022). Assessment of environmental, economic and technical performance of geopolymer concrete: A case study. Journal of Materials Science, 57, 16837–16856. https://doi.org/10.1007/s10853-022-07820-6

[9] Ogundiran, M. B., & Ikotun, O. J. (2014). Investigating the suitability of Nigerian calcined kaolins as raw materials for geopolymer binders. Transactions of the Indian Ceramic Society, 73(2), 138–142.

[10] Zhou, D., Wang, R., Tyrer, M., Wong, H., & Cheeseman, C. R. (2017). Sustainable infrastructure development through use of calcined excavated waste clay as a supplementary cementitious material. Journal of Cleaner Production, 168, 1180–1192. https://doi.org/10.1016/j.jclepro.2017.09.098

[11] Adeniyi, F. I., Ogundiran, M. B., Hemalatha, T., et al. (2020). Characterisation of raw and thermally treated Nigerian kaolinite-containing clays using instrumental techniques. SN Applied Sciences, 2, 821. https://doi.org/10.1007/s42452-020-2610-x

[12] Selmani, S., Essaidi, N., Gouny, F., Joussein, E., & Rossignol, S. (2015). Physical-chemical characterization of Tunisian clays for the synthesis of geopolymers materials. Journal of African Earth Sciences, 103, 76–84. https://doi.org/10.1016/j.jafrearsci.2014.12.009

ISBN: 978-978-67-0285-8 DOI: https://doi.org/10.55455/acsnigeria.1.3.50-55

Effects of operational conditions on biosynthesized silver nanoparticles using *Anogeissus leiocarpus* leaf extract

[1]Dorcas A. Fadare*, [2]Toluwani I. Korede, [2]Babatunde O. Ogunsile
[1] Chemical Sciences Department, Anchor University, Lagos, Nigeria.
[2]Department of Chemistry, University of Ibadan, Nigeria
Corresponding Author's email: dfadare@aul.edu.ng
DOI: https://doi.org/10.55455/acsnigeria.1.3.50-55

ABSTRACT

The yield of synthesized silver nanoparticles from *Anogeissus leiocarpus* leaf (ALNP) was investigated by varying some operational parameters such as time, ratio of extract to $AgNO_3$ and concentration on the production of the nanoparticles for optimization. The effects of the operating parameters on the biosynthesis of ALNP was monitored using the UV-Vis Spectroscopy. The biosynthesized AgNPs was evaluated for activities against some fungi and bacteria pathogens. Dose dependent activities against the pathogens used were observed with zones of inhibition ranging from 16-26 mm. *Pseudomonas aeruginosa* was the most susceptible organism. Optimization of the synthesis of *Anogeissus leiocarpus* silver nanoparticle was obtained at 60 minutes, concentration; 3 mM, ratio 1:2 of $AgNO_3$ and 50 % of ethanol.

KEYWORDS: Nanoparticles, operational variables, *Anogeissus leiocarpus.*

1. INTRODUCTION

Nanotechnology impacts every aspect of human life every day (1-3). Use of nanomaterials has increased significantly in devices such as nanofilms, nanoparticles, nanowires and nanoclusters due to biomedical applications in tissue engineering, drug-gene delivery, and biosensors [4-6].

Nanomaterials from copper, zinc, magnesium, titanium, gold, silver, dielectric and semiconductor been developed [7-11]. Silver and gold nanoparticles showed highest possibilities as they displayed significant antibacterial activities [12-14]. Of all the methods involve in nanoparticle production, the use of plants extract eliminates the conditions of high temperature, pressure, energy and the use of harmful and less expensive reducing agents [15].

Increase in risk of spread of disease, debility, severe illness and mortality due to antimicrobial resistance is a major worldwide health challenge. It was estimated to be associated with close to 5 million deaths across the globe in 2021. This is caused majorly due to drug misuse, and also lack of adequate access to appropriate new and existing vaccines and medicines among locals [16].

Recently efforts are directed on developing new antimicrobial agents that can effectively eliminate bacteria, hence, it is imperative to find novel antimicrobial treatment agents. Nature holds an unlimited pool of agents that could serve as alternatives to combat the growing threat of antimicrobial resistance. In the recent time, there is an increase interest in phytochemicals from medicinal plants which could serve as potential sources of antimicrobial drugs as reliable alternative which have been affirmed from scientific sources.

Anogeissus latifolia is a member of Combretaceae family. It's a medium-sized tree of 20-36 meters in height. Several studies have reported that *Anogeissus leiocarpus* possess potentials for activities against microorganisms, parasitic worms and other parasitic disease agents [17-19]. Lately, the use of plant nanoparticles as antimicrobial agent is a new field of study. Synthesis and antimicrobial properties of some AgNPs with several plant extracts have been reported [20-22]. Our group have reported synthesis, characterization and antimicrobial activity of some AgNPs using different plant extracts [23-25]. In the present study, AgNPs was prepared using a low cost, simple and environmentally friendly method using the leaf extracts of *A. leiocarpus*. The effect of different experimental variables, such as concentration of $AgNO_3$, time, percentage of ethanolic plant extract used and volume ratio of plant extract to $AgNO_3$ solution on the synthesis of the silver nanoparticles were studied. The characteristics (size and morphology) of metal nanoparticles are influenced by the various synthesis parameters which determines the uses and applications of nanoparticles [26]. In this study, AgNPs was prepared using

the leaf *A*. *leiocarpus.* This study aims at examining the best conditions of synthesis of *A*. *leiocarpus* silver nanoparticle and also to determine their usefulness as potential alternative antimicrobials.

2. MATERIALS AND METHODS

2.1 Preparation of plant extract

Anogeissus leiocarpus leaves were collected and identified at Forest Research Institute of Nigeria. $AgNO_3$ salt used was prepared from Merck Company (Germany). Freshly collected leaves were washed and air-dried at 32°C for 48 hours. Leaves were ground and boiled for 10 minutes in 40% ethanol in the ratio 1:10.

Figure 1: *Anogeissus leiocarpus* leaves

2.2 Synthesis of silver nanoparticles

Equal amount (10 mL) of extract and aqueous solution of $AgNO_3$ were heated at 70°C for 60 minutes. A colour changed from light brown to deep brown was noticed which confirms production of nanoparticle. The formation of *A. leiocarpus* silver nanoparticles (ALNP) was also confirmed by UV spectrophotometer.

2.3 Effect of amount of $AgNO_3$

About 5 mL of 1 mM solution of $AgNO_3$ was added to 5 mL extract and heated at 70 °C for 10 mins. A change in colour was observed which indicates the formation of nanoparticles. The absorbance of the resulting solutions was measured spectrophotometrically. This was repeated with various amount of silver salt solution (2 and 3mM).

2.4 Effect of time

Mixture of equal volume of plant extracts and 1 mM $AgNO_3$ was incubated. Sample of the mixtures was taken at time intervals of 0, 15, 30, 45 and 60 minutes of the reaction and the absorbance taken.

2.5 Effect of ratio of volume of plant extract to $AgNO_3$ *solution*

An equal volume of extract ratios (1:1, 1:2 and 1:3) and the silver salt was heated at 70 °C and colour changed from light brown to dark brown. The UV absorbance of the mixture was taken.

2.6 Effect of Concentration of ethanol solvent used in preparing the extract

Equal volume of different concentrations (10%, 20%, 30%, 40% and 50%) of ethanol solvent was reacted with the same volume of leaf extract at 70°C for about an hour. A change in the colour of the reaction was used to confirm the formation of nanoparticles.

2.7 Antimicrobial assay

The agar diffusion plate method was used for the antibacterial assay while surface plate method was employed for the antifungal assay. Human pathogenic organisms consisting of four bacteria; 2 Gram positive (*Bacillus subtilis* and *Staphyloccocus aureus*) and 2 Gram-negative bacteria (*Pseudomonas aeruginosa* and *Escherichia coli*) were used for the antibacterial assay. For antifungal assay, one yeast (*Candida albicans*) and three molds (*Aspergillus niger, Penicillium notatum Rhizobium stolonifer*) were used. The microorganisms were obtained from the Faculty of Pharmacy, University of Ibadan. Nutrient agar, nutrient broth, sabourand dextrose agar (SDA), tryptone soya broth agar from Oxoid Laboratories, U.K were used in the study. Methanol (40%) was in used to dissolve the drugs and also served as negative control in the assay. The agar cup well (diameter =8 mm) diffusion and agar broth tube dilution procedures were in the study. Gentamicin (0.5 mg\ml) and Tioconazole (70 µg/mL) served as reference antibacterial and antifungal drug.

2.8 Statistical analysis

Results were analyzed with SPSS software, while the analysis of variance was used to determine significant differences between the values under the experimental conditions examined.

3. RESULTS AND DISCUSSION

3.1 The effect of various operational variables

The rate of formation of AgNs increased with increase in reaction time (from 0-60 minutes) with slight shift in the absorption maxima indicative of variation in the particle size. (Figure 3a). Optimum concentation for *A. leiocarpus* was10^{-3} M (Figure 3b).Excess silver ion is required for optimum synthesis of ALNP (Figure 3c).Change in the concentration of ethanol solvent used during formation of AgNPs is negligible Figures 3d.

3.2 Antimicrobial Result

Anogeissus leiocarpus NP showed dose dependent inhibitory activity against the whole organism in the antimicrobial assay. *P. aeruginosa* was the most susceptible organism while *Rhizobium stolonifera* showed least activity. Other members of the family Combretaceae such as *Anogeisuss acuminata* and *Anogeissus latifolia* palladium nanoparticle have demonstrated similar antimicrobial activity [27, 28]. In all the assays, the synthesized AgNPs demonstrated lower activities than the reference drugs Table 1.

3.3. Discussion

Addition of leaf extract of *A. leocarpus* reduced Ag^+ to Ag metal nanoparticles which caused the observed colour change from faint brown to dark brown ascribed to the surface plasmon resonance phenomenon (SPR) [29]. The synthesized nanoparticles showed a spectrum range around 420 to 460 nm which agree to literature reports that gave AgNPs spectrophotometric absorption measurements in the wavelength ranges between 400-450 nm [30]. The aggregation of the silver nanoparticles in the solution is shown by the presence of broad resonance (Figure 2). The green reduction of the Ag^+ occurs speedily with over 90% of reduction of Ag^+ ions accomplished in less than 1 h after its addition to the leaf extract. Higher SPR peaks intensities were observed at the higher time intervals which indicate the increase in the production of silver nanoparticles (Figure 2a). After addition of the leaf extract to silver nitrate solution at different ratios, the curve shows increased absorbance at higher concentration (3mM) (Figure 2b) and high volume ratio.

The antimicrobial activity of silver nanoparticles synthesized by natural plants extract was investigated against various pathogenic organisms. The synthesized silver nanoparticles showed efficient antimicrobial property due to their extremely large surface area, which provides better contact with microorganisms. The antibacterial activities of metal nanoparticles from *A. leocarpus* leaf extract showed similar and comparable results to other silver nanoparticles from other plant [31,32].

Table 1: Antimicrobial activity of AgNP

Plant/Concentration (mg/mL)	S.a	E.c	B. sub	Ps.a	C.a	A.u	P.n	R.n
A. Leiocarpus								
100	20	24	24	26	20	18	18	16
50	18	20	22	20	18	16	16	14
25	14	18	18	18	16	14	14	12
12.5	12	14	16	14	14	12	12	10
6.25	10	12	12	12	12	10	10	_
3.125	_	10	10	10	10	_	_	_
-ve (40% Methanol)	_	_	_	_	_	_	_	_
+ve	40	38	38	40	28	26	28	28

Key: +ve = Gentamicin 10 µg/mL (Bacteria), Tioconazole 70 µg/mL (Fungi), *Staphylococcus aureus* (S. a), *Esherichia coli* (E.c), *Bacillus subtilis* (B.sub), *Pseudomonas aeruginosa* (Ps.a), *Candida albicans* (C.a), *Aspergillusniger* (A.u), *Penicilliumnotatum* (P.n), *Rhizobium stolonifer* (R.s).

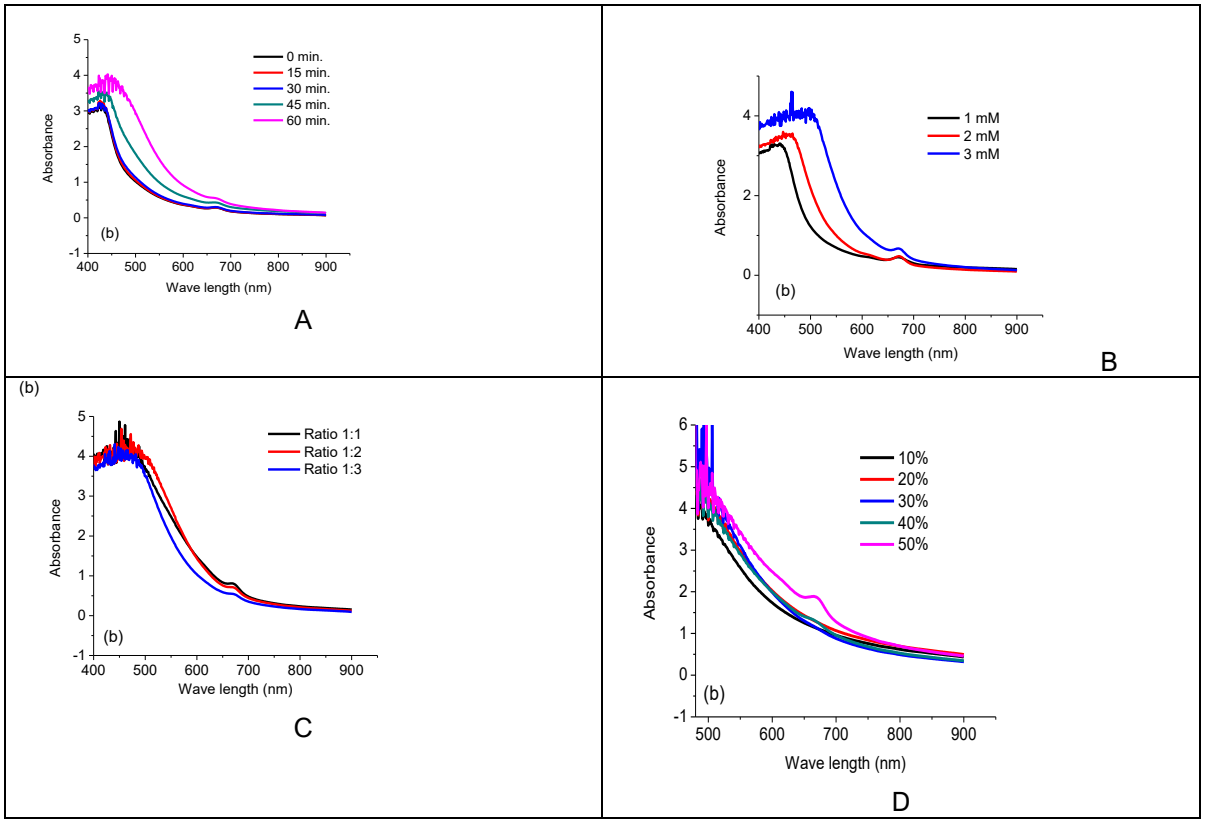

Figure 2a: Effects of time on AgNPs formation *A. leiocarpus*, 2b: Effects of concentration of $AgNO_3$ on AgNPs formation *A. leiocarpus*
2c: Results of change in ratio of $AgNO_3$ solution to plant extracts on AgNPs formation *A. leiocarpus*,
2d: Effects of concentration of ethanolic solvents on AgNPs formation *A. leiocarpus*

4. CONCLUSION

Anogeissus leiocarpus leaf extracts demonstrated reducing ability for the synthesis of the Ag nanoparticles. The concentration of the extract was the most effective parameter for optimization. The synthesized AgNPs showed effective antifungal and antibacterial activities.

REFERENCES

1. Islam, S., Ahmed, M. M. S., Islam, M. A., Hossain, N. and Chowdhury, M. A. 2025. Advances in Nanotechnology in targeted drug delivery–A review. Results in Surfaces Interfaces. 19:100529.
2. Kumari, S., Raturi, S., Kulshrestha, S., Chauhan, K., Dhingra, S., András, K., and Singh, T. 2023. A comprehensive review on various techniques used for synthesizing nanoparticles. Journal of Materials Research and Technology 27:1739-1763.
3. Zheng, X., Zhang, P., Fu, Z., Meng, S., Dai, L. and Yang, H. 2021. Applications of nanomaterials in tissue engineering. RSC advances 11(31):19041-19058.
4. Melchor-Martínez, E. M., Torres Castillo, N.E., Macias-Garbett, R., Lucero-Saucedo, S. L., Parra-Saldívar, R. and Sosa-Hernández, J. E. 2021. Modern world applications for nano-bio materials: tissue engineering and COVID-19. Frontiers in Bioengineering and Biotechnology 9:597958.
5. Jamkhande, P. G., Ghule, N. W., Bamer, A. H. and Kalaskar, M. G. 2019. Metal nanoparticles synthesis: An overview on methods of preparation, advantages and disadvantages, and applications. Journal of Drug Delivery Science and Technology 53: 101174.
6. Roldan, C. B. 2013. Metal nanoparticle catalysts beginning to shape-up. Accounts of Chemical Research 46(8):1682-1691.
7. Srivastava, S., Usmani, Z., Atanasov, A.G., Singh, V.K., Singh, N.P., Abdel-Azeem, A.M., Prasad, R., Gupta, G., Sharma, M. and Bhargava, A. 2021. Biological nanofactories: Using living forms for metal nanoparticle synthesis. Mini Reviews in Medicinal Chemistry 21(2):245-265.
8. Kumar, H., Venkatesh, N., Bhowmik, H. and Kuila, A. 2018. Metallic nanoparticle: a review. Biomedical Journal of Science Technology Research 4(2):3765-3775.
9. Rim, Y. S., Bae, S. H., Chen, H., De Marco, N. and Yang, Y. 2016. Recent progress in materials and devices toward printable and flexible sensors. Advanced Materials 28(22): 4415-4440.
10. Khalil, M. M., Ismail, E. H., El-Baghdady, K. Z. and Mohamed, D. 2014. Green synthesis of silver nanoparticles using olive leaf extract and its antibacterial activity. Arabian Journal of Chemistry 7(6): 1131-1139.
11. Zhang, X. F., Liu, Z. G., Shen, W. and Gurunathan, S. 2016. Silver nanoparticles: synthesis, characterization, properties, applications, and therapeutic approaches. International Journal of Molecular Sciences 17(9):1534.
12. Bruna, T., Maldonado-Bravo, F., Jara, P. and Caro, N. 2021. Silver nanoparticles and their antibacterial applications. International Journal of Molecular Sciences 22(13): 7202.
13. Burdușel, A. C., Gherasim, O., Grumezescu, A. M., Mogoantă, L., Ficai, A. and Andronescu, E. 2018. Biomedical applications of silver nanoparticles: an up-to-date overview. Nanomaterials 8(9):681.
14. Dauthal, P. and Mukhopadhyay, M. 2016. Noble metal nanoparticles: plant-mediated synthesis, mechanistic aspects of synthesis, and applications. Industrial & Engineering Chemistry Research 55(36):.9557-9577.
15. Khan, S., Ahsan, F., Mahmood, T., & Bano, S. 2024. *Anogeissus latifolia*: a comprehensive review from ethanobotanical insights to future pharmacological frontiers. Chemistry & Biodiversity, 21:12, e202401378.
16. Salih, E. Y., Julkunen-Tiitto, R., Luukkanen, O., Sipi, M., Fahmi, M. K., and Fyhrquist, P. J. 2020. Potential anti-tuberculosis activity of the extracts and their active components of *Anogeissus leiocarpa* (Dc.) guill. and perr. with special emphasis on polyphenols. Antibiotics 9(7):364.
17. Qubtia, M., Ghumman, S. A., Noreen, S., Hameed, H., Noureen, S., Kausar, R. and Jardan, Y. A. B. 2024. Evaluation of plant-based silver nanoparticles for antioxidant activity and promising wound-healing applications. ACS omega, 9(10): 12146.
18. Mukhtar, Y., Abdu, K., and Maigari, A. K. 2017. Efficacy of *Anogeissus leiocarpus* (DC.) as potential therapeutic agent against Trypanosomiasis diseases: A review. International Journal of Health and Pharmaceutical Research, 3(3):1-9.

19. Thomas, S., Gonsalves, R. A., Jose, J., Zyoud, S. H., Prasad, A. R. and Garvasis, J. 2024. Plant-based synthesis, characterization approaches, applications and toxicity of silver nanoparticles: a comprehensive review. Journal of Biotechnology 394:135-149.
20. Sampath, S., Hari, A., George, B., Law, D., Omarov, Y., Eftekhari, A., Shukurova, A. Hasanova, A. and Mohamed, A. J. 2026. Green synthesized silver nanoparticles from *Artocarpus hirsutus* flower extract induced cytotoxicity and apoptosis in HT29 colon cancer cells. Discover Nano 21: 384
21. Shahzadi, S., Fatima, S., Shafiq, Z., and Janjua, M. R. S. A. 2025. A review on green synthesis of silver nanoparticles using plant extracts: a multifaceted approach in photocatalysis, environmental remediation, and biomedicine. RSC advances 15(5): 3858-3903.
22. Jiang, X., Khan, S., Dykes, A., Stulz, E., and Zhang, X. 2025. Biogenic synthesis of silver nanoparticles and their diverse biomedical applications. Molecules 30(15): 3104.
23. Ogunsile, B. O., Seyinde, D. O. and Salako, B. A. 2020. Green synthesis of silver nanoparticles from leaf extract of *Tetrapleura tetraptera* and its antimicrobial activity. In IOP Conference Series: Materials Science and Engineering 805(1):012032.
24. Fadare, D. A., Yussuf, L. A., Oladokun, M. S. and Ogunsile, B. O. 2025. Mushroom-Mediated Synthesis of Ag, Fe, and Ag-Fe Nanoparticles of *Pleorotus ostreatus*: Surface Characterization and Antimicrobial Activity. Archives of Basic and Applied Medicine, 13(2):80-90.
25. Ogunsile, O. B., Okoh, O. S., Ejidike, I. P. and Omolaja, O. R. 2024. Biosynthesis and optimization of AgNPs yield from *Chromolaena odorata* leaf extract using response surface methodology (RSM).
26. Dada, A. O., Adekola, F. A., Dada, F. E., Adelani-Akande, A. T., Bello, M. O., Okonkwo, C. R., ... and Adetunji, C. O. 2019. Silver nanoparticle synthesis by *Acalypha wilkesiana* extract: phytochemical screening, characterization, influence of operational parameters, and preliminary antibacterial testing. Heliyon, 5:10.
27. Mishra, M. P., and Padhy, R. N. 2018. Antibacterial activity of green silver nanoparticles synthesized from *Anogeissus acuminata* against multidrug resistant urinary tract infecting bacteria *in vitro* and host-toxicity testing. Journal of Applied Biomedicine, 16(2):120-125.
28. Kumar, R., Tanwar, B., Sharma, V., and Hajam, Y. A. 2025. Botany, traditional uses, phytochemistry, and pharmacological profile of *Anogeissus latifolia* (Roxb. Ex Dc) Wall. a review. Discover Plants, 2(1): 99.
29. Shivaji, K., Mani, S., Ponmurugan, P., De Castro, C. S., Lloyd Davies, M., Balasubramanian, M. G., & Pitchaimuthu, S. 2018. Green-synthesis-derived CdS quantum dots using tea leaf extract: antimicrobial, bioimaging, and therapeutic applications in lung cancer cells. ACS Applied Nano Materials, 1(4):1683-1693.
30. Niloy, M. S., Hossain, M. M., Takikawa, M., Shakil, M. S., Polash, S. A., Mahmud, K. M.,.. and Ranjan Sarker, S. 2020. Synthesis of biogenic silver nanoparticles using *Caesalpinia digyna* and investigation of their antimicrobial activity and *in vivo* biocompatibility. ACS Applied Bio Materials, 3(11): 7722-7733.
31. Mishra, S., Sundaram, S., Srivastava, S., and Dhar, R. 2023. Phytosynthesis of silver nanoparticles using *Oscimum sanctum* leaf extract and studies on its antidiabetic, antioxidant, and antibacterial properties. ACS Applied Bio Materials, 6(10): 4127-4137.
32. Abdallah, B. M., and Ali, E. M. 2021. Green synthesis of silver nanoparticles using the *Lotus lalambensis* aqueous leaf extract and their anti-candidal activity against oral candidiasis. ACS omega, 6(12): 8151.

ISBN: 978-978-67-0285-8 DOI: https://doi.org/10.55455/acsnigeria.1.3.56-65

Teacher Education in the Digital Era Through Technological Transformation Pedagogy in Nigeria

Yakubu Rufai[1,2] and Suleiman Kabiru[2]
[1]Department of Chemistry, Faculty of Science, Universiti Teknologi Malaysia (UTM), 81310 Johor Bahru, Johor, MALAYSIA
[2]Chemistry Department, Federal College of Education (FCE) Okene P.M.B 1062 Kogi State, NIGERIA
Corresponding Author's email: yakubu.rufai1852@fceokene.edu.ng; +2348065294211
DOI: https://doi.org/10.55455/acsnigeria.1.3.56-65

ABSTRACT

Teacher education systems worldwide face pressure to integrate digital technologies meaningfully into pre-service preparation. In Nigeria, demographic expansion, infrastructural constraints, and curricular rigidity make this imperative both urgent and complex. This analysis examines Nigeria's teacher education landscape in the digital era, synthesizing policy documents, empirical studies (2020–2025), and institutional audits across 24 teacher education institutions. Grounded in the Technological Pedagogical Content Knowledge (TPACK) framework and Sen's Capability Approach, the study positions digital competence as an enabling capability for pedagogical agency rather than a technocentric end. Findings reveal persistent gaps between national digital-education policies and ground-level practice: inadequate infrastructure (only 28% of institutions report reliable electricity), low ICT self-efficacy among teacher educators (68% use technology solely for administrative tasks), fragmented curriculum integration, and weak public–private partnerships. Emergent initiatives mobile-based micro-credentialing, virtual teaching-practicum platforms, and community driven open educational resource repositories demonstrate scalable potential. The paper advances a four-pillar framework for systems-oriented digital re-professionalization: curriculum infusion, continuous professional learning ecosystems, adaptive infrastructure investment, and robust monitoring-evaluation mechanisms, aligned with SDG 4.c and African Union Agenda 2063.

KEYWORDS: Teacher education; digital pedagogy; ICT integration; digital literacy; capability approach

1. INTRODUCTION

Teacher education is the cornerstone of educational quality and equity. Teacher preparation in Nigeria did not start as a digital enterprise, but as a formal teacher training dated to the immediate post-independence period. The recommendation of Ashby Commission's led to an expansion of teacher training colleges, establishment of colleges of education and the National Teachers' Institute as parallel routes into the profession (Saidu & Saliu, 2025). Also, the National Policy on Education formalized the Nigeria Certificate in Education (NCE) as the minimum qualification for classroom teaching, a standard that has anchored teacher-preparation curricula for over four decades (Federal Republic of Nigeria, 2014). That policy was developed for a print-based, lecture-and-examination model of instruction, produced a teaching corps trained primarily in content delivery, classroom management, and subject mastery, with comparatively little structural attention to instructional technology (Asaya, 2010). Nigeria is Africa's most populous nation, with a population exceeding 200 million people, and an estimated 20.2 million of its children and youth remain out of school, one of the highest national totals recorded globally (UNESCO

Institute for Statistics & Global Education Monitoring Report, 2022). Because teacher supply and quality are central to progress toward Sustainable Development Goal 4, the capacity of Nigeria's teacher-education system carries weight well beyond the colleges of education themselves. Yet as digital technologies reshape global knowledge production and assessment, Nigeria's teacher-education infrastructure remains anchored in an inheritance built for lecture-dominated, examination-focused instruction, rather than for hybrid teaching, open educational resources, or AI-mediated pedagogies.

Global frameworks such as UNESCO's ICT Competency Framework for Teachers (UNESCO, 2018) set out competencies for hybrid instruction, open educational resources, and technology-integrated pedagogy that presuppose an infrastructure and training base Nigerian teacher education was not

originally built to provide. Technology-integrated pedagogy grounded in the Technological Pedagogical Content Knowledge (TPACK) framework treats effective technology use as an interaction between subject knowledge, teaching method, and tool, rather than technology added onto existing instruction; Zhang et al. (2025) found that a technology-enhanced active learning environment measurably improved this integrated competency among pre-service teachers. Flipped-classroom pedagogy, in which content delivery precedes class time so that class time is reserved for application and discussion, has been studied as a variant of blended learning that deliberately recombines face-to-face and digital instruction (Lopes et al., 2024). It is frequently paired with gamified pedagogy as the use of points, badges, and leaderboard mechanics to sustain motivation with Borrás-Gené and Montes Díez (2025) reporting measurable gains in motivation and self-regulated learning among pre-service teachers taught through a gamified flipped-classroom design, and Sanz-Angulo et al. (2025) linking a similar blended, gamified methodology to gains in both academic performance and soft-skill development. Also, Halkiopoulos and Gkintoni (2024) reviewed how AI-based adaptive assessment models draw on cognitive neuropsychology to individualize instructional delivery, while Dharam Singh and Mohamad (2025) caution against conflating adaptive learning, which is largely performance-data driven, with genuine personalization, which requires accounting for learner identity, goals, and context as a distinction with direct implications for how teacher-education curricula should frame AI competency rather than treating it as a single undifferentiated skill.

Empirical assessments of ICT availability in teachers Education have repeatedly found resources largely unavailable, inaccessible, or underutilized in actual content delivery (Zubairu & Tukur, 2015), and evidence from other national contexts suggests this pattern is not unique to Nigeria: Landa (2025) found that infrastructural and training-related technological-pedagogical challenges significantly predicted whether university instructors in Tanzania actually used the technologies available to them. In response, the National Commission for Colleges of Education launched a 2025 review of the NCE Minimum Standards intended to embed AI awareness, data literacy, and adaptive digital pedagogy into teacher preparation (National Commission for Colleges of Education, 2025). Guided by Mishra and Koehler's (2006) TPACK framework and Sen's Capability Approach (1999), the analysis treats digital competence as an enabling capability rather than a hardware target, contributing an evidence-based synthesis of the digital landscape, a critical evaluation of emergent innovations, and a systems-oriented framework for digital re-professionalization.

2. BEYOND TECHNOCENTRIC INTEGRATION: INTEGRATING KNOWLEDGE DOMAINS FOR EFFECTIVE TECHNOLOGY USE

TPACK, developed by Mishra and Koehler (2006), conceptualizes effective technology integration as arising from the interaction of Technological, Pedagogical, and Content Knowledge and their derived combinations (TCK, TPK, PCK, and TPACK itself) (Koehler et al., 2013). Effective use requires understanding how technological affordances intersect with pedagogy and content in specific contexts (Voogt et al., 2013); a rural Katsina mathematics educator, for example, negotiates different digital affordances than an urban Lagos English educator (Adedoja & Adeyemi, 2024). Nigerian institutions, however, have often reduced digital competence to basic computer literacy, treating technology as a standalone subject rather than an integrated pedagogical tool (Okebukola&Okebukola, 2022). This reductionism appears in curriculum designs, in professional development divorced from pedagogical application, and in assessments that evaluate technological knowledge independently of teaching practice (Yusuf & Salawu, 2024). Recent scholarship extends TPACK through the concept of “TPACK-in-practice,” emphasizing sustained, situated application rather than decontextualized skills training (Rosenberg & Koehler, 2015), and shows that pre-service teachers need scaffolded, mentored experiences particularly relevant where Nigerian student teachers move directly from theoretical coursework to under-resourced school placements (Baran et al., 2011).

3. DIGITAL TOOLS AS EXPANSION OF HUMAN FUNCTIONING

Sen's (1999) Capability Approach shifts analytical focus from resource endowment to what individuals can do with available resources their substantive freedoms. Applied to digital teacher education, it redirects attention from inputs (tablets distributed, bandwidth capacity) to outcomes: what teachers can accomplish pedagogically with digital technologies (Zheng et al., 2023). This distinction matters in Nigeria, where mobile-phone ownership exceeds 85% of adults (National Bureau of Statistics, 2024) yet meaningful pedagogical use remains shallow; a teacher's capability to facilitate collaborative learning through cloud-based platforms depends on institutional support, mentoring networks, and incentives for innovation as much as on device access or connectivity (Adebayo &Okebukola, 2024). The approach distinguishes conversion factors—educator digital literacy, institutional culture, infrastructure reliability, policy environment from functionings, the abilities educators realize, such as designing digitally enhanced lessons or assessing learning through technology-mediated tools (Robeyns, 2005). Structural inequalities in geography, institutional resources, gender, and prior technology exposure differentially shape how educators convert resources into capabilities (Zheng et al., 2023), a lens especially relevant to Nigeria's rural–urban divides. Together, TPACK and the Capability Approach frame the analysis that follows: TPACK articulates the knowledge structures required for effective integration, while the Capability Approach attends to the social and institutional conditions that enable or constrain their development.

4. STRUCTURE OF NIGERIAN TEACHER EDUCATION

Nigeria's teacher-education system comprises 36 Federal Colleges of Education, 52 State Colleges of Education, over 100 private colleges, and university Faculties of Education (National Commission for Colleges of Education, 2023). The Nigerian Certificate in Education (NCE), a three-year post-secondary credential, remains the predominant qualification, producing about 85,000 graduates annually (National Commission for Colleges of Education, 2024). The National Commission for Colleges of Education (NCCE), established in 1989, sets academic standards, accredits programs, and conducts institutional audits, most recently revising its Minimum Standards in 2023 (National Commission for Colleges of Education, 2023). The National Teachers' Institute (NTI), established in 1976, offers distance-education programs for in-service teachers, though its reach remains constrained by limited digital infrastructure (National Teachers' Institute, 2024).

5. POLICY FRAMEWORK FOR DIGITAL INTEGRATION

The National Policy on ICT in Education (2018) mandates ICT integration across NCE programs and requires pre-service digital-literacy competencies and systematic educator professional development (Federal Ministry of Education, 2018). The 2023 Revised NCE Curriculum introduced mandatory courses such as Digital Pedagogy, Educational Data Literacy, and Emerging Technologies in Education and requires digitally mediated teaching-practice components and proficiency in at least two digital assessment tools (National Commission for Colleges of Education, 2023). Implementation, however, lags considerably: a 2023 NCCE audit found only 31% of Federal Colleges of Education with functional ICT laboratories, fewer than 15% of educators certified in digital pedagogy, and just 12% of programs implementing the mandatory digital teaching-practice component (National Commission for Colleges of Education, 2023). These deficits reflect low education funding (about 5.7% of the federal budget, well below UNESCO's recommended 15–20%), weak coordination between policymaking and implementing agencies, and limited accountability mechanisms for institutional compliance.

6. PEDAGOGICAL CONSERVATISM AND EDUCATOR PREPAREDNESS

A mixed-methods study using simple random and systematic random sampling method of 412 teacher educators across 12 institutions found that 68% used ICT solely for administrative tasks, 44% believed

technology distracts from core teaching objectives, and only 22% had designed lessons meaningfully integrating open educational resources or interactive simulations (Yusuf & Salawu, 2024). Resistance and psychological unpreparedness were studied by Avakyan (2024), who used nearly 1,800 university teachers across nine Russian institutions treated pedagogical conservatism as a measurable trait, finding it linked to psychological unreadiness for innovation and to emotional burnout, and correlated with job satisfaction levels among teaching staff studied across multiple universities.

Griffiths and Goddard (2015), working from a case study of an educational software deployment, built an explanatory framework combining positioning theory, Heidegger's concept of readiness-to-hand, and Popperian ideas about social engineering to explain why teachers resist adopting technologies even when institutions push them toward it. Mirriahi, Vaid, and Burns (2015) found that resistance among academic staff to integrating technology into language teaching tracked closely with the Technology Acceptance Model's constructs of perceived usefulness and ease of use and argued that adoption decisions often overlook the actual pedagogical value of the tools involved. Also, Institutional and structural conservatism by Zemsky and Massy's (2004) widely cited report "Thwarted Innovation" made the case, discussed in later journal literature, that the spread of ICT and online learning in American higher education had, if anything, entrenched conservative teaching practices rather than displacing them since the implementation of ICT and online learning has increased conservatism in American higher education. This connects to Ibatullina and Vorontsova's (2011) treatment of pedagogical conservatism as a structural barrier that institutions must actively work to overcome through defined organizational conditions, not just individual attitude change. Moreso, Ideological and philosophical framing by Bowers's (1980) much older but still-cited piece in Teachers College Record examined the assumption that technological progress in education is inherently good, framing that assumption itself as a form of conservatism dressed up as innovation, a critique of what he called technicism in curriculum thinking presenting a critique of technological consciousness in education from the perspective of philosophical conservatism. Prestridge's (2017) work in Technology, Pedagogy and Education takes a related but more applied angle, examining how teachers' existing pedagogical orientations shape which uses of technology they accept and which they filter out or reject. This pedagogical conservatism reflects legitimate concerns about assessment validity and classroom management, and a lack of institutional support and professional incentives, rather than mere resistance to change (Okebukola&Okebukola, 2022). Digital self-efficacy is a critical mediating variable: educators with higher self-efficacy are significantly more likely to experiment with innovative pedagogies and persist through technological challenges, yet fewer than 30% of Nigerian teacher educators report high digital self-efficacy, and professional development programs rarely address this affective dimension (Yusuf & Salawu, 2024).

7. CURRICULUM–PRACTICE DISJUNCTURE

Although the 2023 NCE curriculum mandates courses in digital pedagogy, educational data literacy, and emerging technologies, observational research across 18 institutions found such courses taught predominantly as theoretical content, without laboratory components or authentic assessment tasks (Eze et al., 2023). Analysis of 326 teaching-practice placements in 2023 found that 87% of student teachers taught without using any digital tools, even in schools where technological infrastructure existed (National Commission for Colleges of Education, 2024). This misalignment undermines the formation of a “digital habitus,” as student teachers rarely see digital pedagogy modeled by their own instructors during formative field experiences. Contributing factors include teacher educators' outdated technology expertise (Okebukola&Okebukola, 2022), assessment of digital competencies through written examinations rather than authentic performance tasks, and partner schools that themselves lack technological resources for placement.

8. GOVERNANCE FRAGMENTATION AND ACCOUNTABILITY DEFICITS

Responsibility for teacher education in Nigeria is dispersed across the NCCE, the Federal Ministry of Education, State Universal Basic Education Boards, the NTI, and individual autonomous institutions (Afe, 2023). This fragmentation produces coordination challenges, policy redundancies, and monitoring gaps: no integrated national indicator system tracks graduates' digital teaching efficacy post-certification, and independent program evaluations remain rare (National Commission for Colleges of Education, 2023). The NTI's e-learning portal, despite its mandate for continuous professional development, reaches fewer than 5% of registered teachers, constrained by infrastructure and digital-literacy gaps (National Teachers' Institute, 2024). No standardized assessment framework verifies graduates' attainment of mandated digital competencies, allowing significant variation in implementation quality across institutions.

9. EMERGING INNOVATIONS AND SCALABLE OPPORTUNITIES (2020–2025)

Despite formidable systemic constraints, several pandemic-era innovations demonstrate promising, scalable pathways. They share common design features: mobile-first or low-bandwidth delivery, use of existing social technologies, integration with rather than replacement of traditional structures, and measurable impact on educator practice.

Mobile-First Micro-Credentialing Programs

The Digital Teaching Badge program, piloted in Ogun and Kaduna States (2022–2024), delivers competency-based training in mobile-assisted language learning, digital storytelling, and formative e-assessment via USSD and WhatsApp platforms requiring no internet connectivity (EduTech Africa, 2024). Over 1,200 teacher educators completed Level 1 certification, with 78% reporting increased classroom technology use and 65% designing at least one mobile-integrated lesson within three months; the NCCE now accredits these credentials for professional advancement (EduTech Africa, 2024).

Virtual Teaching Practicum Platforms

Obafemi Awolowo University and Ahmadu Bello University developed Virtual Teaching Practicum (VTP) systems combining live-streamed lessons in partner schools, VR-based classroom-management simulations, and AI-assisted feedback on recorded teaching performances (Ojo et al., 2024). A quasi-experimental comparison (VTP participants, n = 210, vs. traditional practicum students, n = 198) found VTP participants scored 23% higher on digital lesson-design rubrics, though traditional-practicum students showed advantages in physical classroom management—suggesting hybrid models may optimize student-teacher development (Ojo et al., 2024). The Tertiary Education Trust Fund's Digital Practicum Grant Initiative has funded 12 universities (₦450 million, roughly $300,000) with plans to reach 30 institutions by 2026 (Tertiary Education Fund, 2024).

Community-Driven Open Educational Resource Repositories

NaijaLessonBank, developed by teacher educators in Enugu and Rivers States, curate’s curriculum-aligned resources in English and Nigerian Pidgin on Kolibri, an offline-capable platform, distributing content via WhatsApp channels and portable storage devices (Nwachukwu &Emejulu, 2024). By late 2024 it had registered over 15,000 users, with 42% demonstrating repeat engagement ata notably higher retention rate than many formal professional development programsreflecting the value of linguistic and cultural contextualization and community-driven, participatory development over donor-dependent models (Nwachukwu &Emejulu, 2024).

10. TOWARD SYSTEMIC DIGITAL RE-PROFESSIONALIZATION: A FOUR-PILLAR FRAMEWORK

Building on this analysis of challenges and emergent innovations, a four-pillar framework integrates curriculum design, professional capacity development, infrastructure investment, and accountability mechanisms toward developing educator capabilities rather than merely installing technological resources.

Curriculum Infusion Rather Than Curriculum Addition

Standalone "ICT for Teachers" courses should be replaced with discipline-specific digital pedagogy infused throughout subject methodology courses—for example, dynamic geometry software in mathematics education or multimodal composition in language education—so that student teachers develop integrated TPACK rather than isolated competencies in each domain (Koehler et al., 2013). Curricula must also address emerging competencies including ethical AI literacy, data privacy in learning management systems, and recognition of algorithmic bias, as artificial intelligence increasingly mediates educational processes (Crompton et al., 2024).

Continuous Professional Learning Ecosystems

Sustainable transformation requires moving beyond episodic, workshop-based development toward embedded support: Digital Mentor Tutor positions within each academic department, incentivized through reduced teaching loads and explicit consideration in promotion criteria, can model effective practice and facilitate professional learning communities embedded within existing institutional structures. Partnerships with technology companies should be structured to build local facilitator capacity rather than create dependency on external providers.

Adaptive Infrastructure Investment

Infrastructure development should prioritize adaptive, sustainable technologies appropriate to Nigerian contexts solar-powered, offline-capable hubs such as RACHEL and Kolibri, and tiered connectivity solutions matching local infrastructure (4G LTE in urban areas, LoRaWAN in rural areas, TV white-space technologies where feasible) rather than importing high-resource models. Device strategies should accommodate the reality that many educators' own smartphones even where institutions lack computer laboratories, using mobile-optimized platforms while ensuring institutional access for students who lack personal devices.

Robust Monitoring, Evaluation, and Learning Systems

National indicators for digital-teaching efficacy should move beyond infrastructure inputs to measure actual practice and outcomes for example, the proportion of graduates regularly using two or more digital formative-assessment tools, and pre- and post-practicum TPACK self-efficacy. Annual NCCE Digital Readiness Audits should assess effective use rather than infrastructure stock alone and inform performance-based resource allocation. Partnerships between teacher-education institutions and research centers, potentially supported through TETFundresearch grants, could generate the rigorous comparative evidence currently lacking.

11. DISCUSSION: IMPLICATIONS AND FUTURE DIRECTIONS

This analysis demonstrates the value of integrating TPACK and the Capability Approach: TPACK articulates necessary knowledge structures, while the Capability Approach directs attention to the

conversion factorsinstitutional support, professional development quality, infrastructure reliability that mediate their translation into practice. It also extends understanding of the gap between policy intentions and institutional practice, illustrating that policy articulation, though necessary, is insufficient without accompanying capacity building, resource allocation, and accountability, consistent with implementation-science research emphasizing context, capacity, and culture (Fixsen et al., 2005). Examination of emergent innovations reveals design principles with applicability beyond Nigeria: leveraging ubiquitous technologies, employing low-bandwidth or offline-capable platforms, integrating with existing institutional structures, and building local capacity through participatory approaches.

Policy Implications

Curriculum revision alone, absent parallel investment in educator capacity, infrastructure, and accountability, will not achieve intended outcomes; policy coherence across these domains is essential. Infrastructure investment should prioritize adaptive, context-appropriate technologies solar power, offline-capable platforms, mobile-first approaches over imported high-resource models dependent on reliable electricity or high-bandwidth connectivity. Professional development must shift from episodic workshops to embedded, ongoing learning ecosystems with genuine institutional incentives, and partnerships with technology companies should emphasize local capacity building. Accountability mechanisms must evolve beyond infrastructure inventories to assess actual use, educator competencies, and graduate outcomes, with performance-based funding tied to demonstrated progress.

Limitations and Future Research

Available evidence concentrates in certain geographic regions and institution types, with limited evidence from smaller private or rural colleges. Most studies employ cross-sectional designs, limiting understanding of how digital competencies develop over time or evolve during graduates' early teaching years. The analysis also focuses predominantly on formal institutions, with limited attention to alternative pathways such as online programs or informal professional learning. Future research should compare professional-development models for building teacher-educator TPACK in Nigerian contexts, examine how different infrastructure configurations affect educator practice and student-teacher outcomes, and identify factors predicting sustained technology integration among graduates during their initial teaching years.

12. CONCLUSION

Nigerian teacher education stands at a critical juncture. Persisting with predominantly analog teacher preparation constitutes pedagogical malpractice in classrooms already shaped by digital-native learners, even in under-resourced communities, yet uncritical techno-solutionism—imported platforms, donor-driven hardware distributions, superficial adoption risks reproducing dependency and inequity. The path forward is digital re-professionalization: reconceiving teaching as a digitally fluent, critically reflective, contextually inventive practice, and repositioning teachers from passive technology recipients to active design partners in Nigeria's digital education future. Success will be measured not by syllabus compliance but by whether newly certified teachers can apply digital tools purposefully toward locally relevant pedagogical goals. Mobile-first approaches, virtual practicum platforms, and community-driven resources demonstrate that pathways exist; scaling these innovations through comprehensive curriculum infusion, professional learning ecosystems, adaptive infrastructure, and robust accountability mechanisms offers a realistic route to sustainable transformation one aligned with Sustainable Development Goal 4.c and African Union Agenda 2063.

REFERENCES

Adebayo, R. A., &Okebukola, P. A. (2024). Beyond gadgetry: Rethinking ICT investment in Nigerian education. *African Educational Review, 21*(1), 112–130.

Adedoja, G., & Adeyemi, T. (2024). Digital divide and teacher preparation in rural Nigeria: A geospatial analysis. *Journal of Research in Innovative Teaching & Learning, 17*(2), 178–194.

Afe, E. S. (2023). Reconceptualizing teacher education for sustainable national development in Nigeria. *Journal of Educational and Social Research, 13*(1), 1–12.

Asaya, S. A. (2010). Management of teaching practice in the preparation of Nigerian Certificate of Education (NCE) teachers. *Journal of College Teaching & Learning, 7*(11), 25–32.

Avakyan, I. B. (2024). Pedagogical conservatism of university teachers. *Izvestiya of Saratov University. Educational Acmeology. Developmental Psychology, 13*(1), 80–90. https://doi.org/10.18500/2304-9790-2024-13-1-80-90

Baran, E., Chuang, H.-H., & Thompson, A. (2011). TPACK: An emerging research and development tool for teacher educators. *Turkish Online Journal of Educational Technology, 10*(4), 370–377.

Borrás-Gené, O., & Montes Díez, R. (2025). Improving motivation in future teachers: Flipped classroom and gamification using digital badges. *Journal of Information Technology Education: Innovations in Practice, 24*, Article 21. https://doi.org/10.28945/5634

Bowers, C. A. (1980). Ideological continuities in technicism, liberalism, and education. *Teachers College Record, 81*(3), 293–321.

Crompton, H., Burke, D., Jordan, K., & Wilson, S. (2024). Learning with technology: A systematic review of artificial intelligence applications in K-12 education. *British Journal of Educational Technology, 55*(1), 18–43.

Crompton, H., Jones, M. V., & Burke, D. (2022). Affordances and challenges of artificial intelligence in K-12 education: A systematic review. *Journal of Research on Technology in Education, 54*(5), 613–635. https://doi.org/10.1080/15391523.2022.2121344

Dharam Singh, H. K., & Mohamad, S. K. (2025). Decoupling personalised and adaptive learning in AI-enhanced education: A narrative review and conceptual clarification.

Innovative Teaching and Learning Journal, 9(2), 470–483. https://doi.org/10.11113/itlj.v9.203

EduTech Africa. (2024). *Digital Teaching Badge impact evaluation: Ogun and Kaduna States pilot program (2022–2024)*. EduTech Africa Research Unit.

Eze, S. C., Chinedu-Eze, V. C., & Bello, A. O. (2023). ICT infrastructure and teacher education in Nigeria: A multilevel analysis of implementation challenges. *International Journal of Educational Development, 96*, Article 102691.

Federal Ministry of Education. (2018). *National policy on ICT in education*. Federal Ministry of Education.

Federal Ministry of Education. (2019). *National policy on information and communication technologies (ICT) in education*. Federal Government of Nigeria. https://education.gov.ng/wp-content/uploads/2019/08/national-policy-on-ict-in-education-2019.pdf

Federal Republic of Nigeria. (2014). *National policy on education* (6th ed.). NERDC Press.

Fixsen, D. L., Naoom, S. F., Blase, K. A., Friedman, R. M., & Wallace, F. (2005). *Implementation research: A synthesis of literature*. National Implementation Research Network, University of South Florida.

Griffiths, D., & Goddard, T. (2015). An explanatory framework for understanding teachers' resistance to adopting educational technology. *Kybernetes, 44*(8/9), 1240–1250. https://doi.org/10.1108/K-11-2014-0274

Halkiopoulos, C., &Gkintoni, E. (2024). Leveraging AI in e-learning: Personalized learning and adaptive assessment through cognitive neuropsychology. A systematic analysis. *Electronics, 13*(18), Article 3762. https://doi.org/10.3390/electronics13183762

Haruna, F. R. (2025). *State of governance and management in Federal Colleges of Education in Nigeria* [Keynote address]. TNTT, 21. https://ncce.gov.ng/uploads/tntt-articles/52d41692-6d91-44ed-869e-b02827c4899c.pdf

Ibatullina, E. Y., & Vorontsova, T. V. (2011). Overcoming pedagogical conservatism in the course of innovative educational process in educational institutions. *RUDN Journal of Psychology and Pedagogics*, (S5), 182–187.

Koehler, M. J., Mishra, P., & Cain, W. (2013). What is technological pedagogical content knowledge (TPACK)? *Journal of Education, 193*(3), 13–19.

Landa, E. (2025). Technological pedagogical challenges associated with the integration of technologies for teaching and learning in higher education. *Journal of Educational Technology Systems, 54*(1), 151–167. https://doi.org/10.1177/00472395251341392

Lopes, S. F. S. F., Simões, J. M. de A. P., Lourenço, J. M. R., & Morais, J. C. P. de. (2024). The flipped classroom optimized through gamification and team-based learning. *Open Education Studies, 6*(1), 1–8. https://doi.org/10.1515/edu-2022-0227

Mirriahi, N., Vaid, B. S., & Burns, D. P. (2015). Meeting the challenge of providing flexible learning opportunities: Considerations for technology adoption amongst academic staff. *Canadian Journal of Learning and Technology, 41*(1), 1–16. https://doi.org/10.21432/t25g71

Mishra, P., & Koehler, M. J. (2006). Technological pedagogical content knowledge: A framework for teacher knowledge. *Teachers College Record, 108*(6), 1017–1054.

National Bureau of Statistics. (2024). *Nigeria general household survey wave 7: ICT and digital access module*. NBS.

National Commission for Colleges of Education. (2023). *Revised minimum standards and guidelines for Nigerian Certificate in Education (NCE)*. NCCE.

National Commission for Colleges of Education. (2024). *Annual institutional audit report 2023: Digital readiness assessment*. NCCE Monitoring Directorate.

National Commission for Colleges of Education. (2025). NCCE reviews curriculum of education colleges [Press statement]. Voice of Nigeria. https://von.gov.ng/ncce-reviews-curriculum-of-education-colleges/

National Teachers' Institute. (2024). *Annual performance report 2023: Digital transformation initiatives*. NTI.

Nwachukwu, C., &Emejulu, C. (2024). Community-led open educational resources in multilingual contexts: Evidence from NaijaLessonBank. *Open Praxis, 16*(1), 45–62.

Ojo, A. B., Adeleke, M. A., & Ibrahim, F. (2024). Efficacy of virtual teaching practicum on pedagogical technology integration: A Nigerian quasi-experimental study. *TechTrends, 68*(4), 612–628.

Prestridge, S. (2017). Examining the shaping of teachers' pedagogical orientation for the use of technology. *Technology, Pedagogy and Education, 26*(4), 367–381. https://doi.org/10.1080/1475939X.2016.1258369

Robeyns, I. (2005). The capability approach: A theoretical survey. *Journal of Human Development, 6*(1), 93–117.

Rosenberg, J. M., & Koehler, M. J. (2015). Context and technological pedagogical content knowledge (TPACK): A systematic review. *Journal of Research on Technology in Education, 47*(3), 186–210.

Saidu, A., & Saliu, K. A. (2025). Teacher education in Nigeria: Trends in policy, reforms and challenges from 1960–2019. *Faculty of Education Journal*, Adekunle Ajasin University.

Sanz-Angulo, P., Galindo-Melero, J., De-Diego-Poncela, S., & Martín, Ó. (2025). Promoting soft skills in higher engineering education: Assessment of the impact of a teaching methodology based on flipped learning, cooperative work and gamification. *Education and Information Technologies, 30*(10), 13463–13506. https://doi.org/10.1007/s10639-025-13322-0

Selwyn, N. (2023). *Education and technology: Key issues and debates* (3rd ed.). Bloomsbury Academic.

Sen, A. (1999). *Development as freedom*. Oxford University Press.

Tertiary Education Trust Fund. (2024). *Digital Practicum Grant Initiative: Implementation report 2022–2024*. TETFund.

UNESCO. (2018). *ICT competency framework for teachers* (Version 3). UNESCO.

UNESCO Institute for Statistics & Global Education Monitoring Report. (2022). *New estimates on out-of-school children*. UNESCO.

UNICEF. (2024). *Nigeria education crisis: Out-of-school children assessment 2024*. UNICEF Nigeria Country Office.

Voogt, J., Fisser, P., Pareja Roblin, N., Tondeur, J., & van Braak, J. (2013). Technological pedagogical content knowledge: A review of literature. *Journal of Computer Assisted Learning, 29*(2), 109–121.

World Bank. (2024). *Nigeria digital economy diagnostic report*. World Bank Group.

Yusuf, M. O., & Salawu, R. O. (2024). Digital self-efficacy and pedagogical use of ICT among Nigerian teacher educators: A comprehensive mixed-methods analysis. *Computers and Education Open, 6*, Article 100168.

Zemsky, R., & Massy, W. F. (2004). *Thwarted innovation: What happened to e-learning and why*. University of Pennsylvania, The Learning Alliance.

Zhang, H., Wang, Z., Jiang, R., & Wu, H. (2025). Exploring the influence of technology-enhanced active learning environments on pre-service teachers' TPACK and technology beliefs. *SAGE Open, 15*(3). https://doi.org/10.1177/21582440251359823

Zheng, Y., Hatakka, M., Sahay, S., & Andersson, A. (2023). Conceptualizing development in information and communication technology for development (ICT4D). *Information Technology for Development, 24*(1), 1–14.

Zubairu, S. A., & Tukur, A. K. (2015). Assessment of availability, accessibility and utilization of information and communication technology resources in content delivery among lecturers in Federal Colleges of Education in Nigeria. *Sokoto Educational Review, 16*(2), 1–15. https://doi.org/10.35386/ser.v16i2.130

ISBN: 978-978-67-0285-8 DOI: https://doi.org/10.55455/acsnigeria.1.3.66-74

Predictive Modeling and Multivariate Optimization of Multi-Feedstock Biodiesel Blends Derived from African Star Apple (*Chrysophyllum albidum*) Seed Oil and Indigenous Lipid Streams

Joseph Nifu Barnabas, Noela Chinyelu Igwemmar, and Oluremi Isola Adeniran
Department of Chemistry, Faculty of Science, University of Abuja, PMB 117, Abuja, Nigeria
Corresponding Author's email: chemistbarnabasedu@gmail.com
DOI: https://doi.org/10.55455/acsnigeria.1.3.66-74

ABSTRACT

This data-driven predictive optimization framework, developed using IBM SPSS, optimizes multi-feedstock biodiesel mixtures derived from non-edible African star apple (*Chrysophyllum albidum*) seed oil (ASASO), palm kernel oil (PKO), and waste cooking oil (WCO). A total of 231 distinct blends were simulated using this approach. The performance of each blend composition with respect to key biodiesel fuel properties was modelled using Multiple Linear Regression Analysis (MLRA). Among the five fuel indices evaluated (kinematic viscosity, density, oxidative stability, higher heating value, and cetane number), kinematic viscosity was the best-predicted property ((R^2 = 0.739)). To identify high-quality fuel blends, blend configurations satisfying the optimal limits specified by ASTM D6751 were classified into three clusters using hierarchical cluster analysis based on Ward's method. A restricted blending window of 20–50% ASASO was identified as a viable range for simultaneously managing fluid flow resistance and oxidative stability. Within this range, the kinematic viscosity was maintained between 3.80 and 4.95 mm²/s, while oxidative stability exceeded 7.5 h. This approach replaces laborious and time-consuming empirical blending trials with a practical predictive framework for biodiesel formulation, thereby supporting the development of the green economy in West Africa through practical formulation indices.

KEYWORDS: *Chrysophyllum albidum*, Blending kinetics, Multiple linear regression, Hierarchical cluster analysis, Fuel property optimization.

1. INTRODUCTION

1.1 Global Energy Transition Context

Facing issues of global warming, energy consumption growing, and long-term energy security, the global energy market is currently undergoing an exceptional energy transition toward low-carbon energy. Being one of the major emitters of greenhouse gases as a result of continued dependence of the road transport system on petroleum, the transport sector Governments & intergovernmental organizations are committed to enhancing the utilization of renewable transport fuels to promote diversification, carbon mitigation, as well as overall energy resiliency[1]. Amongst the potential alternatives, biodiesel got much attention owing to its biodegradable and replenishable properties and compatible usage with conventional compression-ignition engines.

Biodiesel can be made from diverse biological origins, including the use of edible and non-edible oils and other waste products. However, this move is relatively far behind the developed economies. Many developing economies (particularly in Sub-Saharan Africa) are suffering from their dependence on imported petroleum products (owing to a lack of processing capacity) and failure to tap the huge amount of indigenous biomass available on the continent, consequently fuelling the energy security concern. For that, there is a need to harness non-edible oilseeds and waste streams towards designing decentralised biodiesel production to provide environmental benefits and to realize a circular bioeconomy[2,3]. However to capitalize this opportunity in efficiently, fuel compositions are essential scientifically optimized to ensure its adherence with the international standard as well as to capture the synergistic effects of local sources, therefore; data driven approach has opened the door for predicting fuel parameters that may support development of bio- diesel, reduce the cost associated with experiment, while also leading the way to facilitate the design of optimal bio fuel compositions[4].

1.2 Nigerian Energy Crisis and Biofuel Policy

Although Nigeria is endowed with large crude oil deposits, challenges persist in its downstream petroleum sector, including insufficient domestic refinery capacity, reliance on imported refined fuels, and repeated fuel shortages. These structural limitations have been further complicated by the recent removal of fuel subsidies, which has significantly increased transportation and logistics costs and intensified inflationary pressures throughout the economy. Consequently, rising diesel prices have adversely affected industrial activities, agricultural mechanization, electricity production, and road freight transportation, highlighting the need for stable, locally available alternative fuels to strengthen energy security and resilience against global petroleum price fluctuations[1]. In response to these and related challenges, Nigeria has introduced policies to scale up renewable energy and increase biodiesel's contribution to the domestic energy supply.

For example, the National Biofuel Policy and Incentives promotes the use of indigenous plant biomass resources to displace fossil-derived fuels and encourage rural economic development. Nigeria's commitment to achieving net-zero greenhouse gas emissions by 2060 has also renewed interest in producing second-generation biodiesel from non-food oil crops and waste materials. Biodiesel produced from non-edible feedstocks and residues has the added advantage of utilizing abundant but underused plant resources while reducing food-versus-fuel concerns associated with edible crops such as palm and groundnut oil, thereby supporting circular bioeconomy solutions. These government policies provide a strong basis for developing domestically available biodiesel products that can strengthen national energy security and support climate and sustainability goals[1,5].

1.3 African Star Apple Seed Oil as a Sustainable Biodiesel Feedstock

African star apple (Chrysophyllum albidum), an indigenous fruit tree common in West Africa, including Nigeria, is mainly consumed for its fruit, while the seeds are often discarded as municipal or agricultural waste. African star apple seeds represent an abundant and largely unexplored non-food biomass resource with potential for biodiesel production because they do not directly compete with food crops or arable land. Biodiesel produced from African star apple seed oil has favourable ignition characteristics and oxidation stability due to its fatty acid composition. However, its relatively high kinematic viscosity at high blend concentrations may impair fuel flow, atomization, and engine performance, particularly at low temperatures[6]. This suggests that blending African star apple seed biodiesel with other biomass-derived biodiesels may provide a more suitable second-generation fuel.

1.4 Predictive Multi-Feedstock Blending and Multivariate Statistical Modelling

Multi-feedstock blending combines different feedstocks to compensate for the limitations of individual oils. Appropriate combinations of saturated and unsaturated feedstocks can improve oxidative stability, viscosity, and other fuel properties[7,8]. Blending edible oils, where appropriate, with animal fats or non-edible vegetable oils can therefore produce fuel matrices with favourable characteristics. However, traditional experimental formulation can be resource-intensive and may provide limited capacity for developing statistically integrated multivariable models[4,9].

Mathematical and statistical approaches provide more efficient alternatives for blend selection and optimization[10]. Response surface methodology is useful for evaluating interactions among key variables, while Multiple Linear Regression can quantify relationships between dependent and independent variables[11]. IBM SPSS provides a platform for analysing such interrelated data. However, studies integrating West African feedstock matrices within predictive multi-feedstock optimization frameworks remain limited. Therefore, this study addresses this gap by applying an integrated modelling approach to regional renewable fuel resources.

Specifically, this study develops a multivariate predictive optimization framework using previously published physicochemical data. The objectives are to determine optimum blend ranges with consideration of viscosity and stability, develop multivariate regression models, and classify blend formulations using hierarchical cluster analysis to support biodiesel feedstock utilization and West Africa's energy transition.

2. METHODOLOGY AND STATISTICAL FRAMEWORK

2.1 Base Experimental Input and Data Collection

Physical & Physicochemical Properties The biodiesel's physical and chemical attributes for African star apple seed oil (ASASO) were used on the basis of those obtained experimentally through physical measurements, reported in the literature as provided by[1]. These physicochemical property data, namely: Density 0.918 g/ cm 3, kinematic viscosity 6.85 m/ s^2, higher heating values of biodiesel (27.65 MJ/ kg) higher heating values of biodiesel as well as other properties like oxidative stability, the cetane number, the flash point, etc., were collated. To create a broad-based and realistic multi-feedstock biodiesel blending tool to serve various purposes, these physicochemical attributes were used for formulating and modelling similar characteristics for palm kernel oil (PKO) and waste cooking oil (WCO) biodiesels through the review and examination of recorded measured values from other experimental research to constitute input data parameters for blending in binary and ternary mix models[12,13].

2.2 Mathematical Formulation of Biodiesel Blend Simulation

A blending matrix was developed for binary (ASASO–PKO) and ternary (ASASO–PKO–WCO) biodiesel systems. The volumetric blending fractions (X_i) were varied systematically in 5% increments while satisfying the mass-balance constraint:

$$X_{\mathrm{ASASO}} + X_{\mathrm{PKO}} + X_{\mathrm{WCO}} = 1$$

A 5% increment was selected to provide sufficiently fine compositional resolution across the blending space while maintaining a manageable number of simulated formulations. Under the 100% mass-balance constraint, this systematic grid generated 231 unique biodiesel blend compositions, which were subsequently evaluated statistically. The density (ρ_b) and higher heating value (HHV_b) of each blend were estimated using linear volumetric mixing rules:

$$\rho_b = \sum_i X_i \, \rho_i$$

$$HHV_b = \sum_i X_i \, HHV_i$$

where X_i, ρ_i, and HHV_irepresent the volumetric fraction, density, and higher heating value, respectively, of each constituent biodiesel.

Because kinematic viscosity exhibits non-linear blending behaviour, the viscosity of each blend (ν_b) was estimated using the Arrhenius–Grunberg–Nissan logarithmic mixing model:

$$\ln \nu_b = \sum_i X_i \ln \nu_i + \sum_i \sum_{j>i} X_i \, X_j d_{ij}$$

where $\nu_i$is the kinematic viscosity of constituent biodiesel i, and $d_{ij}$is the binary interaction parameter between components $i$and j. In the present simulation, the binary interaction parameters were set to $d_{\mathrm{ASASO-PKO}} = 0.000$, $d_{\mathrm{ASASO-WCO}} = 0.000$, and $d_{\mathrm{PKO-WCO}} = 0.000$. Thus, the viscosity calculations employed the ideal logarithmic form of the Arrhenius–Grunberg–Nissan model without an additional binary non-ideality correction. The pure-component kinematic viscosities used were 6.85, 5.24, and 4.82 mm²/s for ASASO, PKO, and WCO biodiesels, respectively. These mixing models provide a systematic means of estimating the physicochemical properties of multi-component biodiesel blends from the corresponding constituent properties.[14,15].

2.3 Statistical Analysis Using IBM SPSS

The simulated dataset containing the 231 binary and ternary biodiesel blends was analysed using IBM SPSS Statistics Version 27 (IBM Corp., Armonk, NY, USA). Two complementary multivariate statistical techniques were employed to evaluate the relationships between blend composition and fuel performance.

2.3.1 Multiple Linear Regression Analysis (MLRA)

Multiple Linear Regression Analysis (MLRA) was performed to quantify the influence of the volumetric blending fractions of ASASO (X_{ASASO}) and PKO (X_{PKO}) on the predicted physicochemical properties of the biodiesel blends. Six independent regression models were developed using kinematic viscosity, density, oxidative stability, higher heating value, cetane number, and flash point as dependent variables, while the blend fractions served as independent predictors. The Enter method was employed to estimate the regression coefficients, and statistical significance was evaluated at the 95% confidence level ($p < 0.05$). Multiple linear regression has been widely applied for modelling fuel-property relationships and evaluating the influence of compositional variables on biodiesel quality[15,16].

2.3.2 Hierarchical Cluster Analysis (HCA)

The HCA was applied to group the generated biodiesel mixtures according to similarities existing among physicochemical parameters. Before performing clustering, all variables were standardized to Z-scores in order to remove variation related to the different scale measurements. For the analysis, the squared Euclidean distance was selected as the similarity criterion and Ward's minimum variance was employed as the agglomeration rule. Based on the resultant dendrogram, homogeneous groups of biodiesels with similar quality characteristics could be distinguished. HCA has been established as an important multivariate data tool for distinguishing performance groups of complex fuel mixtures and has been utilized in the optimisation of biofuel[17].

2.3.3 Model Validation

Regression models' predictive performance was tested by R^2, Adjusted R^2, ANOVA, and the standard error of the estimate calculated by SPSS. Variance Inflation Factor (VIF) was used to test the multicollinearity between explanatory variables, and those lower than 5.0 may imply good predictor independence and stable coefficients of the explanatory variable. These statistical measures are routinely employed to ensure the robustness of the regression and prediction accuracy.[18,19].

3. RESULTS AND DISCUSSION

3.1 Multivariate Regression Modelling and Predictive Fuel Properties

The 231 simulated biodiesel blends were analysed using IBM SPSS Statistics to evaluate the effects of ASASO and PKO fractions on the selected fuel properties. Regression coefficients and collinearity diagnostics are presented in **Table 1**. VIF values (1.333–1.343) indicated no substantial multicollinearity.

Table 1. SPSS Model Coefficient Outputs and Collinearity Diagnostics

Dependent Variable	Predictor Term	B	Std. Error	β	*t*	*p*	VIF
Kinematic Viscosity (mm²/s)	Constant	4.824	0.053	—	91.864	<0.001	—
	(X_{ASASO})	1.989	0.085	0.914	23.357	<0.001	1.343
	(X_{PKO})	0.256	0.084	0.119	3.039	0.003	1.343
Density (kg/m³)	Constant	0.845	0.032	—	26.472	<0.001	—
	(X_{ASASO})	0.045	0.052	0.066	0.869	0.386	1.343
	(X_{PKO})	0.070	0.051	0.104	1.363	0.174	1.343
Oxidative Stability (h)	Constant	3.174	0.356	—	8.927	<0.001	—
	(X_{ASASO})	–0.110	0.577	–0.014	–0.191	0.849	1.343
	(X_{PKO})	1.430	0.570	0.188	2.506	0.013	1.343
Higher Heating Value (MJ/kg)	Constant	32.819	0.384	—	85.486	<0.001	—
	(X_{ASASO})	–5.500	0.623	–0.562	–8.831	<0.001	1.343
	(X_{PKO})	–0.077	0.616	–0.008	–0.126	0.900	1.343
Cetane Number	Constant	62.760	0.940	—	66.776	<0.001	—
	(X_{ASASO})	3.960	1.525	0.183	2.597	0.010	1.343
	(X_{PKO})	9.769	1.508	0.456	6.479	<0.001	1.343
Flash Point (°C)	Constant	148.000	0.000	—	—	—	—

(X_{ASASO})	–9.000	0.000	–1.152	—	—	1.333
(X_{PKO})	–5.000	0.000	–0.640	—	—	1.333

Flash point was generated directly from the blending relationship, resulting in a deterministic fit ($R^2 = 1.000$) with zero residual error. Thus, standard errors, *t*- and *p*-values were not estimable and are not interpreted as conventional statistical evidence. The regression output is retained in **Table 3.1** for completeness. The resulting empirical regression equations derived from the unstandardized coefficients are expressed as:

$$\nu_b = 4.824 + 1.989(X_{ASASO}) + 0.256(X_{PKO})$$
$$\rho_b = 0.845 + 0.045(X_{ASASO}) + 0.070(X_{PKO})$$
$$OS_b = 3.174 - 0.110(X_{ASASO}) + 1.430(X_{PKO})$$
$$HHV_b = 32.819 - 5.500(X_{ASASO}) - 0.077(X_{PKO})$$
$$CN_b = 62.760 + 3.960(X_{ASASO}) + 9.769(X_{PKO})$$
$$FP_b = 148.000 - 9.000(X_{ASASO}) - 5.000(X_{PKO})$$

The regression models revealed that blend composition influenced the investigated fuel properties to varying degrees. Kinematic viscosity exhibited the strongest statistically meaningful dependence on blend composition ($R^2 = 0.739$, $p < 0.001$), with ASASO exerting the dominant positive effect ($\beta = 0.914$), while PKO also contributed positively but with a comparatively smaller influence ($\beta = 0.119$). These findings indicate that increasing the ASASO fraction substantially increases resistance to flow, reflecting the influence of its fatty acid ester composition on intermolecular interactions. Similar relationships between biodiesel composition and viscosity have been reported for multi-feedstock biodiesel systems and predictive fuel-property models[7,10].

The resulting empirical regression equations derived from the unstandardized coefficients are expressed as Equations 3 through 8. To visually map these interrelated mathematical dependencies, a response surface optimization contour was constructed (Figure 1A). As illustrated in the contour topography, the fluid friction boundary scales sharply toward the primary axis vertex, confirming that increasing the *Chrysophyllum albidum* fraction drives structural flow resistance upward due to its high density and underlying saturation metrics.

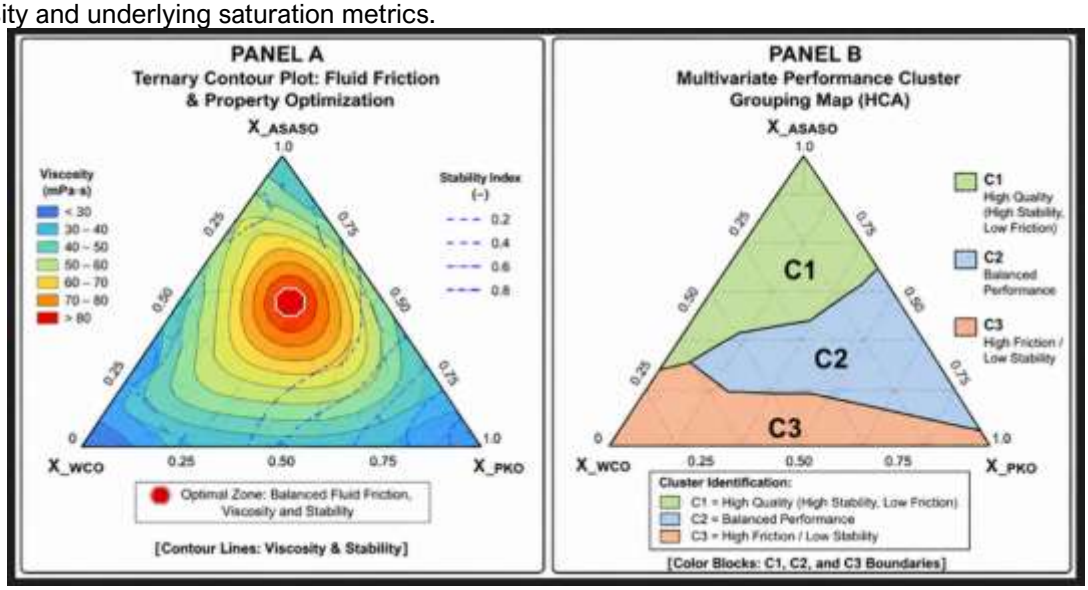

Figure 1: *Multivariate optimization space and hierarchical performance classification mappings for binary and ternary fuel systems: (A) Response surface contour showing the interaction of fluid resistance and oxidative stability parameters across different mixing fractions; (B) Formatted ternary distribution tracking the three distinct homogeneous performance windows isolated via Ward's hierarchical cluster analysis (HCA).*

Density showed only a weak dependence on blend composition, with neither ASASO ($p = 0.386$) nor PKO ($p = 0.174$) exerting a statistically significant effect. The low coefficient of determination ($R^2 = 0.008$) suggests that the constituent biodiesels possess comparable molecular packing characteristics, resulting in only minor variations in blend density.

Oxidative stability also exhibited limited predictive capability ($R^2 = 0.038$); however, PKO significantly improved oxidation resistance ($\beta = 0.188$, $p = 0.013$), whereas ASASO showed no significant contribution ($p = 0.849$). This behaviour indicates that oxidative stability depends not only on

blend ratio but also on intrinsic fuel chemistry, including fatty acid saturation, antioxidant composition and oxidation kinetics[7,8]

The higher heating value model demonstrated moderate predictive performance ($R^2 = 0.311$), with increasing ASASO significantly reducing the energy content of the blends ($\beta = -0.562, p < 0.001$), while PKO exhibited no statistically significant effect. Conversely, both ASASO ($\beta = 0.183$, $p = 0.010$) and PKO ($\beta = 0.456$, $p < 0.001$) significantly increased cetane number, indicating that blend composition can be strategically adjusted to improve ignition quality. Flash point followed a deterministic relationship with blend composition because it was generated directly from the prescribed blending equation; consequently, the regression produced a perfect mathematical fit rather than an independently validated statistical prediction.

Table 2. Regression ANOVA and Model Fit Summary

Target Model	R	R²	Adjusted R²	Std. Error of Estimate	F	Sig.
Kinematic Viscosity	0.860	0.739	0.737	0.235	324.415	<0.001
Density	0.091	0.008	0.000	0.141	0.947	0.389
Oxidative Stability	0.194	0.038	0.029	2.474	4.568	0.011
Higher Heating Value	0.557	0.311	0.305	2.670	51.280	<0.001
Cetane Number	0.396	0.157	0.150	6.536	21.218	<0.001
Flash Point*	1.000	1.000	1.000	0.000	—	—

*Flash point was generated directly from the blending equation; therefore, the regression produced a deterministic fit with zero residual error.

From statistical fitness measures reported in Table 2, it could be inferred that the prediction ability of the regression models differed with different fuel properties evaluated. The parameters that possessed relatively higher predictive accuracy in a statistically meaningful way were kinematic viscosity, next being higher heating value and cetane number, whereas those with relatively poorer fit were density and oxidative stability. Further, the absence of multicollinearity among predictor variables, VIF < 5.0, and statistical independence was indicated by very low values (VIF = 1.333–1.343), validating the use of MLRA. Taken together, these findings suggest that MLRA can be successfully used for the prediction of major physicochemical properties of biodiesel blends and offer scope for its usage in subsequent analyses of hierarchical cluster analysis and blend optimisation studies.

3.2 Cluster Analysis (HCA) Breakdown

The 231 simulated biodiesel mixtures were classified into three performance regions using HCA based on six standardized fuel properties. Cluster 1 comprised high-ASASO blends with greater stability, Cluster 2 represented the preferred optimization region with balanced fuel properties, and Cluster 3 comprised more fluid blends with lower thermal capacity. The cluster distributions were visualized in the ternary optimization space (Figure 1B), while recommended Cluster 2 formulations and their predicted properties are presented in Table 3.

Table 3: Recommended Cluster 2 formulations and predicted properties

ASASO (%)	PKO (%)	WCO (%)	Kinematic viscosity (mm²/s)	Density (g/cm³)	Oxidative stability (h)	HHV (MJ/kg)	Cetane number	Flash point (°C)
30	35	35	5.51	0.87	3.54	30.99	66.98	143.55
35	30	35	5.59	0.87	3.53	30.78	66.86	143.35
35	35	30	5.61	0.87	3.52	30.71	67.18	143.10

i. Cluster 1: High-ASASO Stability Zone

Cluster 1 comprised ASASO-rich blends with higher viscosity but favourable oxidative stability and flash point. Thus, increasing ASASO improves stability and fire characteristics but requires compositional balancing to maintain acceptable fluidity.

ii. Cluster 2: Optimised Blending Zone

Cluster 2 provided the best overall balance of fuel properties. Representative formulations (Table 3.3) showed acceptable ASTM D6751 compliance for viscosity, cetane number, and flash point, although viscosity and oxidative stability did not fully satisfy EN 14214 limits. These blends therefore represent promising candidates for further optimisation and experimental validation.

iii. Cluster 3: PKO/WCO-Dominated Flow Zone

Cluster 3 contained PKO/WCO-rich blends with lower viscosity and improved fluidity but reduced oxidative stability. Such formulations may require antioxidant treatment and appropriate storage. Overall, HCA identified distinct compositional-performance domains, with Cluster 2 offering the most balanced formulation window.

Model limitation: PKO and WCO properties were obtained from literature rather than measured directly. Variations in feedstock composition and measurement conditions may therefore affect prediction accuracy; hence, the recommended blends should be experimentally validated before being considered standards-compliant.

3.3 Policy Implications

The regression models and the cluster analysis offer a useful decision-making platform in designing biodiesel blend compositions that optimally harness the potential of ASASO, PKO and WCO feedstocks and are conducive to standardising the production of biodiesel that ultimately decreases reliance on fossil fuel diesel. Such modelling approaches for predictive analysis have a crucial role in speeding up industrial commercialization of green biodiesel technology and in more efficient assurance of fuel properties[1,10]. The potential of incorporating other underexploited non-edible feedstocks, when combined with waste oil biodiesel, would improve utilisation of resources and ensure sustainable circular bioeconomy strategies were applied; in developing countries with access to feedstocks such as Nigeria's waste and non-edible sources like ASASO and PKO, it would guarantee sustainable energy source security while lowering emissions and promoting transport systems with a low carbon footprint[2,20].

4. CONCLUSION

This study developed a multivariate predictive optimization framework for multi-feedstock biodiesel blends derived from African star apple seed oil (ASASO), palm kernel oil (PKO), and waste cooking oil (WCO) using IBM SPSS. By integrating blend simulation, multiple linear regression analysis (MLRA), and hierarchical cluster analysis (HCA), the study demonstrated that statistical modelling can effectively predict key physicochemical fuel properties while identifying optimal blend compositions without extensive experimental trial-and-error. Among the investigated fuel properties, kinematic viscosity exhibited the highest predictive accuracy, indicating that blend composition, particularly the proportion of ASASO, strongly governs fuel flow behaviour. Conversely, density and oxidative stability showed weaker dependence on blend ratio, suggesting that these properties are influenced by additional intrinsic fuel characteristics.

Hierarchical cluster analysis further classified the simulated biodiesel blends into three distinct performance groups, enabling the identification of an optimized blending region that balances viscosity, oxidative stability, cetane number, and higher heating value within acceptable biodiesel quality limits. The results demonstrate that combining complementary non-edible and waste-derived feedstocks provides a practical strategy for overcoming the limitations associated with individual biodiesel sources while improving overall fuel quality.

The predictive framework developed in this study provides a rapid and cost-effective decision-support tool for biodiesel formulation and optimization. By reducing dependence on extensive laboratory experimentation and facilitating the rational design of multi-feedstock biodiesel blends, the proposed approach offers a scalable methodology for sustainable biodiesel production. Furthermore, the integration of indigenous non-edible biomass resources with waste lipid streams supports circular bioeconomy principles, promotes efficient resource utilization, and contributes to enhanced energy security and the broader transition toward sustainable transportation fuels in Sub-Saharan Africa.The preferred blending region was a ternary formulation containing approximately 30–40% ASASO

biodiesel, 30–40% PKO biodiesel, and 20–40% WCO biodiesel, which provided the most balanced predicted fuel properties. However, these model-derived blends require experimental validation to confirm their fuel performance and compliance with applicable biodiesel standards.

REFERENCES

1. International Energy Agency. Renewables 2023: Analysis and Forecasts to 2028; International Energy Agency: Paris, France, 2024.
2. International Renewable Energy Agency. *World Energy Transitions Outlook 2022: 1.5°C Pathway*; International Renewable Energy Agency: Abu Dhabi, United Arab Emirates, 2022. https://www.irena.org/publications/2022/Mar/World-Energy-Transitions-Outlook-2022
3. Muhammad, K. M.; Adeyemi, M. M.; Jacob, J.; Koko, A. R.; Dauda, K.; Tamasi, A. A.; Yahuza, I. Biodiesel Production in Africa from Non-Edible Sources: Sources, Production, Properties and Policies. *Sustainable Chem. Environ.***2025**, *9*, 100201. https://doi.org/10.1016/j.scenv.2024.100201.
4. Ishola, N. B.; Epelle, E. I.; Betiku, E. Machine Learning Approaches to Modeling and Optimization of Biodiesel Production Systems: State of the Art and Future Outlook. *Energy Convers. Manage. X* 2024, *23*, 100669. https://doi.org/10.1016/j.ecmx.2024.100669
5. Federal Republic of Nigeria.*Nigerian Bio-Fuel Policy and Incentives*; Federal Government of Nigeria: Abuja, Nigeria, 2020. https://moman.org/wp-content/uploads/2024/07/Biofuels-Policy-2007.pdf
6. Adeniran, O. I.; Joseph, N. B.; Aransiola, S. A.; Maddela, N. R.; Prasad, R. Sustainable Biodiesel Production: A Comparative Analysis of Fuel Properties from Non-Edible Oil and Waste-Derived Feedstock. *Environmental Progress & Sustainable Energy***2026**, *45* (2), e70354. https://doi.org/10.1002/ep.70354.
7. Longanesi, L.; Pereira, A. P.; Johnston, N.; Chuck, C. J. Oxidative Stability of Biodiesel: Recent Insights. *Biofuels, Bioproducts and Biorefining* 2022, *16* (1), 265–289. https://doi.org/10.1002/bbb.2306
8. Hassan, T.; Rahman, M. M.; Rahman, M. A.; Nabi, M. N. Opportunities and Challenges for the Application of Biodiesel as Automotive Fuel in the 21st Century. *Biofuels, Bioproducts and Biorefining***2022**, *16* (5), 1353–1387. https://doi.org/10.1002/bbb.2375
9. Osman, A. I.; Nasr, M.; Farghali, M.; Rashwan, A. K.; Abdelkader, A.; Al-Muhtaseb, A. H.; Ihara, I.; Rooney, D. W. Optimizing Biodiesel Production from Waste with Computational Chemistry, Machine Learning and Policy Insights: A Review. *Environ. Chem. Lett.* 2024, *22*, 1005–1071. https://doi.org/10.1007/s10311-024-01700-y
10. Bhan, S.; Yadav, P. S.; Bibhu, V.; Gautam, G. D.; Gautam, R. Optimization of Biodiesel Properties Using Free Fatty Acid-Based Blending, Artificial and Machine Learning Modelling, and Advanced Production Technologies: A Comprehensive Review. Environ. Prog. Sustainable Energy 2026, 45 (2), e70250. https://doi.org/10.1002/ep.70250.
11. Knothe, G.; Krahl, J.; Van Gerpen, J., Eds. *The Biodiesel Handbook*, 2nd ed.; AOCS Press: Urbana, IL, 2010. https://shop.elsevier.com/books/the-biodiesel-handbook/knothe/978-1-893997-62-2
12. Yaqoob, H.; Teoh, Y. H.; Sher, F.; Jamil, M. A.; Gulzar, M.; Bashir, M. N.; et al. Prospects of Biodiesel as an Alternative Fuel: A Comprehensive Review. Fuel 2022, 308, 122114. https://doi.org/10.1016/j.fuel.2021.122114.
13. de Mattos, R. A., Bastos, F. A., & Tubino, M. (2015). Correlation between the composition and flash point of diesel-biodiesel blends. *Journal of the Brazilian Chemical Society, 26*(2), 393–395.
14. Messaâdi, A.; Ouerfelli, N.; Das, D.; Hamda, H.; Hamzaoui, A. H. Correspondence Between Grunberg–Nissan, Arrhenius and Jouyban–Acree Parameters for Viscosity of Isobutyric Acid + Water Binary Mixtures from 302.15 to 313.15 K. *J. Solution Chem.***2012**, *41* (12), 2186–2208. https://doi.org/10.1007/s10953-012-9931-3
15. Osamudiamen, P. M., & Afolabi, L. O. (2014). Fatty acid composition of the seed oil of *Chrysophyllum albidum* (G.Don). *African Journal of Plant Science, 8*(7), 364–365. https://doi.org/10.5897/AJPS2014.1154.
16. Bello, U.; Adamu, H.; Faizan, M.; Ourimi, M.; Alzoubi, R.; Jallow, A.; Siddiqui, M. N.; Jameel, A. G. A. Advancing Biodiesel Quality Assessment Using Machine Learning Algorithms: A Mini-

Review on Oxidative Stability Prediction and Models Benchmarking. Energy Fuels 2026, 40 (7), 3485–3508. https://doi.org/10.1021/acs.energyfuels.5c06424.
17. Hair, J. F.; Black, W. C.; Babin, B. J.; Anderson, R. E. Multivariate Data Analysis, 9th ed.; Cengage Learning: Boston, MA, 2022.
18. James, G.; Witten, D.; Hastie, T.; Tibshirani, R. An Introduction to Statistical Learning with Applications in R, 2nd ed.; Springer: New York, NY, 2021. https://doi.org/10.1007/978-1-0716-1418-1.
19. Montgomery, D. C.; Peck, E. A.; Vining, G. G. Introduction to Linear Regression Analysis, 6th ed.; Wiley: Hoboken, NJ, 2021.
20. United Nations. The Sustainable Development Goals Report 2023: Special Edition; United Nations: New York, NY, 2023. https://doi.org/10.18356/9789210024914.

ISBN: 978-978-67-0285-8 DOI: https://doi.org/10.55455/acsnigeria.1.3.75-79

Effects of Selected Soil Properties on the Chemical Speciation of Heavy Metals in Oghara, Delta State, Nigeria

Gladys Ugochukwu, Paulina Okogbenin and Theresa Ataine
Department of Chemistry, Delta State College of Education, Mosogar, Delta State. Nigeria
Corresponding Author's email: gladyscugochukwu@gmail.com
DOI: https://doi.org/10.55455/acsnigeria.1.3.75-79

ABSTRACT

This study investigated the relationship between soil physicochemical properties and heavy metal speciation in soils from Oghara, Delta State, Nigeria. Surface soil samples (0–20 cm) were collected from ten sampling locations and analysed using standard analytical procedures. Heavy metal speciation was determined using the five-step sequential extraction method, while Fe, Zn, Cu, Cr, Ni, Pb, and Mn were quantified by Atomic Absorption Spectrophotometry (AAS). Pearson correlation analysis was employed to evaluate the relationships between soil particle-size fractions and heavy metal speciation. The soils were slightly acidic (pH 6.4 ± 0.1) and predominantly sandy (61.28%), with low organic matter (1.55 ± 0.03%) and cation exchange capacity (3.99 ± 0.05 cmol(+) kg^{-1}). Zinc (230.79 ± 0.20 mg kg^{-1}) and nickel (141.15 ± 0.10 mg kg^{-1}) recorded the highest total concentrations. Zinc occurred mainly in the Fe–Mn oxide-bound and organic matter-bound fractions, whereas nickel was predominantly associated with the residual fraction. Significant correlations ($p < 0.001$) between soil particle-size fractions and heavy metal forms indicated that soil texture strongly influenced metal distribution and retention. The study concludes that soil physicochemical properties, particularly particle-size distribution, play a significant role in controlling heavy metal speciation and potential mobility in Oghara soils. These findings provide baseline information for environmental monitoring, ecological risk assessment, and sustainable soil management.

KEYWORDS: Heavy metal speciation; soil physicochemical properties; sequential extraction; soil texture; Oghara; Niger Delta.

1. INTRODUCTION

Soil is a critical environmental resource that supports agricultural productivity, nutrient cycling, water regulation, and ecosystem sustainability. However, rapid industrialization, urbanization, agricultural intensification, petroleum exploration, and indiscriminate waste disposal have increased heavy metal contamination of soils [1]. Because heavy metals are persistent and non-biodegradable, they accumulate in the environment and may enter the food chain, posing significant ecological and public health risks [1].

Environmental risk associated with heavy metals depends not only on their total concentrations but also on their chemical forms (speciation), which determine their mobility, bioavailability, and toxicity. Consequently, heavy metal speciation has become an important approach for evaluating contaminant behaviour in soils [2]. The distribution of metals among geochemical fractions is strongly influenced by soil physicochemical properties such as pH, organic matter, cation exchange capacity, electrical conductivity, and soil texture, all of which regulate metal adsorption, retention, and release under changing environmental conditions [3].

Previous studies in the Niger Delta have largely focused on determining total heavy metal concentrations in soils, sediments, and water bodies, providing limited information on the relationships between soil physicochemical properties and heavy metal speciation[4], [5], [6]. As a result, the factors controlling heavy metal mobility and potential ecological risks in many locations remain insufficiently understood. Oghara, Delta State, is characterised by expanding residential development, agricultural activities, transportation, and proximity to petroleum-producing communities, all of which may influence soil quality and heavy metal dynamics. Despite these environmental pressures, information on the relationship between soil physicochemical properties and heavy metal speciation in Oghara soils is scarce.This study therefore investigated the relationship between selected soil physicochemical properties and heavy metal speciation in soils from Oghara, Delta State, Nigeria. The findings will improve understanding of heavy metal mobility and bioavailability and provide scientific evidence to

support environmental monitoring, ecological risk assessment, and sustainable soil management in the study area.

2. MATERIALS AND METHODS

2.1 Study Area

The study was conducted in Oghara, Ethiope West Local Government Area, Delta State, Nigeria (5°55′–5°59′ N, 5°40′–5°46′ E). The area has a humid tropical climate with annual rainfall of 2,000–2,500 mm and mean temperatures of 27–32 °C. It is underlain by the Benin Formation, with predominantly sandy loam soils. Agriculture, residential development, commercial activities, transportation, and proximity to petroleum-related operations constitute potential sources of heavy metal contamination.

2.2 Soil Sampling

Surface soil samples (0–20 cm) were collected from selected locations representing different anthropogenic activities using a stainless-steel auger. Five subsamples from each location were composited to obtain representative samples. Samples were air-dried, sieved (<2 mm) for physicochemical analyses, and further ground (<0.15 mm) for heavy metal determination.

2.3 Soil Physicochemical Analysis

Soil pH, electrical conductivity (EC), particle size distribution, organic carbon, organic matter, cation exchange capacity (CEC), moisture content, available phosphorus, and total nitrogen were determined using standard analytical procedures[7], [8], [9]

2.4 Heavy Metal Speciation and Determination

Heavy metal speciation was performed using the five-step sequential extraction procedure of [10], which fractionates metals into exchangeable, carbonate-bound, Fe–Mn oxide-bound, organic matter-bound, and residual forms. Concentrations of Cd, Pb, Cu, Zn, Cr, Ni, Fe, and Mn in each fraction were determined using Atomic Absorption Spectrophotometer (AAS)Labnicsmodel 2000

2.5 Quality Assurance and Data Analysis

Analytical quality was assured through the use of acid-washed glassware, analytical-grade reagents, procedural blanks, duplicate analyses, certified reference materials, and recovery tests. Data were analysed using descriptive statistics and Pearson's correlation to evaluate relationships between soil physicochemical properties and heavy metal speciation at a 95% confidence level.

3. RESULTS AND DISCUSSION

3.1 Results

3.1.1 Physicochemical properties of soil samples

Table 1. *Physicochemical properties of soil samples collected from Oghara, Delta State, Nigeria*

Parameter	Value
Available phosphorus (mg kg^{-1})	14.5 ± 0.1
Calcium (cmol(+) kg^{-1})	3.10 ± 0.02
Cation exchange capacity, CEC (cmol(+) kg^{-1})	3.99 ± 0.05
Clay (%)	9.29
Magnesium (cmol(+) kg^{-1})	0.52 ± 0.04
Organic matter (%)	1.55 ± 0.03
pH	6.4 ± 0.1
Potassium (cmol(+) kg^{-1})	0.05 ± 0.001
Sand (%)	61.28
Silt (%)	29.43
Sodium (cmol(+) kg^{-1})	0.32 ± 0.01
Total nitrogen (%)	0.11 ± 0.05

Values are expressed as mean ± standard deviation (SD)

Table 1 presents the physicochemical properties of soils collected from Oghara, Delta State. The soils were slightly acidic (pH 6.4 ± 0.1) and sandy in texture, comprising 61.28% sand, 29.43% silt, and 9.29%

clay. Organic matter, total nitrogen, and available phosphorus contents were 1.55 ± 0.03%, 0.11 ± 0.05%, and 14.5 ± 0.1 mg kg^{-1}, respectively. The cation exchange capacity was 3.99 ± 0.05 cmol(+) kg^{-1}, with calcium being the dominant exchangeable base (3.10 ± 0.02 cmol(+) kg^{-1}), followed by magnesium, sodium, and potassium.

3.1.2 Heavy metal speciation and total concentrations in soil samples

Table 2. *Heavy metal speciation and total concentrations in soil samples from Oghara, Delta State, Nigeria*.

Metal	Total (mg kg^{-1})	Exchangeable	Carbonate-bound	Fe–Mn oxide-bound	Organic matter-bound	Residual
Fe	12.36 ± 0.01	3.47 ± 0.01	3.28 ± 0.01	3.91 ± 0.01	1.70 ± 0.01	ND
Zn	230.79 ± 0.20	36.61 ± 1.00	35.96 ± 1.00	78.46 ± 1.60	77.48 ± 1.60	1.96 ± 0.06
Cu	0.95 ± 0.01	ND	ND	ND	0.63 ± 0.02	0.31 ± 0.01
Cr	4.94 ± 0.03	ND	ND	1.56 ± 0.10	2.60 ± 0.20	**0.78 ± 0.05**
Ni	141.15 ± 0.10	5.87 ± 0.30	4.99 ± 0.30	1.17 ± 0.10	51.07 ± 1.20	**78.05 ± 1.70**
Pb	9.05 ± 0.02	ND	ND	4.79 ± 0.20	ND	4.26 ± 0.20
Mn	11.26 ± 1.04	ND	8.24 ± 0.30	0.55 ± 0.02	ND	**2.47 ± 0.12**

Values are presented as mean ± standard deviation (SD) of triplicate determinations (n = 3). ND = Not detected (below the limit of detection)

Table 2 presents the total concentrations and geochemical fractions of heavy metals in soils from Oghara. Zinc recorded the highest total concentration (230.79 ± 0.20 mg kg^{-1}), followed by nickel (141.15 ± 0.10 mg kg^{-1}), whereas copper had the lowest concentration (0.95 ± 0.01 mg kg^{-1}). Iron occurred mainly in the exchangeable, carbonate-bound, Fe–Mn oxide-bound and organic matter-bound fractions, while zinc was predominantly associated with the Fe–Mn oxide-bound and organic matter-bound fractions. Nickel was largely concentrated in the residual and organic matter-bound fractions, whereas lead was detected only in the Fe–Mn oxide-bound and residual fractions. Copper and chromium were primarily associated with the organic matter-bound and residual fractions, while manganese occurred mainly in the carbonate-bound fraction

3.1.3 Heavy Metal Fractions and Soil Particle-Size Fractions In Soils.

Table 3. *Pearson correlation coefficients (r) between heavy metal fractions and soil particle-size fractions in soils in Oghara, Delta State, Nigeria*

Metal	Fraction	Clay	Sand
Iron (Fe)	Exchangeable	0.655	0.596
	Carbonate-bound	0.000	0.000
	Fe–Mn oxide-bound	0.217	.512
	Organic matter-bound	–0.143	–0.197
	Residual	0.645	–0.115
Zinc (Zn)	Exchangeable	0.466	0.565
	Carbonate-bound	0.818	0.738
	Fe–Mn oxide-bound	0.327	0.693
	Organic matter-bound	–0.436	0.784
	Residual	0.393	–0.813
Lead (Pb)	Exchangeable	0.000	0.000
	Carbonate-bound	0.000	0.000
	Fe–Mn oxide-bound	NC	0.776
	Organic matter-bound	0.000	0.000
	Residual	–0.782	–0.393

Table 3 shows significant correlations between soil particle-size fractions and heavy metal speciation ($p < 0.001$). Iron exhibited moderate positive correlations between its exchangeable and residual fractions and clay, whereas zinc showed strong positive correlations in the carbonate-bound fraction with clay ($r = 0.818$) and the organic-bound fraction with sand ($r = 0.784$). In contrast, the residual fractions of zinc ($r = –0.813$) and lead ($r = –0.782$) were negatively correlated with sand and clay, respectively. These

findings indicate that soil texture significantly influences the distribution and retention of heavy metals in Oghara soils.

3.2 Discussion

The physicochemical properties of the Oghara soils showed that they were slightly acidic (pH 6.4), sandy in texture, and contained relatively low organic matter and cation exchange capacity (CEC). These characteristics suggest a moderate capacity for heavy metal retention and increased susceptibility to metal mobility. Soil pH, texture, organic matter, and CEC are widely recognized as the primary factors controlling the adsorption, mobility, and bioavailability of heavy metals in soils. Clay- and organic matter-rich soils generally retain metals more effectively than sandy soils because of their greater surface area and higher cation exchange capacity [11], [12]. In the Oghara samples, however, the prevalence of a sandy texture and low organic matter content likely limits the formation of stable metal-organic complexes and insoluble precipitates, thereby increasing the risk of heavy metal leaching into groundwater [13], [14].

The heavy metal speciation results revealed that zinc and nickel had the highest total concentrations, while copper occurred at the lowest concentration. Zinc was mainly associated with the Fe–Mn oxide-bound and organic matter-bound fractions, whereas nickel was predominantly present in the residual fraction. This distribution indicates that a substantial proportion of these metals occurs in relatively stable forms with lower immediate bioavailability. Previous studies have similarly reported that Fe–Mn oxides, soil organic matter, and residual mineral fractions serve as important sinks for heavy metals, thereby reducing their mobility under stable environmental conditions [15], [16], [17].

The correlation analysis further demonstrated significant relationships between soil texture and heavy metal fractions. The positive correlations of several iron and zinc fractions with clay indicate that clay minerals enhance heavy metal adsorption and retention [18]. Conversely, the negative correlations observed for the residual fractions of zinc and lead with sand suggest that coarse-textured soils have a lower capacity to retain metals, thereby increasing their potential mobility. These findings are consistent with previous reports that clay-rich soils immobilize heavy metals more effectively than sandy soils because of their larger surface area and greater adsorption capacity[19], [20], [21].

4. CONCLUSION

The study demonstrated that soil physicochemical properties significantly influence heavy metal speciation in soils from Oghara, Delta State. The soils were slightly acidic and predominantly sandy, with zinc and nickel recording the highest total concentrations. Most heavy metals occurred in the Fe–Mn oxide-bound, organic matter-bound, and residual fractions, indicating differences in their mobility and bioavailability. Significant correlations between soil particle-size fractions and heavy metal forms confirmed that soil texture plays an important role in controlling metal distribution. These findings provide baseline information for environmental monitoring, ecological risk assessment, and the sustainable management of contaminated soils in the Niger Delta.

REFERENCES

1. Hanif, S.; Ali, S.; Chaudhry, A. H.; Sial, N.; Marium, A.; Mehmood, T. A review on soil metal contamination and its environmental implications. Nature Environ. *Pollut. Technol*. 2025, *24*, D1684. doi: 10.46488/nept.2025.v24i01.d1684
2. Tack, F.; Verloo, M. Chemical speciation and fractionation in soil and sediment heavy metal analysis: A review. *Int. J. Environ. Anal. Chem.* 1995, *59*, 225–238. doi: 10.1080/03067319508041330
3. Murillo-Tovar, M. A.; Saldarriaga-Noreña, H.; Saeid, A. Trace Metals in the Environment - New Approaches and Recent Advances; IntechOpen, 2019. doi: 10.5772/intechopen.83504
4. Ebong, G. A.; Anyalebechi, P. E.; Udosen, E. D. Physicochemical properties and metal speciation in gas flare-impacted soils in Ibeno, Nigeria. World J. Adv. Res. Rev. 2022, 14, 103–115. doi: 10.30574/wjarr.2022.14.1.0266
5. Cipullo, S.; Snapir, B.; Tardif, S.; Campo, P.; Prpich, G.; Coulon, F. Insights into mixed contaminants interactions and its implication for heavy metals and metalloids mobility, bioavailability and risk assessment. Sci. Total Environ. 2018, 645, 662–673. doi: 10.1016/j.scitotenv.2018.07.179

6. Ngozi, V. E.; Oguchukwu, U. L.; Verla, A. W. First assessment of ecological health, human health, and public health implications of sitespecific speciation of heavy metals in Ohaji-Egbema, Niger Delta, Nigeria. *J. Environ. Ecol*. 2025, *1*, 15–25. doi: 10.64229/aserx194
7. Selassie, Y. G.; Anemut, F.; Addisu, S. The effects of land use types, management practices and slope classes on selected soil physico-chemical properties in Zikre watershed, North-Western Ethiopia. *Environ. Syst. Res*. 2015, *4*, 3. doi: 10.1186/s40068-015-0027-0
8. Wang, J.; et al. Impact of cultivation duration and methods on soil physicochemical properties, ginseng growth, and arbuscularmycorrhizal fungi community structure. *Front. Microbiol*. 2025, *16*, 1628889. doi: 10.3389/fmicb.2025.1628889
9. Taeprayoon, P.; Homyog, K.; Meeinkuirt, W. Organic amendment additions to cadmium-contaminated soils for phytostabilization of three bioenergy crops. *Sci. Rep*. 2022, *12*, 13070. doi: 10.1038/s41598-022-17385-8
10. Tessier, A.; Campbell, P. G. C.; Bisson, M. Sequential extraction procedure for the speciation of particulate trace metals. *Anal. Chem*. 1979, *51*, 844–851. doi: 10.1021/ac50043a017
11. Ukonmaanaho, L.; et al. Heavy metal concentrations in various aqueous and biotic media in Finnish Integrated Monitoring catchments. *Jukuri* 2024. doi: 10.60910/2u2m-ebdd
12. Petruzzelli, G.; Pezzarossa, B.; Pedron, F. The fate of chemical contaminants in soil with a view to potential risk to human health: A review. *Environments* 2025, *12*, 183. doi: 10.3390/environments12060183
13. Okorie, M. N.; Okechukwu, V. U.; Omokpariola, D. O. Physicochemical properties and health risk assessment of selected heavy metals from soil and borehole water in Ifite-Awka, Anambra State, Nigeria. *Discover Appl. Sci*. 2024, *6*, 112. doi: 10.1007/s42452-024-05767-8
14. Wuana, R. A.; Okieimen, F. E.; Imborvungu, J. A. Removal of heavy metals from a contaminated soil using organic chelating acids. Int. J. Environ. Sci. Technol. 2010, 7, 485–496. doi: 10.1007/bf03326158
15. Violante, A.; Cozzolino, V.; Perelomov, L.; Caporale, A. G.; Pigna, M. Mobility and bioavailability of heavy metals and metalloids in soil environments. J. Soil Sci. Plant Nutr. 2010, 10, 3. doi: 10.4067/s0718-95162010000100005
16. Caporale, A. G.; Violante, A. Chemical processes affecting the mobility of heavy metals and metalloids in soil environments. *Curr. Pollut. Rep*. 2015, *2*, 15–27. doi: 10.1007/s40726-015-0024-y
17. Basta, N. T.; Ryan, J. A.; Chaney, R. L. Trace element chemistry in residual-treated soil: Key concepts and metal bioavailability. *J. Environ. Qual.* 2005, 34, 49–63. doi: 10.2134/jeq2005.0049dup
18. Dharmayasa, I. G. N. P.; Sugiana, I. P.; Putri, P. Y. A.; Maw, M. M. Investigating the relationship between heavy metals concentration and soil fractions in Benoa Bay, Indonesia. Ecol. *Eng. Environ. Technol*. 2025, *26*, 365–375. doi: 10.12912/27197050/205559
19. Boros-Lajszner, E.; Wyszkowska, J.; Kucharski, J. Use of zeolite to neutralise nickel in a soil environment. *Environ. Monit. Assess*. 2017, *190*, 54. doi: 10.1007/s10661-017-6427-z
20. Miller, W. P.; Fee, W. W. M.; Kelly, J. M. Mobility and retention of heavy metals in sandy soils. *J. Environ. Qual*. 1983, *12*, 579–584. doi: 10.2134/jeq1983.00472425001200040030x
21. Mielke, H. W.; Anderson, J.; Berry, K. J.; Mielke, P. W.; Chaney, R. L.; Leech, M. M. Lead concentrations in inner-city soils as a factor in the child lead problem. *Am. J. Public Health* 1983, *73*, 1366–1369. doi: 10.2105/ajph.73.12.1366

ISBN: 978-978-67-0285-8 DOI: https://doi.org/10.55455/acsnigeria.1.3.80-87

Antimicrobial evaluation of Rhizome Extracts and Chemical Characterization of the hexane Extracts of *Costuslucanusianus J. Braun&Shum*

Adesegun O. Onanuga[1*] and Ganiyat K. Oloyede[2]
[1]Department of Chemistry, Bowen University, Iwo, Osun State, Nigeria.
[2]Department of Chemistry, University of Ibadan, Ibadan, Nigeria.
Corresponding Author's email: adesegunonas@gmail.com
DOI: https://doi.org/10.55455/acsnigeria.1.3.80-87

ABSTRACT

Micro-organisms resistance to antimicrobial agents has prompted a quest for novel potent antimicrobial agents which are particularly derived from natural sources. *Costuslucanusianus*(*J.Braun&Shum*) is a plant generally utilized in traditional medicine for the treatment of innumerable infectious diseases including venereal diseases. However, there is limited information on the antimicrobial potency of its rhizome crude extracts and chemical compositions. This study is aimed at determining the chemical composition and antimicrobial potency of *C. lucanusianus* rhizome organ. The antimicrobial potency of various concentrations (12.5-100 µg/mL) of the ethyl acetate, hexane and methanol extracts of the rhizome was evaluated against six bacterial and four fungal strains using the Agar well diffusion techniques. Minimum inhibition concentration (MICs) of the most potent extracts was determined using Agar Microdilution method. The most potent plant extract was further subjected to chromatographic separation and then structural elucidation using NMR spectroscopy. The extracts displayed varying antimicrobial activity against the micro-organisms, and MICs for the most potent extracts ranged from 3.125 µg /ml to 6.25 µg/ml. Chromatographic studies of the hexane extract led to the isolation of a compound Z, a mixture of isonuatigenin and diosgenin whose structures were established with NMR and comparison with literature data. The *in vitro* antimicrobial activity displayed by the crude extracts from *C. lucanusianus* rhizomes highlights its potential for the treatment of infectious diseases in ethnomedicine.

KEYWORDS: *Costuslucanusianus*, Antimicrobial activity, Isonutiagenin, Diosgenin, Infectious diseases

1. INTRODUCTION

Infectious diseases continue to pose a significant world health concern, especially in low- and average-income regions where access to effective treatment remains limited[1]. The enormous burden of infectious diseases in developing countries is due to the emergence and spread of drug-resistant infections[2]2. A major challenge encountered in treating infectious diseases is the antimicrobial resistance. There is therefore an urgent requirement for new drugs that can counteract antimicrobial agent resistance mechanisms 3. Medicinal plants have traditionally served as a vital origin of bioactive compounds used to treat various diseases. These plants contain significant organic compounds such as carbohydrates, steroids, terpenes, alkaloids and flavonoids, many of which are liable for the antimicrobial properties displayed *in vitro* conditions [4].As a result, the interest in making use of compounds derived from plants as potential alternatives to conventional antimicrobial agents has increased.

Costuslucanusianus, commonly referred to as the Spiral ginger and African spiral flag, is a popular plant widely famous for its efficiency in the treatment of cough, urethral discharge, urinary tract infection, venereal diseases amongst others 5. The rhizome is frequently used in decoctions for therapeutic purposes in cases like leprosy and malaria 6. Various biological activities such like hepatoprotective, antimicrobial, anti-inflammatory and antihyperglycemic effects have been reported [7-9].

Despite this, limited information is available on the plant's chemical components 9. The *Costus* genus is rich in steroidal saponins, starches, oxalates, and sapogenins and other bioactive compounds [10], suggesting that C. lucanusianus may contain structurally relevant compounds with significant pharmacological potential. This study aims to evaluate the antimicrobial activity of rhizome extracts and characterize the chemical bioactive constituents accountable for these effects.

2. MATERIALS AND METHODS

2.1 Plant material

Fresh rhizomes of Costuslucanusianus italicize were collected from General gas area, Akobo Ibadan, Oyo state, Nigeria (at a geographical coordinate of 7 ° 25! 45.4" N 3 ° 56 ' 10.9" E; altitude 830 ft.). Voucher specimens (FH110048) of the plant were dropped at the FRIN herbarium.

2.2 Instrumentation

The NMR spectra were acquired by the use of BrukerTopSpin 600 and 150 MHz spectrometers for ^{1}H and ^{13}C, respectively, in $CDCl_3$. Silica gel 60-200 mesh size was utilized for column chromatographic procedures.

2.3 Study method

2.3.1 Extraction of plant organ

Air-dried and ground rhizome (50 g) was deffated with hexane using the cold-maceration extraction method repeatedly. The extract filtered usingWhatman filter paper number 1 and a Buchner funnel. The filtrate was concentrated under reduced pressure with a rotary evaporator at 40°c to obtain the crude extract. The defatted plant material was then extracted with Ethyl acetate and methanol sequentially with the same cold maceration technique. Subsequently, more extracts were obtained from the rhizome organ (2.70kg) using a Soxhlet apparatus. The rhizome organ was defatted with hexane, extracted with ethyl acetate and methanol successively. The percentage yields (w/w) of the extracts were determined.

2.3.2 Purification of the hexane extract

Hexane extract (6.80 g) was purified on silica gel (60-200 mesh, 205 g, 32.5 mm x 66 mm) using various concentrations of ethyl acetate in hexane to give 125 fractions of 200 mL each. Fractions 64-73 (1.03 g) were subjected to repeated column chromatography using a gradient of ethyl acetate in hexane to give a mixture of diosgenin (3) bold and isonutiagenin (4) bold (12 mg).

2.3.3 Antimicrobial activity of crude extracts

A total of six clinical bacterial strains (*Pseudomonas aeruginosa, Bacillus subtilis, Staphylococcus aureus, Salmonella typhi, Klebsiellapneumoniae and Escherichia coli*) and four fungal strains (*Candida albicans, Rhizopusstolonifer, Penicilliumnotatum and Aspergillusniger*) were used in this study. All test organisms were provided by the laboratory of pharmaceutical microbiology, University of Ibadan. The antibacterial and antifungal potency of methanol, hexane and ethyl acetate extracts from *C. lucanusianus* were determined using Agar well diffusion techniques on Mueller-Hinton Agar medium (MHA) and Sabouraud Dextrose Agar medium (SDA), respectively, against the above-mentioned microorganisms. Culture media were sterilized by autoclaving prior to use

2.3.4 Preparation of graded concentrations

An initial concentration of 100 µg /ml of each extract was prepared by dissolving,extracts (1.0 mg each) into 10 ml of methanol. Double-fold serial dilution method was used to obtainfour different concentration solutions ranging from 12.5 µg/ml to 100 µg/ml

(a). Antibacterial assay

A mixture of micro-organisms andsterile nutrient agar was cautiously poured into sterilized petri dishes and permitted to solidify for about 45 minutes. Extracts (30µl), methanol and gentamicin were poured into the wells (8 mm diameter hole pierced in the Agar at distance of 25 mm apart using a sterilized cork borer). For adequate diffusion of the extracts into the medium, the plates were left at room temperature, afterwards incubated at 37 °C for 24 hours.

The bacterial growth zones were observed after the duration and inhibition zones were measured in mm. Tests were carried out in triplicates [11].

(b). Antifungal assay

The prepared sterile SDA (62 g/L) was permitted to solidify for about 45 minutes in sterile plates. The SDA plate surfaces were covered with fungal strain suspension using sterile cotton swabs under aseptic conditions. Different concentrations of the extracts, along with methanol and tioconazole{please chech the name} 70% were transferred into the wells for 120 minutes to allow perfect diffusion into the agar. After that, they were incubated uprightly for 48 hours at 28 °C. Measurements of inhibition zone diameter (IZD) in mm were determined [12.]

2.3.5 Determination of Minimum Inhibitory Concentration (MIC)

The hexane and methanol extracts solutions in methanol were prepared. The MIC was determined by making use of the Agar dilution technique (micro/dilution technique) in a 96-well micro-titer plate (MTP). Prepared sterilized and cooled Agar (18 mL each) was properly mixed with various concentrations of the extracts (2 mL each). The spreading of the resulting mixtures was evenly in (MTP) which was maintained in an oven for 24 hours at 37 °C for bacteria and 48 hours for fungi. Then, unto the surfaces were applied microorganisms. For the fungi, the visualization of turbidity in the wells, which represented the least concentration at which no microorganism growth was seen, was used to determine the MIC 12. The experiment was carried out in triplicate. MIC of the extracts in millilitres was determined,

2.3.6 Statistical Analysis

Statistical analysis of data obtained was determined by the use of one-way analysis of variance (ANOVA). A significant difference between obtained data was considered at $P \leq 0.05$.

3. RESULTS AND DISCUSSION

3.1 Results

3.1.1 Crude extract percentage yields

The percentage yields of the cold hexane, ethyl acetate and methanol extracts were 0.05 g, 0.01 g and 1.20 g, respectively. On the other hand, the hot methanol, hexane and ethyl acetate extracts yields were 0.26 g, 0.08 g and 1.41 g, respectively.

3.1.2 Isolation of bioactive constituents

In this study, we report the isolation of a mixture of isonutiagenin (3) and diosgenin (4) from the rhizomes of Costuslucanusianus. Fig.1 &2).

The known compounds (3 and 41) were identified by comparison of their NMR spectra data (Supplementary Figures A and (Tables 1-2) with the literature 13-15.

Fig.3 and 4.Chemicalcompoundsisolated fromtherhizomesof *Costuslucanusianus*J.Braun&K.Shum

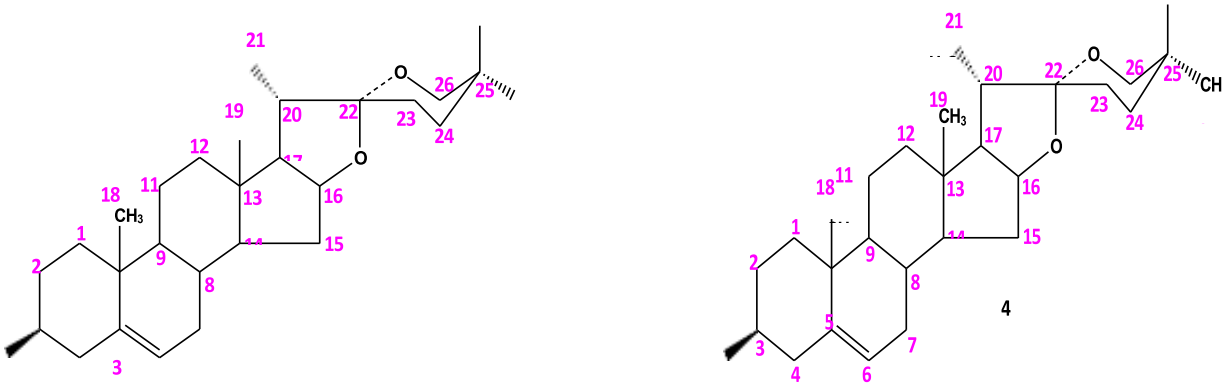

The1H NMRand13CNMRdataofcompounds3&4 are reported inTables1 and2,respectively.

Compd.	H-3	H-6	H-18	H-19	H-21	H-26	H-27
3	3.35-3.37,m	5.36,d,1.9Hz	0.79,s,3H	1.02,s,3H	0.96, d, 7.0Hz	3.28,dd, 10.3,2.4, 3.6Hz	1.20,s,3H
4	3.45-3.47,m	5.73,d,1.9Hz	0.80,s,3H	1.02,s,3H	0.98,d,6.7 Hz	3.34, d,11.0, 3.44,d,11	0.82,s,3H

[1]H NMR(600Hz).3*,4*13-15

Table2:13CNMR dataofcompounds**3** and**4**

CarbonPosition	Compound**3***		Compound**4***	
	Experimental	Literature	Experimental	Literature
1	37.38	37.10	37.38	37.43
2	31.78	31.60	31.78	31.79
3	71.89	71.30	71.89	71.89
4	42.43	42.30	42.43	42.46
5	140.95	141.5	140.95	141.02
6	121.59	121.5	121.59	121.60
7	32.96	32.90	32.29	32.25
8	31.87	31.80	31.60	31.64
9	50.89	50.60	50.22	50.25
10	36.80	37.00	36.80	36.84
11	20.98	21.20	21.03	21.07
12	39.95	40.10	39.95	39.99
13	40.52	40.60	40.42	40.46
14	56.68	56.90	55.82	56.72
15	32.01	31.90	32.21	32.04
16	80.77	81.60	80.97	81.03
17	62.20	62.40	62.26	62.28
18	16.40	16.40	16.44	16.49
19	19.50	19.50	19.57	19.63
20	41.77	41.40	41.88	41.80
21	14.63	14.30	14.67	14.73
22	109.42	109.5	109.44	109.50
23	31.52	29.90	31.55	31.59
24	34.11	34.60	28.96	28.99
25	80.66	81.60	30.46	30.49
26	67.00	69.20	67.02	67.04
27	30.43	23.80	17.56	17.35

13CSpectrum(CDL_3)recordedonBrukerAvanceIIIat150.0MHz.3*,4*(*3= 13,16*4=14-15.

3.2 Discussion

3.2.1 Extract yields

Low extraction yields were recorded for both the cold (0.01-1.20%) and hot (0.08-1.41%) extracts. This aligns with previous reports, which have attributed low recovery of crude extracts to the limited abundance of extractable secondary metabolites 17-18.

3.2.2 Isolation of bioactive constituents

This was the initial isolation of steroids from the hexane extract of the *C. lucanusianus* rhizome. *Costus* genus rhizomes are known as the major sourceof diosgenin and similar compounds have been identified from its other parts such as leaves, stems and flowers. In addition, steroidal saponins, steroids and sapogenins have also been reported to be characteristic constituents of the genus [10]. In this study, isonuatigenin was identified alongside diosgenin, marking its first reported occurrence within the Costus genus. The examination of

spectroscopic data of compound Z, in comparison with the published data for (25R)-isonuatigenin and diosgenin confirmed that it was a mixture of two identical steroidal sapogenins13-16

Few proton signals were easily recognizable due to extensive interproton coupling in the 1H NMR. A total of eight methyl signals at (18-CH_3, 19-CH_3) and (21-CH_3, 27-CH_3) were observed as the upfield signals. The overlapping multiplets in the methylene envelope (δ 2.23-1.6 ppm) were as a result of the remaining methylene and methine signals. Overlapping downfield signals greater than 3ppm were assigned to the olefinic signals at δ 5.3-5.7ppm and oxysubstitutedmethine resonance at δ 3.3-3.4 ppm. The signals for H-16 appeared as a doublet of doublet at δ 4.4 ppm and H-26 at δ 3.2-3.3 ppm. The overlapping of signals observed in the H NMR can be attributed to the presence of two similar compounds with similar chemical shifts. The signal corresponding to the H-27 is of particular diagnostic value in distinguishing between the two compounds. The chemical shift value of the C-27 protons at 30.43ppm further confirmed that the structure is isonuatigenin.

A total of fifty-four (54) carbon signals observed were assigned to compounds 3 and 4.

The characteristic signals of the steroidal sapogenin are those of C-16, C-26 and C-22, which are usually between (80-110 ppm). 16

The angular methyl groups, and C-21 chemical shifts were established to be similar to those reported for isonuatigenin and diosgenin. The signals of diosgenin and isonuatigenin were nearly identical except for the induction of the expected chemical shift of the carbon atoms (25-C and 27-C) of ring F by the addition of a -OH group at C-25 and a small downfield shift of the C-27 value. Some ^{1}H-^{1}H and ^{1}H-^{13}C couplings were also established with the 2D NMR

3.2.3 Antibacterial and antifungal activity

High inhibition zones were observed by the hexane extract against *S. typhi* (30 mm), followed by *S. aureus* and *K. pneumonia* (28 mm) while the methanol extract exhibited a high inhibition zone against *B. subtilis* (24 mm) and *P. aeruginosa* (23 mm). These findings are comparable to previous studies on the antibacterial potency of *C. igneus, C. pictus* and *C. speciosus* rhizome petroleum ether (non -polar) extracts against *E. coli*, *S. aureus, P. aeruginosa*and *B. subtilis* at (500-2000 µg/mL) 19. Also, *C. speciosus* rhizome hexane, ethyl acetate and methanol extracts inhibited the growth of *S. aureus* and *B. subtilis* (9 mm-15mm) at 2.5-5.0 mg/disc 17.

A similar trend was observed in antifungal assays where maximum antifungal activity was also observed at 100 µg/ml (Table 4). Hexane extract displayed a slightly higher antifungal activity than the methanol and ethyl acetate extracts. Antifungal activity of the extracts against tested fungal strains is in line with previous reports on the antifungal potency of the root and leaf ethanol extracts of *Costusafer*, a related African species, against *C. albicans* and *A. niger*20.

Antibacterial and antifungal activity resultsof the crude extracts revealed that the active components liable for the observed properties are predominantly present in the non-polar extract (hexane extract).

SolventExtracts	***S.aureus***				***E.coli***				***P.aeruginosa***				***K.pneumonia***				
(µg/mL)Concentration	**100**	**50**	**25**	**12.5**	**100**	**50**	**25**	**12.5**	**100**	**50**	**25**	**12.5**	**100**	**50**	**25**	**12.5**	**100**
Hexane(Rhizome)	- 28.0± 1.848	- 24.3± 1.067	- 20	- 18	- 27.3 ±1.06 7	- 25.3 ±1.067	- 22-3 ±0.53 3	- 19.0 ±1.60 0	- 26.7 ±1. 067	- 26	- 21.7 ±1.41 1	- 20	- 28	- 25.3 ±1.06 7	- 22.7 ±1.41 1	- 19.7± 1.411	- 25.3 ±1.067
Ethylacetate(Rhizome)	16.7± 1.067	14	12	10	18	16.7 ±1.067	14.7 ±1.06 7	12.7 ±1.06 7	18	16	14	12	17.3± 1.067	15.3 ±1.06 7	12.7 ±1.06 7	10	20
Methanol(Rhizome)	20 ±1.848 0.533	17.3 ±1.067	15.3± 1.067	13. 3± 1. 06	22.7 ±1.06 7	19.7± 1.411	17.7 ±1.41 1	15.0 ±1.60 0	23	20.7 ±0.53 3	17.7 ±0.53	15.7 ±0.5 3	22	18	16	14	24
+vestandardGentamicin	40						38										
-veStandardDMSO	-	-	-	-	-	-	-	-	-	-	-	-	-	-	-	-	-

S.auereus=Staphylococcusaureus,B.subtilis = Bacillus subtilis,E.coli=Escherichiacoli,P.aureginosa=Pseudomonasaureginosa,K.pneumonia=Klebsiellapneumonia,S.typhi =Salmonellatyphi

Table4:AntifungalActivityOfCrudeExtracts

Partsofplant used	SolventExtracts	*C.albicans*				*A.niger*				*P.notatu*		
	Concentration (µg/mL)	100	50	25	12.5	100	50	25	12.5	100	50	2
		-	-	-	-	-	-	-	-	-	-	-
Rhizome	Hexane	18.7± 1.067	16.7± 1.067	15	14	19.3±1.067	17.3± 1.067	15.3±1.067	13.3± 1.067	19.0± 0.924	17.3± 0.533	1 ±
	Ethylacetate	17.3± 1.067	14.7± 1.067	12	10	17.3±1.067	15.3± 1.067	12.7 ± 1.067	10	19.3± 1.067	17.3± 1.067	1
	Methanol	18.7± 1.067	17.3± 1.067	14.7± 1.067	12	17.3±1.067	14	12	10	16.7 ±1.067	14	1
	+ve Standard Tioconazole(70%)	28				26				28		
	-ve Standard DMSO	-				-				-		

C.albicans= Candidaalbicans, P. notatum= Penicilliumnotatum,A.niger=Aspergillusniger ,R.stolonifer

3.3.4 Minimum Inhibitory Concentration (MIC) Results

The hexane extract exhibited MIC values at 3.125 µg /ml against tested microorganisms except *A. niger* and *P. notatum*, which displayed no prominent growth (Table 5) while the MIC of the methanol extract was at 6.25 µg /ml against all tested microorganisms (Table 6). C. speciosus rhizome hexane extract displayed a MIC value of 1.25 mg /ml against *B. subtilis*and *S. aureus*and 500 mg /ml against *A. niger*. Also, a MIC of 1.25 mg /ml was displayed by *C. speciosus* rhizome methanol and ethyl acetate extracts against *B. subtilis* and *S. aureus* respectively. The methanol extract also displayed a MIC of 0.625 mg/mL against *S. aureus* 17. *Costusigneus* rhizome petroleum ether extract also displayed a MIC value of 0.25mg /ml against *P. aeruginosa, S. aureus* and *B. subtilis*, while *CostusPictus* petroleum ether exhibited MIC of 0.25 mg /ml for *B. subtilis, S. aureus,* and 0.5 mg /ml for *P. aeruginosa and E. coli*[19].

4. CONCLUSION

The Chromatographic studies of the rhizome hexane extract led to the isolation of a mixture of diosgenin and isonuatigenin. The antimicrobial activity displayed by the rhizome extracts validates its application in the treatment of infectious diseases traditionally. Further work is ongoing to purify and separate the compounds for individual antimicrobial activities.

ACKNOWLEDGEMENTS

The authors gratefully acknowledge Dr. Adeniyi Ogunlaja of Nelson Mandellaa University for his valuable assistance with the NMR spectroscopy measurements and Dr. Olutimilehin Oladele and Dr. Oludamilola Oladele for their financial contributions to the success of the research.

REFERENCES

1. Kuete, V. Medicinal spices and vegetable from Africa. Therapeutic potential against metabolic, inflammatory, infectious and systemic diseases 2017. Academic press:133-151.check ACS reference template??

2. Okeke, I.N; Laxmaninarayan, R; Bhutta, Z.A; Duse, A.G; Jenkins, P, O"BrienTF;Pablos-Mendez, A; Klugman, K.P . Antimicrobial resistance in developing countries, Part 1. Recent trends and current status. Lancet Infectious Diseases 2005, 5, 481-493.

3. Cascioferro, S; Carbone, D; Parrino, B; Pecoraro, C; Giovannetti, E; Cirrincione, G; Diana, P. Therapeutic strategies to counteract antibiotic resistance in MRSA biofilm-associated infections 2021. Chem Med Chem (16), 65-80.

4. Cowan, M.M.Plant products as antimicrobial agents. Clinical Microbiology Review 1999, 12(4), 564-582.

5. Burkill, H.M. Costuslucanusianus. The Useful Plants of West Tropical Africa 1985, (Vol 1), 520.

6. Lambert, N; Baccou, J.C, Sauvalre, Y. Screening of diosgenin in rhizome from 3 Costus species (C. deistellii, C. igneus, C. lucanusianus). PlantaMedica 1988, 54(4):366-367.

7. Haruna, B; Onanuga, A. Preliminary phytochemical screening and antimicrobial evaluation of three medicinal plants used in Nigeria. African Journal of Traditional Complement and Alternative Medicine 2011, 8(4):387-390.

8. Owolabi, O.J; Nworgu, Z.A.M. Anti-inflammatory and anti-nociceptive activities of Costuslucanusianus (Costaceae). Pharmacologyonline 2009, 1:1230-1238.

9. Saliu, J.A; Fapohunda, O. The antihyperglycemic, hepatoprotective and renoprotective potentials of the aqueous extract of Costuslucanusianus on streptozotocin-induced diabetic rats. Journal of Applied Life Science 2016, 4(2):1-10.

10 Oliver, B. Medicinal Plants in Tropical West Africa 1986. Cambridge University Press, Cambridge:198-199.

11. Perez, C; Paul, M; Bazerque, P. Antibiotic assay by Agar well diffusion method. Acta Biol. Medica. Exp. 1990, 15:113-115.

12. Akinpelu, D.A.; Alayande, K.A.; Aiyegoro, O.A.; Akinpelu, O.F.; Okoh, A.I (2015). Probable mechanisms of biocidal action of Cocosnucifera Husk extract and fractions on bacterial isolates. BMC Complement Medical Therapies 2015. 15:116.

13. Faini, F., Torres, R.; Castillo, M. (25R)-Isonuatigenin, an unusual steroidal sapogenin from Vestialycioides, Phytochemistry 1984,23(6):1301–1303.

14. Puri, R; Wong, T.C; Puri, R.K. Solasodine and diosgenin: 1H and 13C assignments by two-dimensional NMR spectroscopy. Magnetic Resonance Chemistry 1993, 31:278-282.

15. Abdel-Aziz, A.M.E.; Brain, K.R.; Bluden, G.; Crabb, T.; Bashir, A.K . Steroidal sapogenins from Taicaleontopetaloides. PlantaMedica 1990, 56: 218-221.

16. Agrawal, P.K.; Jain, D.C.; Pathak, A.K.NMR spectroscopy of steroidal sapogenins and steroidal saponins:An update, Magnetic Resonance Chemistry 1995,33(12) :923–953.

17. Duraipandiayn, V.; Al- Harbi, N.A.; Ignacimuthu, S.; Muthukumar, C. Antimicrobial activity of sesquiterpene lactones isolated from traditional medicinal plant, Costusspeciosus.BMC Complement. Alternative Medicine 2012, 12(13): 1-6.

18. Shiny T (2013). Phytochemical investigation of the insulin plant 'Costuspictus' D.Don. International Journal of Resource Pharmaceutical Biomedical Science 2013, 4(2):97-104.

19. Sulakshana, G.; Rani, A.S.; Saidulu B. Evaluation of antibacterial activity in three species of Costus, International Journal of Current Microbiology Applied Science 2013, 2(10):26-30.

20. Nnaoma, I.E; Unegbu, C.C; .Nnrom, C.M; Rich, J. Phytochemical composition and antifungal activity of the leaf and root extracts of Costusafer. Journal of Chemical Pharmaceutical Resources. 2018, 10 (11):84-87.

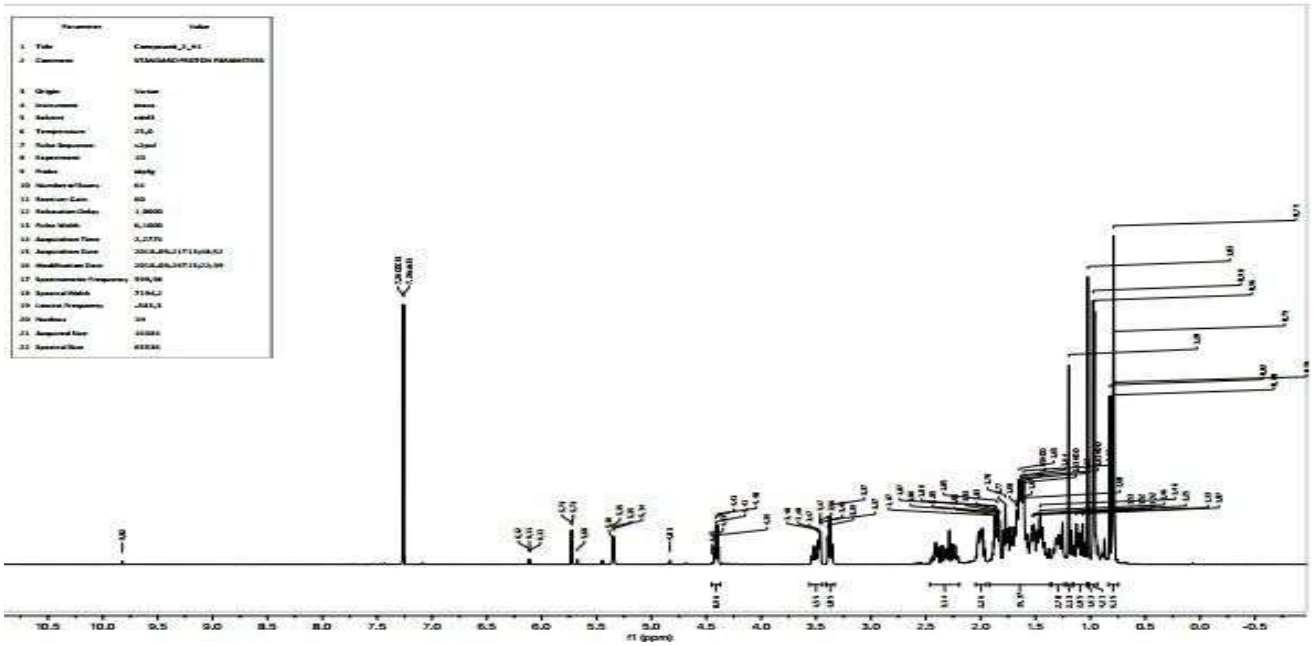

FigureB1:ProtonNMRofCompounds**3**and**4**

FigureB2:Carbon13NMRofCompounds**3**and**4**

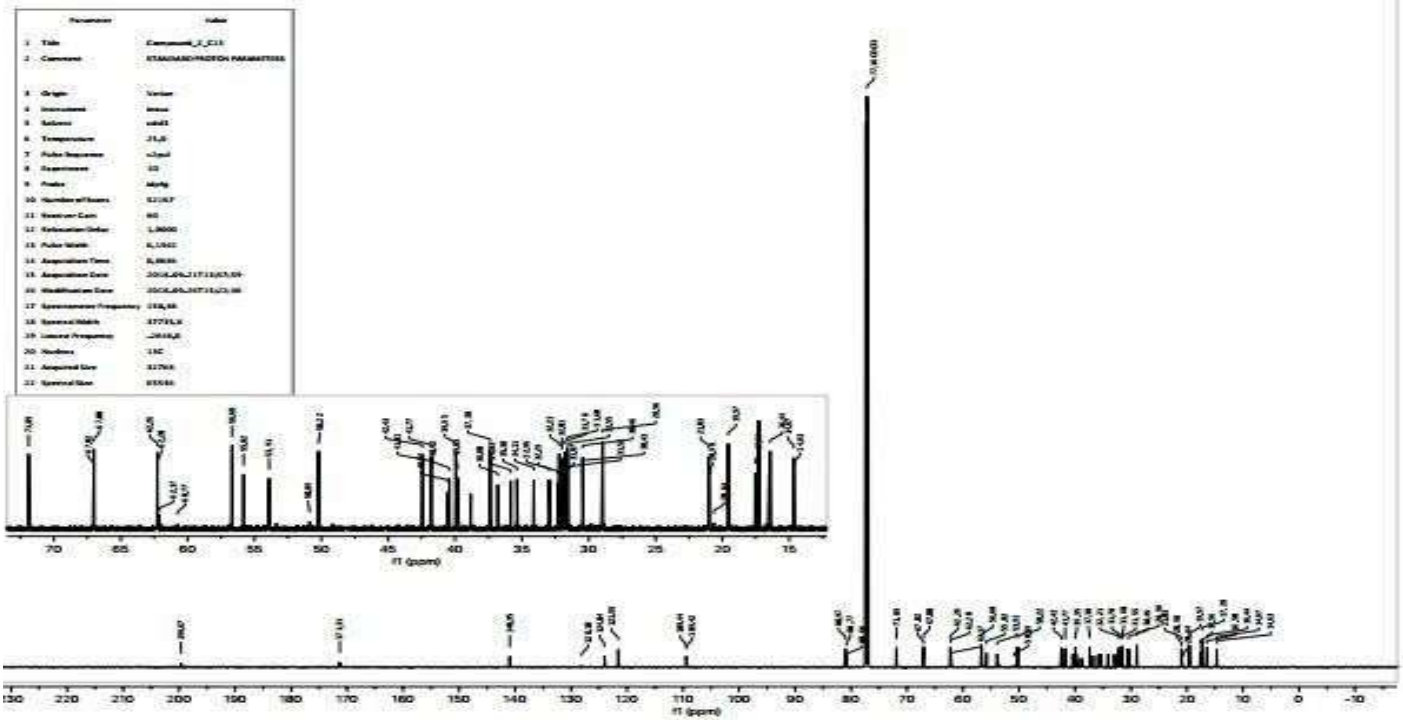

ISBN: 978-978-67-0285-8 DOI: https://doi.org/10.55455/acsnigeria.1.3.88-92

Profiling Organic Biomarkers in Petroleum Depot and Its Biogeochemical Relevance

Adeniji, Taiwo Husani[1], Adeosun, Abimbola Latifat[2], Adeniji, Ajarat Tolulope[3], Sojinu, Olatunbosun Samuel[4], Akinlabi, Akinola Kehinde[5] and Arowolo, Toyin A.[6]

[1, 2] Chemistry Department, Federal College of Education, Abeokuta

[3] Lagos State University, Federal College of Education, Abeokuta Centre

[4, 5] Department of Pure and Applied Chemistry, Federal University of Agriculture, Abeokuta

[6] Hallmark University, Ijebu-Itele, Ogun-State

Corresponding Author's email: thadeniji28@gmail.com

DOI: https://doi.org/10.55455/acsnigeria.1.3.88-92

ABSTRACT

The occurrence of organic biomarkers in an ecosystem should be of great concern due to their effects on the environment and health of residents. The study profiled the organic biomarkers in soil and sediment samples towards identifying the various classes of organic biomarkers present and their biogeochemical relevance. Soil and sediment samples were collected from the petroleum depot at Mosinmi, Ogun State. The extraction of the samples (soil and sediments) were done with the aid of sonicator. Silica-alumina column chromatography was used for further clean-up of the extracts into polar, aromatic and saturate fractions. Gas chromatography-Mass spectrometer (GC-MS) was used for the analysis of the organic biomarkers from the concentrated fractions. The National Institute of Standards and Technology (NIST) library reference was used as basis of comparison of mass spectra for the identification of the organic biomarkers. Biogeochemical parameters including Pristane/Phytane (Pr/Ph), Odd-Even Carbon Prevalence (OEP), Pristane/Carbon-17 (Pr/nC17) were determined. The values obtained gave indication of the state of the environment and anthropogenic activities of the sampled area.

KEYWORDS: Organic biomarkers, Odd-Even carbon preference (OEP), Sonicator, Mass Spectra, petroleum depot.

1. INTRODUCTION

Biomarkers are organic matter whose identity can be traced back to biologically synthesized organic molecules. They occur in sediments, rock, and crude oils and show little or no change in structure from their parent organic molecules in living organisms. Their chemical fingerprint in petroleum provide unique clues to indicate source rocks and biological sources of organisms that generated the organic matter, environmental conditions, thermal maturation and level of microbial biodegradation. Biomarkers generally retain their source information after burial in soil and sediment regardless of any alteration (Derrien *et al*., 2017). Soil and sediment contain organic matter with very complex sources (Ortiz *et al*., 2013), hence, different tools such as stable isotopic, total organic carbon (TOC) and specific biomarker methods are used to identify their origin of organic carbon. Specifically, n-alkanes and geochemical parameters such as: carbon preference index (CPI), average chain length (ACL), pristine/phytane (Pr/Ph) ratio are widely used in identification and oil-source rock correlations, origin and environment of depositions determination (Cheng *et al.*, 2023). Only a few reports, including Olayinka *et al*., (2020) exists on organic biomarkers in the petroleum depots. However, to ensure a clean and safe environment, proper profiling of organic biomarkers in sediments and soils of petroleum depots is essential.

2. MATERIALS AND METHODS

The soil and sediment samples were collected at the identified locations at a depth of 0 – 30 cm each using hand shovel. 20 g of the freeze-dried composite soil and sediment samples were weighed into 100 ml beaker. 25 cm^3 of dichloromethane was added and sonicated for 15 minutes at 25 ^oC. The sonication was done three times, and all the extracts collected together into a beaker covered with perforated aluminum foil. The beaker was labeled and set for purification with column chromatography.

3. RESULTS AND DISCUSSION

3.1 Occurrence of saturated organic biomarkers in sediment samples of Mosinmi, Sagamu

Aliphatic compounds detected in the sediment sample of Mosinmi, Sagamu ranged from nC_8 to nC_{17} (table 1).Cetene and E-15- heptadecenal both have high similarity indices of 92% and 91% respectively. 1- Ethyl -2- methylcyclopentane which is an n- alkane nC_8 show the least similarity index of 59%, it is however the most predominant as it exhibited the highest area percentage of 33.26 (table 1). This is an indication of petrogenic input of hydrocarbons in the surface sediments, supported by Hassaan *et al.*, (2024). The high predominance of low molecular weight n-alkane indicates oil contamination in the sample while its petroleum source input is corroborated by Sojinu *et al.*, (2012).

Table 1: Occurrence of compounds in sediment sample of Mosinmi, Sagamu

S/N	RT (mins)	Name	CAS Number	%Quality	%Area
1.	2.26	1-ethyl-2-methylcyclopentane	019781-68-1	59	33.26
2.	14.16	Cetene	000629-73-2	92	0.63
3.	16.03	E-15-Heptadecenal	100130-97-9	91	1.74

3.2 Occurrence of aliphatic Compounds in sediment sample of Mosinmi (outside depot), Sagamu

The n-alkanes in the sample ranged from nC_6 to nC_{26} (table 2). Hexacosene, 2, 6, 11-trimethyldodecane, nonadecene, hexadecane and tetradecane have similarity indices of 97%, 96%, 95%, 93% and 94% respectively. 1, 2- dimethylaziridine, 3methylene heptane and (E)- 2- octane show moderate similarity indices of 59%, 59% and 58% respectively. (Z)- 2- hexane is the saturate with the least similarity index of 53%.,indicating sensitive response to anthropogenic interactions and petroleum hydrocarbon pollution (Zhan *et al.*, 2022).The predominantly low to medium molecular weight nC_8 to nC_{19} n- alkanes reveals the abundant algal organic matter biomakers with terrigenous inputs (Egbeola *et al.*, 2024).

Table 2: Occurrence of compounds in sediment sample of Mosinmi (outside) depot, Sagamu

S/N	RT (mins)	Name	CAS Number	%Quality	%Area
1.	2.27	1,2-Dimethylaziridine	030757-96-1	59	2.68
2.	3.09	(Z)- 2-Hexene	007688-21-3	53	0.89
3.	4.33	3-methyleneheptane	001632-16-2	59	1.79
4.	4.46	(E)- 2- octane	013389-42-9	58	0.60
5.	12.15	Tetradecane	000629-59-4	94	0.63
6.	14.22	Hexadecane	000544-76-3	93	0.88
7.	16.06	1-Nonadecene	018435-45-5	95	8.80
8.	16.10	2,6,11-trimethyldodecane	031295-56-4	96	0.61

9.	22.06	1-Hexacosene	018835-33-1	97	0.84

3.3 Occurrence of aliphatic compounds in soil sample, Mosinmi (inside) depot, Sagamu

The n-alkanes ranged from nC_6 to nC_{35} (table 3), most of the compounds have similarity index above 70% while 1-bromo–4-bromomethylpetane and 1- methylpentane have similarity indices of 64% and 56% respectively. 2- Cyclopropylpentane and 1- docosene have relatively high area percentage of 13.39 and 11.64 respectively.

Table 3: Occurrence of compounds in soil sample of Mosinmi (inside) depot, Sagamu

S/N	RT (mins)	Name	CAS Number	%Quality	%Area
1.	2.21	2- methyl -Pentane	000107-83-5	56	5.34
2.	2.97	2-cyclopropyl-Pentane	005458-16-2	78	13.39
3.	12.08	(E)-5-Tetradecene	041446-66-6	96	1.04
4.	12.17	Tetradecane	000629-59-4	94	1.91
5.	13.21	Nonadecane	000629-92-5	83	0.38
6.	14.18	1-Octadecene	000112-88-9	94	5.32
7.	14.26	Hexadecane	000544-76-3	97	3.94
8.	15.18	Heptadecane	000629-78-7	90	0.24
9.	15.25	1-bromo-Octadecane	000112-89-0	83	0.42
10.	16.13	Hentriacontane	000630-04-6	91	2.39
11.	17.79	1-Docosene	001599-67-3	99	11.64
12.	20.11	1-Bromo-4-bromo-Methyldecane	061639-11-0	64	0.34
13.	26.40	17-Pentatriacontene	006971-40-0	87	0.44

3.4 Occurrence of aliphatic compounds in soil sample, Mosinmi (outside) depot, Sagamu

The compounds present in the soil sample of Mosinmi (outside depot) are n-alkanes ranging from nC_8 to nC_{19} (table 4). The number of saturated compounds detected was relatively small but with considerably high similarity index with octadecane having the highest index of 94% and 2-hexyloctylcyclopentane with the least similarity index of 70%. This is an indication of sensitive response to anthropogenic interactions and petroleum hydrocarbon pollution (Zhan *et al.*, 2022).

Table 4: Occurrence of compounds in soil sample of Mosinmi (outside) depot, Sagamu

S/N	RT (mins)	Name	CAS Number	% Quality	% Area
1.	2.99	2-cyclopropyl- pentane	005458-16-2	72	30.34
2.	16.01	1-Nonadecene	018435-45-5	91	2.13
3.	16.06	Octadecane	000593-45-3	94	0.42
4.	17.55	(2-hexyloctyl)-Cyclopentane	055044-77-4	70	0.78

3.5 Biogeochemical significance of organic biomarkers in selected ecosystems

The biogeochemical parameters determined were carbon Preference Index 1 (CPI_1), Natural alkane Ratio (NAR), Carbon Preference Index 2 (CPI_2), Odd-Even Carbon Prevalence (OEP), Pristane/Phytane (Pr/Ph), Pristane/Carbon-17 (Pr/nC_{17}), Phytane/Carbon-18 (Ph/nC_{18}), Average
Chain Length (ACL), Low Molecular Weight/ High Molecular Weight (LMW/HMW) and Carbon- 31/ Carbon-29 ($n\text{-}C_{31}/C_{29}$) (table5).

The CPI_1 values of less than 1 are for n-alkanes derived from petroleum and other anthropogenic activities such as combustion of fuel, wood and agricultural debris and values greater than 1 is source indicator of n-alkanes in marine sediments (Nascimeto *et al.*, 2023), CPI_2 values greater than 1 is an indication of input from terrestrial higher plant wax.

The LMW/HMW values of less than 1 is an indication of n-alkanes in marine sediments, contribution from higher plants, marine animals and sedimentary bacteria and values greater than 1 showed contribution from petroleum and plankton sources. The n-alkane ratio (nC_{31}/nC_{19}) differentiates sources inputs of n-alkanes in marine sediments, serving a measure of relative proportions of allochthonous and autochthonous hydrocarbon inputs, values greater than 0.4 is associated with non-marine sources. The values of OEP less than 1 suggested an input from petroleum, strong bacteria activities or low flux of terrestrial vascular plant debris and NAR values less than 1 indicated an input from petroleum hydrocarbons, values greater than 1, origin from terrestrial higher plants or marine plants. The environment of deposition is inferred from the Pr/Ph values with values less 1 indicating anoxic, aquatic environment and greater than 1, oxic, terrestrial with contribution from terrigenous plants.

Table 5: Geochemical parameters in samples

Indices	Mosinmi(1)	Mosinmi(2)	Mosinmi (in)	Mosinmi (out)
CPI_1	6.73	3.27	1.12	1.21
CPI_2	0.05	1.28	2.37	4.26
NAR	0.74	0.72	0.21	-0.10
OEP	0.08	3.46	0.31	0.00
Pr/Ph	0.00	2.18	0.00	2.35
Pr/C_{17}	1.32	0.00	0.06	0.81
Ph/C_{18}	0.00	2.86	0.00	3.00
ACL	0.04	1.13	0.05	3.85
LMW/HMW	1.31	3.49	0.30	4.08

C_{31}/C_{19}	0.00	0.00	0.00	0.00

The samples depositional environments ranged from oxic, sub-oxic to anoxic in the terrestrial and aquatic environment while the anthropogenuc activities and possible pollution indication have been established.

4. CONCLUSION

Aliphatic compounds including Cetene, E-15- heptadecenal and. 1- ethyl -2- methylcyclopentane, nonadecene, hexadecane, tetradecane, 2- cyclopropyl- pentane, and 1- methylpentane were identified in the petroleum depot. The anthropogenic and petrogenic sources indications established while the origin of the biomarkers such as terrestrial, aquatic, lacustrine and environment of depositions including oxic, sub-oxic and anoxic determined.

REFERENCES

1. Derrien, M.; Yang, L.; Hur, J. Lipid Biomarkers and Spectroscopic Indices for Identifying Organic Matter Sources in Aquatic Environments: A Review. *Water Res.* **2017**, *112*, 58–71. DOI: 10.1016/j.watres.2017.01.023.
2. Egbeola, M. A.; Adeigbe, O. C.; Adamolekun, O. J. n-Alkane Bound Biomarker Fingerprints from Asphaltenes in the Bitumens of Eastern Dahomey Basin, Nigeria: Source and Genetic Implications. *Pet. Res.* **2024**, *9* (1), 85–91. DOI: 10.1016/j.ptlrs.2023.07.005.
3. Hassaan, M. A.; Ragab, S.; El Sikaily, A.; El Nemr, A. Sources of Hydrocarbons and Their Risk Assessment in Seawater and Sediment Samples Collected from the Nile Delta Coast of the Mediterranean Sea. *Sci. Rep.* **2024**, *14*, 5082. DOI: 10.1038/s41598-024-55339-4.
4. Olayinka, O. O.; Adedeji, O. H.; Ahmed, S. A. Oil Spillage Measures Caused Drastic Reduction in Total Petroleum Hydrocarbon Levels in Petroleum Depot in Ibadan, Southwestern Nigeria. *Cogent Environ. Sci.* **2020**, *6* (1), 1826744. DOI: 10.1080/23311843.2020.1826744.
5. Ortiz, J. E.; Moreno, L.; Torres, T.; Vegas, J.; Ruiz-Zapata, B.; García-Cortés, Á.; Galán, L.; Pérez-González, A. A 220 ka Palaeoenvironmental Reconstruction of the Fuentillejo Maar Lake Record (Central Spain) Using Biomarker Analysis. *Org. Geochem.* **2013**, *55*, 85–97. DOI: 10.1016/j.orggeochem.2012.11.012.
6. Cheng, P.; Gai, H.; Xiao, X.; Zhou, L.; Zhao, W.; Zhou, Q.; Tian, H. Evolution of the Pristane/Phytane Ratio with Maturity of Lacustrine Source Rocks: Implications of a Thermal Simulation Experiment. *ACS Earth Space Chem.* **2023**, *7* (5), 1072–1082. DOI: 10.1021/acsearthspacechem.3c00011.
7. Sojinu, S. O.; Sonibare, O. O.; Ekundayo, O.; Zeng, E. Y. Assessing Anthropogenic Contamination in Surface Sediments of Niger Delta, Nigeria with Fecal Sterols and n-Alkanes as Indicators. *Sci. Total Environ.* **2012**, *441*, 89–96. DOI: 10.1016/j.scitotenv.2012.09.015.
8. Zhan, S.; Wu, J.; Zhang, H.; Jin, M. Occurrence, Sources, and Spatial Distribution of n-Alkanes in Surface Soils from the Amu Darya Delta, Uzbekistan, Arid Central Asia. *Environ. Res.* **2022**, *214*, 114063. DOI: 10.1016/j.envres.2022.114063.